Northwest Atlantic Fisheries Organization

Serial No. N7030 **NAFO SCR Doc. 19/058**

SCIENTIFIC COUNCIL MEETING – NOVEMBER 2019

Vulnerable Marine Ecosystems in the NAFO Regulatory Area: Updated Kernel Density Analyses of Vulnerable Marine Ecosystem Indicators

by

E. Kenchington[1], C. Lirette[1], F.J. Murillo[1], L. Beazley[1], A.-L. Downie[2]

[1]Department of Fisheries and Oceans, Dartmouth, Nova Scotia, Canada.

[2]CEFAS, Lowestoft, Suffolk, United Kingdom.

Abstract

In support of the 2020 NAFO review of the closed areas to protect vulnerable marine ecosystems (VMEs) in the NAFO Regulatory Area, kernel density analyses (KDE) of Large-sized Sponges, Sea Pens, Small and Large Gorgonian Corals, Erect Bryozoans, Sea Squirts (*Boltenia ovifera*), and Black Corals were undertaken using all available research vessel survey data (1995 – 2019). This is the first KDE analysis of black corals for this area. KDE polygons equating to VMEs were overlain on binary outputs of predicted suitable versus unsuitable habitat from species distribution models (SDMs) for each taxon where available, and for sponges and large gorgonian corals, polygons were modified to areas of predicted suitable habitat consistent with previous practices. New SDMs were prepared for Erect Bryozoans and Sea Squirts (*Boltenia ovifera*). For Tube-dwelling (Cerianthid) Anemones and Sea Lilies (Crinoids), updated distribution maps were provided, drawing on data from research vessel trawl surveys, NEREIDA rock dredge samples and NEREIDA underwater imagery. The effectiveness of the closed areas was for the first time assessed by examining the proportion of VME area and biomass protected for each VME indicator type. The results of these analyses were compared with those previously conducted in 2013 and reviewed by the NAFO Working Group on Ecosystem Science and Assessment (WGESA) at its 12th meeting in November 2019.

Contents

Introduction 3
Summary of Data Sources 3
Overview of Analytical Methods 5
Kernel Surfaces and Significant Area Polygons 5
Species Distribution Modeling 6
Previously Adopted Definitions 6
New Predictive Models of Distribution for Erect Bryozoans and Sea Squirts (*Boltenia ovifera*) 7
Methods 7
Results and Discussion 10
Review of Significant Concentrations of Large-sized Sponges 14
Modified VME Polygon Boundaries for Large-sized Sponges 20
Review of Significant Concentrations of Sea Pens 22
Modified VME Polygon Boundaries for Sea Pens 27
Review of Significant Concentrations of Small Gorgonian Corals 29
Review of Significant Concentrations of Large Gorgonian Corals 33
Modified VME Polygon Boundaries for Large Gorgonian Corals 37
Review of Significant Concentrations of Tube-dwelling Anemones 37
Review of Significant Concentrations of Erect Bryozoans 38
Review of Significant Concentrations of Sea Lilies (Crinoids) 42
Review of Significant Concentrations of Sea Squirts 43
Modified VME Polygon Boundaries for Sea Squirts (Boltenia ovifera) 47
Review of Black Coral Biology, Distribution, and Functional Significance 48
Kernel Density Analysis of Black Corals 49
Modified VME Polygon Boundaries for Black Corals 53
Conclusions of the 2019 Analyses of VME Indicator Taxa 55
Indicators for the Effectiveness of the NAFO Closed Areas 58
References 64

Introduction

The United Nations General Assembly Resolution 61/105, concerning sustainable fisheries in marine ecosystems, calls for the protection of vulnerable marine ecosystems (VME) from destructive fishing practices. Subsequently, the Food and Agriculture Organization (FAO) produced guidelines for the identification of VME indicator species/taxa to assist in the implementation of the resolution, but recommended the development of case-specific operational definitions for their application. The Northwest Atlantic Fisheries Organization (NAFO) undertook a review of the closed areas in 2013/2014 (NAFO, 2013) and applied kernel density estimation (KDE) to research vessel trawl survey data to identify significant concentrations of VME indicator taxa in the NAFO Regulatory Area (NRA). In response to a request from the NAFO Commission and following the procedures applied in 2013, these analyses were updated using all available data from the Canadian and EU/Spanish trawl survey data in support of the current review of the closed areas.

Kernel density estimation (KDE) utilizes spatially explicit data to model the distribution of a variable of interest. It is a simple non-parametric neighbour-based smoothing function that relies on few assumptions about the structure of the observed data. It has been used in ecology to identify hotspots, that is, areas of relatively high biomass/abundance. With respect to marine benthic invertebrate species, it was first applied to the identification of significant concentrations of sponges in the NAFO Regulatory Area in 2009 (Kenchington et al., 2009) followed by an application to sea pens (Murillo et al., 2010). Since then it has been used to identify significant concentrations (VMEs) of corals, sponges and other VME indicators from research vessel (RV) trawl survey catch data in both Canada (Kenchington et al., 2016) and in the NRA (NAFO, 2013; Kenchington et al., 2014). Here, KDE biomass surfaces for seven VME indicator taxa were created: Large-sized Sponges, Sea Pens, Small Gorgonian Corals, Large Gorgonian Corals, Erect Bryozoans, Sea Squirts (*Boltenia ovifera*), and Black Corals, and the RV catch threshold that delineates the VME polygons determined. The congruence between the KDE-generated VME polygons and areas of predicted occurrence derived from species distribution models (SDM) were examined, where available, and were used to modify the polygons to eliminate areas where the taxon was not predicted to occur (as was done previously; NAFO, 2015). New SDMs were created for Sea Squirts (*Boltenia ovifera*) and Erect Bryozoans using a suite of terrain variables as predictors along with physical oceanographic variables. For two VME indicator groups (Tube-dwelling Anemones (Cerianthids) and Sea Lilies (Crinoids)), updated distribution maps were provided, drawing on up-to-date data from the RV trawl surveys, NEREIDA rock dredge samples and NEREIDA underwater imagery. Lastly, the effectiveness of the closed areas was for the first time assessed by examining the proportion of VME area (km^2) and biomass (kg) derived from the kernel density biomass surfaces under protection. These metrics may serve as potential indicators of the status and long-term trends of the VMEs and the management measures in place to protect them, and will be used to inform the ecosystem overview summary sheets.

Summary of Data Sources

Available data for each VME indicator type were obtained from research vessel trawl surveys (Table 1), benthic imagery collected through the NEREIDA program (Tables 2 and 3) and from NEREIDA rock and scallop dredges (Table 4). Only the trawl survey data (Table 1) has changed substantially since the last review of closed areas. One record was updated from the video imagery (Table 3).

Table 1. Data sources from contracting party research vessel surveys; EU, European Union; DFO, Department of Fisheries and Oceans; NL, Newfoundland and Labrador; IEO, Instituto Español de Oceanografia; IIM, Instituto de Investigaciones Marinas; IPMA, Instituto Português do Mar e da Atmosfera.

Programme	Period	NAFO Division	Gear	Mesh Size in Codend Liner (mm)	Trawl Duration (min)	Average Wingspread (m)
Spanish 3NO Survey (IEO)	2002 - 2019	3NO	Campelen 1800	20	30	24.2 – 31.9
EU Flemish Cap Survey (IEO, IIM, IPIMAR)	2003 - 2019	3M	Lofoten	35	30	13.89
Spanish 3L Survey (IEO)	2003 - 2019	3L	Campelen 1800	20	30	24.2 – 31.9
DFO NL Multi-species Surveys (DFO)	1995 - 2019	3LNO	Campelen 1800	12.7	15	15 - 20

During the CCGS *Hudson* NEREIDA cruise in 2009, 9 benthic imagery transects were conducted on the Sackville Spur and western Flemish Cap slope/Flemish Pass region using the 4K camera (4KCam) and Campod (Beazley et al., 2013a). Although video footage of the seabed was continuously recorded on the 'Campod' transects, only images have been analyzed to date.

Table 2. Summary of the benthic imagery collected and analyzed from the CCGS *Hudson* NEREIDA 2009 cruise to the Flemish Cap area.

Location	Transect ID	Inside Closure?	Gear	Transect Length (m)	Depth Range (m)	# Photos
Sackville Spur	11	Mostly	4KCam	6 211	1080 – 1545	167
	12	Yes	4KCam	6 343	1313 – 1723	172
	18	Yes	4KCam	5 238	1336 – 1478	92
	24	Yes	4KCam	4 974	1290 – 1427	145
	26	Yes	4KCam	3 212	1381 - 1409	38
Flemish Pass area	28	No	Campod	2 431	461 - 479	92
	29	No	Campod	3 197	444 - 471	132
	30	No	4KCam	6 101	455 - 940	174
	38	Yes	4KCam	2 978	1328 - 1411	75

Table 3 summarizes the details of the analyzed transects that were collected using the ROV ROPOS during the CCGS *Hudson* NEREIDA 2010 cruise to the Flemish Cap. Downward- and forward-facing video was continuously recorded during each ROPOS dive (only downward-facing video has been analyzed to date). Due to their different objectives, the method used to analyze each transect varied. The ROV operated in two modes. In transect mode it kept a near constant speed and distance from bottom, did not stop and travelled to a predetermined waypoint. In explorer mode it stopped to collect specimens and although end waypoints were set the route to the waypoints was directed by

the investigators and was biased towards interesting observations. Speed and distance from the bottom varied. For instance, for transect 1335 and the explorer mode portions of transect 1337, only those megafauna that were large (~10 cm) and clearly visible were recorded. Transect 1336 was not analyzed in detail after its collection, and thus only the megafauna recorded during the *in situ* recording of the dive was summarized. For transect 1338, three sections of the transect (one trawled line, two untrawled lines; ~ 3 km in total) were analyzed every 10 m for corals and sponges only, but non-coral and sponge VME indicators were extracted from the *in situ* collection of the video. All visible megafauna were analyzed from the entire length of transect 1339.

Table 3. Summary of the benthic video collected and analyzed using the ROV ROPOS in 2010 during the CCGS *Hudson* NEREIDA cruise to the Flemish Cap (FC) area.

Location	Transect ID	Inside Closure?	Transect Length (m)	Depth Range (m)	Analysis Details
Southern FC slope	1335	No	8,292	873 – 1,853	Explorer mode. Analyzed in detail; frame by frame.
	1336	No	11,555	2,212 – 2,970	Explorer mode. Transect not analyzed in detail ('live' recordings summarized).
Southeast FC slope	1337	No	14,475	1,011 – 2,191	Transect and explorer mode. Explorer mode analyzed frame by frame; every 10 m analyzed for transect modes.
	1338	Yes	11,195	1,029 – 1,088	Explorer and transect. Three lines were analyzed (1 trawled, 2 untrawled) every 10 m for the abundance of sponges and corals. Non-coral and sponge observations extracted from 'live' recordings.
Northeast FC slope	1339	Yes	8,624	1,344 – 2,462	Explorer mode. Data extracted from 10 m intervals.

Table 4. Summary of the rock dredge and scallop gear sets collected and analyzed from the NEREIDA Programme on board the RV *Miguel Oliver*.

Programme	Period	NAFO Division	Depth Range (m)	Gear	N Valid Sets	Trawl Duration (min)
NEREIDA	2009 - 2010	3LMN	502 - 1991	Rock dredge	88	15
NEREIDA	2009	3M	870 - 1137	Scallop gear	7	15

Overview of Analytical Methods

Kernel Surfaces and Significant Area Polygons

The primary tool used previously to quantitatively determine significant concentrations of VMEs is kernel density estimation (KDE) analysis. As applied here, this analysis identifies "hotspots" in catch biomass distribution. Using the output kernel biomass density surfaces, polygons are drawn around successively smaller catch values and the area occupied by each polygon is calculated (Kenchington et al., 2014). The catch value associated with the largest change in area between successive values is considered to be the VME, distinguishing habitat-forming dense aggregations from the broader occurrence of individuals as identified through rule-based decisions (NAFO, 2013).

Species Distribution Modeling

Species distribution modeling (SDM) predicts the presence, absence or abundance/biomass of a species or habitat (the response variable) from environmental variables thought to influence it (the predictor variables). SDM for sponge grounds (Knudby et al., 2013 a, b), black corals, large gorgonian corals and sea pen corals (Knudby et al., 2013c), the glass sponge *Asconema foliata*, erect bryozoans and sea squirts (*Boltenia ovifera*) are incorporated into the assessment of VMEs. These models are particularly valuable in areas where the survey vessels do not sample (e.g., rough bottom, cliffs, depths greater than 1500 m) and for non-aggregating taxa such as the black corals that are present in low frequency and their past occurrence (noted after removal by the trawl) may or may not reflect the presences of other colonies in the same area. They can also be used to evaluate the area between trawl sets to determine if the full KDE polygon is potential habitat. With the exception of the SDM for *Asconema foliata* (Murillo et al., in revision), erect bryozoans and sea squirts, it was previously decided (NAFO, 2018a) that the SDMs used for the 2013 assessment (NAFO, 2013) would be presented. The new SDM for the erect bryozoans and the sea squirts were undertaken building on previous requests (NAFO, 2017) to refine the distributions of those taxa.

The analyses used for each VME indicator were:

1. Large-sized Sponges: kernel analyses, SDM
2. Large gorgonian corals: kernel analyses, SDM
3. Small gorgonian corals: kernel analyses
4. Sea pens: kernel analyses, SDM
5. Erect bryozoans: kernel analyses, SDM (new)
6. Sea squirts: kernel analyses, SDM (new)
7. Tube-dwelling (Cerianthid) anemones: distribution
8. Sea lilies (Crinoids): distribution
9. Black coral: kernel analyses, SDM.

Previously Adopted Definitions

In this general context, NAFO (NAFO, 2013) has followed the FAO guidelines (FAO, 2009) in defining and identifying:

VME indicator species. These are species that met one or more of the FAO Guidelines criteria for possible VMEs. Their simple presence is not an automatic indication of VMEs, but when found in significant aggregations with conspecifics, or other VME indicator species, they can constitute a VME. NAFO has approved a list of taxa that qualify as VME indicator species (NCEM Annex I.E.VI).

VME elements. These are topographical, hydrophysical or geological features which are associated with VME indicator species in a global context and have the potential to support VMEs. NAFO has approved a list of features that qualify as physical VME indicator elements (NCEM Annex I.E.VII).

Higher concentration observations of VME indicator species (a.k.a. "Significant concentrations"). These are specific locations where there are individual records of VME indicator species at densities at or above a threshold value that, for that specific VME indicator species, is associated with the formation of highly aggregated groups of that species. These higher concentration locations have been the basis for the delineation of the polygons referred as "Areas of higher sponge and coral concentrations" in NCEM Article 16.5, which are closed to bottom fishing activities.

Vulnerable Marine Ecosystem (VME). Under the structure-forming criterion, it is a regional habitat that contains VME indicator species at or above significant concentration levels. These habitats are structurally complex, characterized by higher diversities and/or different benthic communities, and provide a platform for ecosystem functions/processes closely linked to these characteristics. The

spatial scale of these habitats is larger than the footprint of a higher concentration observation. NAFO has used quantitative methods to objectively define areas that contain VME indicator species at or above significant concentration levels. These areas are not simply defined by the individual tows above the threshold value but also all of the smaller catches within the delimited polygon. These smaller catches may represent recruitment or smaller species in the VME indicator group. These larger areas **are** the VMEs proper unless post-hoc considerations suggest otherwise. VMEs occur throughout the NRA and their spatial arrangement may be important to recruitment processes and to overall ecosystem function.

New Predictive Models of Distribution for Erect Bryozoans and Sea Squirts (*Boltenia ovifera*)

Methods

Environmental data

A bathymetry layer covering the study area was produced by mosaicking the multibeam echosounder bathymetry (gridded to 75 m cell size) produced by the NEREIDA project with a bathymetry layer sourced from The Global Multi-Resolution Topography synthesis v3.6 (GMRT, 100 m grid downloaded 14/10/2019 from https://www.gmrt.org). GMRT is a multi-resolution compilation of bathymetric data compiled from multiple sources of gridded seafloor depth data (at a variety of scales) and multibeam swath bathymetry data contributed by the international science community and the 30 arc-second gridded General Bathymetric Chart of the Oceans (GEBCO) product merged into a single continuously updated compilation of global elevation data (Ryan et al., 2009). The combined bathymetry layer has a cell size of 250 m. The SAGA 'Fill sinks (Wang & Liu)' tool with a slope threshold of 0.005 was used to smooth out artefacts in the bathymetry before calculating a set of derivative layers describing terrain attributes (Wang and Liu, 2006).

SAGA GIS tools for QGIS (v. 3.2; Conrad et al., 2015) were used to calculate a set of **terrain variables** described below. Terrain variables can be divided into locally and regionally derived types. The local variables are calculated using a moving window neighbourhood and include geometric attributes such as slope. Regional variables represent attributes connected with hydrological properties (Olaya, 2009). Local terrain variables calculated include slope and Topographic Position Index (TPI). Slope was derived as degrees using a 5-cell neighbourhood. TPI was calculated with both 5 and 10-cell neighbourhoods.

The regional terrain variables calculated include Channel Network Base Level, Channel Network Distance, Valley Depth, Relative Slope Position, LS-Factor, Positive and Negative Openness and the Wind Exposition Index (Figure 1). The concept of the channel network base level (Figure 1) is used to distinguish topographic highs and lows. The approach uses the Digital Elevation Model (DEM) to create a channel network attributed with a Strahler order. Two channel networks with their associated terrain layers were created limiting channels to Strahler orders of three and five, respectively. The lower Strahler order channel network includes smaller 'streams', hence delineating finer topographic features. The channel network base level is an interpolated elevation surface connecting the channel elevations. The channel network distance is calculated as the vertical distance between the DEM elevation and the channel network base level elevation. Valley depth is calculated as the vertical distance to the lowest elevation of source flow. The LS-factor, a combination of slope length and steepness (gradient over the length), which predicts erosion potential in the terrestrial environment (Desmet and Govers, 1996), can also be applied in the marine context to reflect the potential stability of sediment deposits and hence the likelihood of exposed hard substrata. The relative slope position (Boehner and Selige, 2006), location along the entire length of a slope, can again be interpreted to represent different current conditions nearer the bottom or top of the slope.

Positive and negative topographic openness (Yokoyama et al., 2002) provide information on how prominent or sheltered an area is in relation to surrounding topography. Topographic openness was calculated using 8 directions. Similarly, the Wind Effect Index indicates to how exposed an area is (Boehner and Antonic, 2009). In the marine context, instead of wind the exposure relates to currents and tides. The topographic layers, their units of measure and the tools used to produce them are summarised in Table 5.

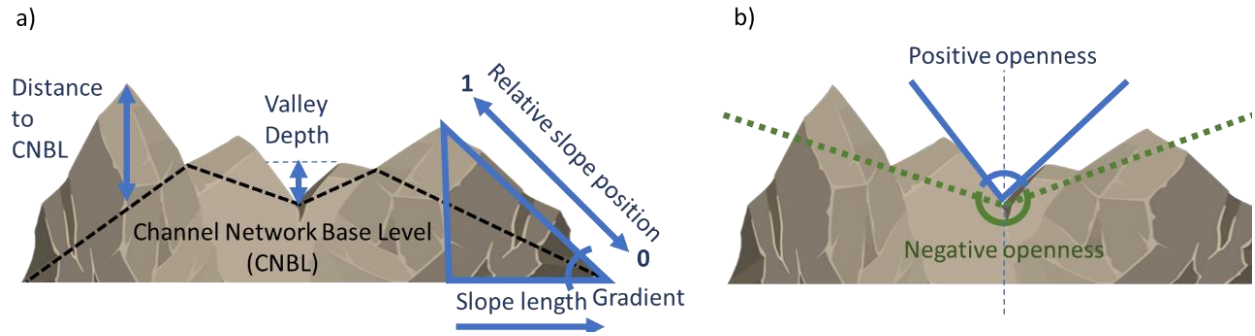

Figure 1. Derivation of topographic attributes from a DSM in relation to (a) channel network base level and (b) topographic openness.

Table 5. Description of topographic derivative layers calculated from MBES bathymetry.

Variable	Short name	Measure	SAGA for QGIS – Tool
Slope	SL	Radians	Basic terrain analysis
LS-factor	LSF	Index value	Basic terrain analysis
Channel Network Base Level (3/5)	CNBL3/5	Metres	Basic terrain analysis
Channel Network Distance (3/5)	CND3/5	Metres	Basic terrain analysis
Valley Depth (3/5)	VD3/5	Metres	Basic terrain analysis
Relative slope position (3/5)	RSP3/5	From 0 (bottom) to 1 (top)	Basic terrain analysis
Positive / Negative topographic openness	POP / NOP	Radians	Topographic openness
Wind Exposition Index	WEX	Sheltered < 1 > Exposed	Wind exposition index
Bathymetric Position Index (BPI, 5/10)	BPI5/10	Standardised index value	Topographic position index

In addition to the terrain variables, eleven water column variables, derived from different sources and with varying spatial resolutions, were used in the modelling (Table 6). The variables were chosen based on availability of data and assumed relevance to the taxa being modelled. They included measures associated with food supply, water mass and currents. Specific details on these variables are documented in Guijarro et al. (2016a).

Table 6. Water column variables used in the random forest models (Max: maximum; Min: minimum; MLD: mixed layer depth; SST: sea surface temperature; PP: primary production; BNAM: Bedford Institute of Oceanography North Atlantic model (Wang et al., 2017); RSU-BIO: Remote Sensing Unit at the Bedford Institute of Oceanography).

Variable	Short name	Unit	Native Resolution	Source
Max Annual MLD Oct-Dec	MLD12_ave_max	m	1/12th degree	BNAM
Max Annual MLD Apr-Jun	MLD46_ave_max	m	1/12th degree	BNAM
Max Annual SST	sst_av_max	°C	1/12th degree	BNAM
Max Annual Bottom Temperature	bt_av_max	°C	1/12th degree	BNAM
Max Annual Bottom Salinity	sal_av_max	N/A	1/12th degree	BNAM
Max Annual Bottom Current Velocity	cur_av_max	m s^{-1}	1/12th degree	BNAM
Mean Annual PP	ppa_mean	mg C m^{-2} day^{-1}	9 km	RSU-BIO
Max Annual PP	ppa_av_max	mg C m^{-2} day^{-1}	9 km	RSU-BIO
Min Annual Spring PP	pps_av_min	mg C m^{-2} day^{-1}	9 km	RSU-BIO
Max Annual Fall PP	ppf_av_max	mg C m^{-2} day^{-1}	9 km	RSU-BIO
Range of Annual Summer PP	ppsu_av_r	mg C m^{-2} day^{-1}	9 km	RSU-BIO

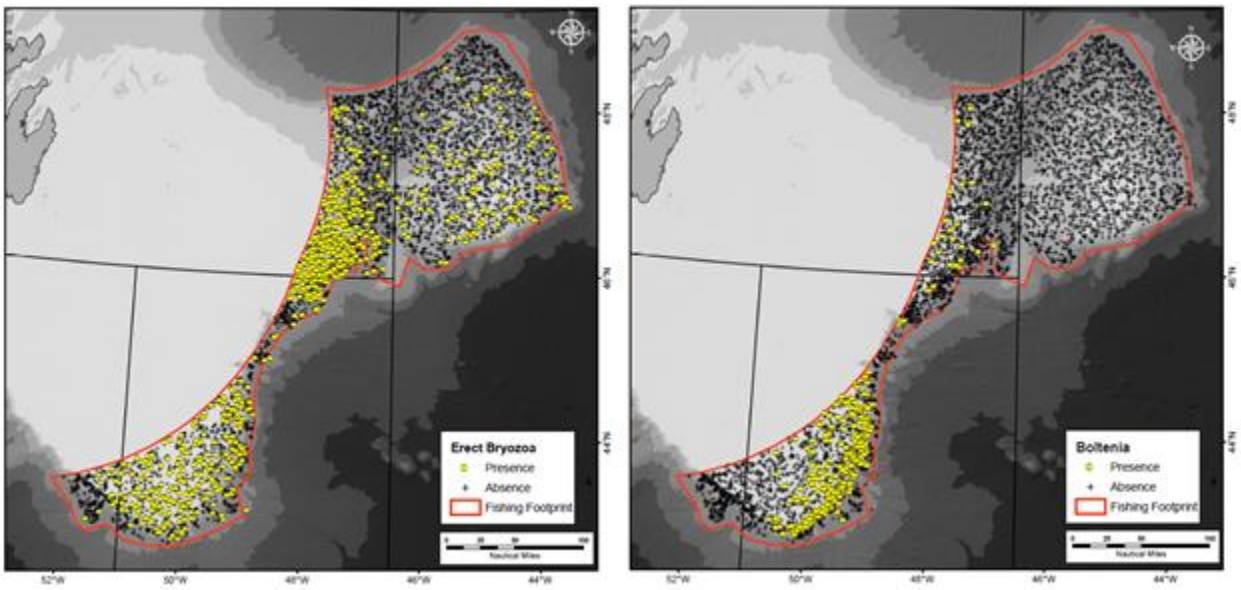

Figure 2. Location of scientific trawls and model extent (red outline, also the NAFO fishing footprint) showing presence/absence of Erect Bryozoans (left) and Sea Squirts (*Boltenia ovifera*) (right).

Biological data

Data on catches of Erect Bryozoans and Sea Squirts were obtained from survey trawls acquired during annual fishery surveys conducted by Fisheries and Oceans Canada and the European Union (Spain) between 2006 and 2019. The species composition of the sea squirt catch was composed of the stalked tunicate *Boltenia ovifera*, and so the SDM on that VME indicator conducted below is a model of that species. In contrast the catch of Erect Bryozoans is comprised of a number of species

with different distributions, not consistently or accurately identified at sea. This has implications for the performance and interpretation of the SDM for that taxon. The study area, delineated by the extent of the fishing footprint in the NAFO Regulatory Area Divisions 3L, 3M and 3N, contained 5863 and 6285 survey trawls with known presences and absences of Erect Bryozoans and *Boltenia ovifera*, respectively and full corresponding environmental data. Points that had null values for one or more of the environmental variables (26 erect bryozoan records; 36 sea squirt records) were excluded. Data points have a good geographic cover of the area (Figure 2).

Modelling approach

Models predicting the probability of presence for each species were built using classification Random Forest models. Random Forest is an ensemble method, where a large number of decision trees (typically 500-1000) are built using random subsets of the data. Regression trees are used for response variables consisting of continuous data and classification trees for factor variables. In the regression models predictions are based on averages from all trees (Breiman, 2001; Cutler et al., 2007). The models were built in the free statistical computing software R (v.3.5.1, R Development Core Team, 2018) using the 'randomForest' package (Liaw and Wiener, 2002). The models were run using the default settings of the randomForest function, using 1000 trees.

Preliminary predictor variable selection was done by applying an iterative permutation procedure testing the effect the removal of each variable in turn has on the decrease in mean internal model accuracy in comparison to randomised variables. The *boruta* algorithm in the 'Boruta' package in R (Kursa and Rudnicki, 2010) compares the importance of a variable as calculated by random forest to the importance of a random permutation of the same variables over several iterations. The variables included as predictors were further reduced by inspecting correlations among predictors and removing any variables that had a higher than 0.65 correlation score with another predictor. Out of a pair of highly correlated variables the one with a higher random forest importance score was retained in the model.

Models were validated using a bootstrap cross-validation procedure. For each response variable, the data was randomly subsampled 10 times into train and test data (80/20 split). Models were built using each train set and validation statistics calculated for each corresponding test dataset. A cross-validation approach, such as this, gives an average cross-validation score, but also an estimate of variability around the mean. The variability can be used as an indicator of the stability of the model fit, and to check for the arbitrary effects from subsetting data for training and testing a model. Accuracy measures used to validate the models included Sensitivity, Specificity, Kappa, and AUC, calculated using the 'PresenceAbsence' package (Freeman and Moisen, 2008). Final predictions were done with a full model including all available data and binary presence/absence maps were created by using a prevalence threshold.

Results and Discussion

The results from model cross-validation are shown in Table 7. Accuracy statistics for Erect Bryozoans indicate acceptable model performance, whilst the model for Sea Squirts (*Boltenia ovifera*) can be considered outstanding (Mandrekar, 2010). The reduced performance of the Erect Bryozoan model is likely due to the inclusion of multiple species with different niche requirements and the equal weight placed on low catches in the presence/absence model. The performance and applicability of the Erect Bryozoan model could potentially be improved by reducing the presences to catches above the threshold identified in the KDE analysis or by limiting the data to the continental shelf of the Grand Bank (<200 m) where the bryozoan species which form the dense aggregations (*Eucratea loricata*) is known to occur (Murillo et al., 2011b; 2016). WGESA concluded that the model for the Sea Squirts (*Boltenia ovifera*) could be used to modify the KDE polygons (see below). However, given the lower performance of the Erect Bryozoan model and its relatively low sensitivity and specificity,

WGESA suggested that it be considered as supporting information at this time until model improvements could be undertaken. As the predicted presence encompassed the KDE polygons for that VME this decision had no consequences to the delineation of the VME area.

Table 7. Mean and standard deviation of accuracy statistics for the 10 cross-validation runs for presence/absence Random Forest models for erect Bryozoans and Sea Squirts (*Boltenia ovifera*).

Accuracy Measure	Erect Bryozoans	Sea Squirts (*Boltenia ovifera*)
Sensitivity	0.70 (±0.02)	0.85 (±0.02)
Specificity	0.70 (±0.01)	0.86 (±0.01)
Kappa	0.24 (±0.02)	0.34 (±0.03)
AUC	0.77 (±0.01)	0.92 (±0.01)

The environmental variables with significant contributions to improving model accuracy and their importance in the model (measured by the mean decrease in node impurities (represented by the Gini index) from splitting on the variable) are shown in Table 8. The predictors included in the models covered a wide range of attributes from depth to variables describing water column conditions, such as temperature, salinity and mixed layer depth, to bottom current velocity, to primary productivity and variables describing the terrain attributes such as the LS-Factor, BPI and Relative Slope Position. Although the temperature and primary productivity variables had the highest contributions in both models, there were no large differences in the contributions of individual variables.

Table 8. Predictor variables (see Tables 5, 6) included in random forest models for Erect Bryozoans and Sea Squirts (*Boltenia ovifera*) and their contribution to each model. The values given in the table are the percentage contributions of each variable to total overall predictor importance measured by the mean decrease in node impurities (represented by the Gini index) from splitting on the variable. The highest five values for each taxon are highlighted in bold.

Predictor variable	Erect Bryozoans	Sea Squirts (*Boltenia ovifera*)
Depth	**8.0**	**9.6**
LS-Factor	6.5	7.8
BPI10	5.4	7.7
Relative Slope Position - Coarse	-	3.8
Relative Slope Position - Fine	2.8	-
Max Annual MLD Oct-Dec	7.1	-
Max Annual MLD Apr-Jun	-	**11.2**
Max Annual SST	**8.5**	-
Max Annual Bottom Temperature	7.6	**9.7**
Max Annual Bottom Salinity	7.7	8.4
Max Annual Bottom Current Velocity	7.2	7.5
Mean Annual PP	**9.3**	**9.2**
Max Annual PP	**8.5**	**9.0**
Min Annual Spring PP	6.1	8.2
Max Annual Fall PP	7.8	7.1
Range of Annual Summer PP	7.5	-

The model shows that *Boltenia ovifera* occurs on the edge of Grand Bank, mainly at depths above 500 m with a mixed layer depth around 15 m. Probability of presence increases towards the tops of slopes in areas of relatively steep terrain with high bottom currents (Figure 3.). The trends in the responses to primary production variables are more complicated to interpret. The mean of annual maximum primary production and the mean annual minimum spring primary productivity are high in areas with higher probability of *Boltenia ovifera* presence which is consistent with this species being a filter feeder. The trend for the mean of annual mean primary production and the mean of maximum fall primary production (Figure 3.3), on the other hand, shows low values.

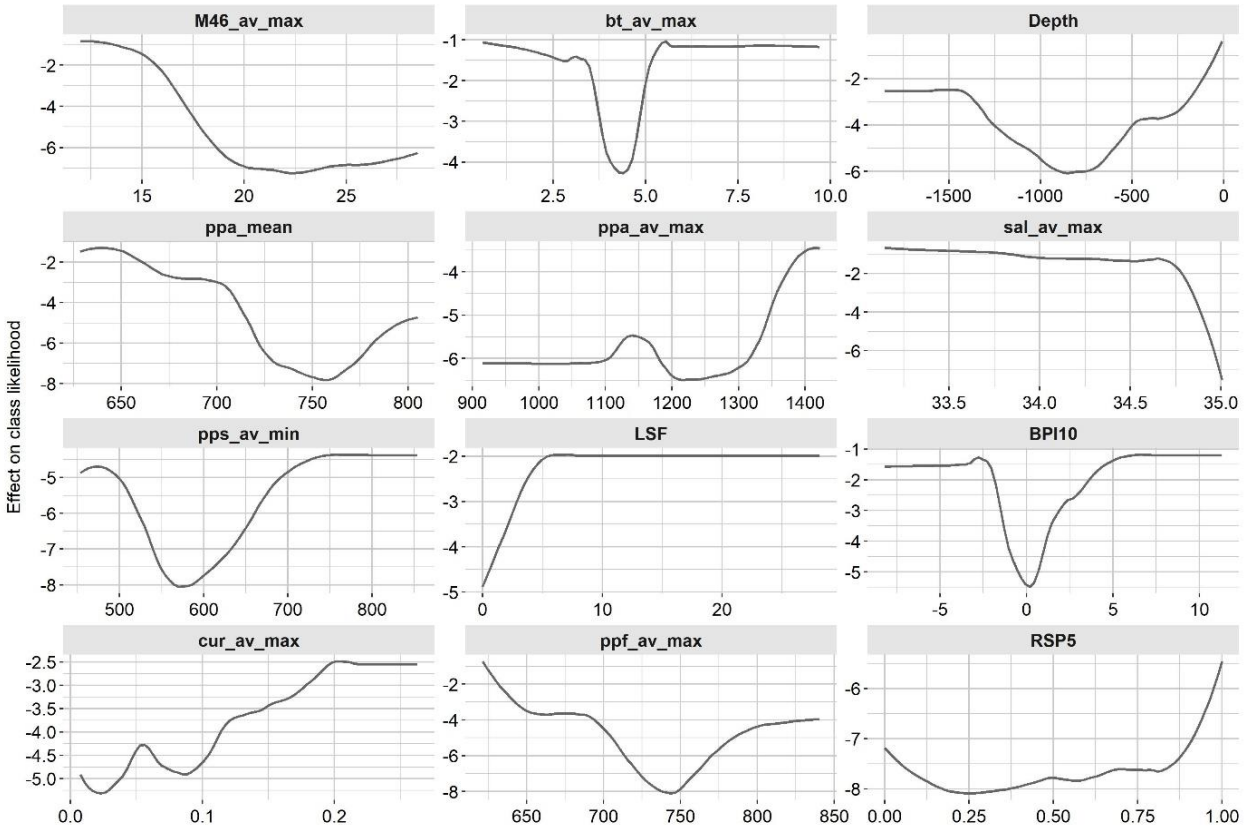

Figure 3. Response curves for the full random forest models for the Sea Squirt, *Boltenia ovifera*. Explanations of the variables are given in Tables 5 and 6.

The Erect Bryozoan model shows similar, although not as strong, trends towards steep topography and high bottom current conditions. Depth shows a more bimodal distribution, and predictions of high probability are present both on the top of Grand Bank in waters shallower than 500 m as well as on the continental slope in waters deeper than 1500 m. The same dichotomy is seen in high probabilities both mid-slope and on top of the slope, and in the mixed layer depth and the primary production variables (Figure 4). The bimodal trends suggest the presence observations combine two or more species of bryozoa with different habitat preferences. Bryozoa are not recorded at species level in the survey data, thus it is not possible to tease these apart.

The predictive surface for the Erect Bryozoans is shown in Figure 32 below and that for the Sea Squirts (*Boltenia ovifera*) in Figure 38.

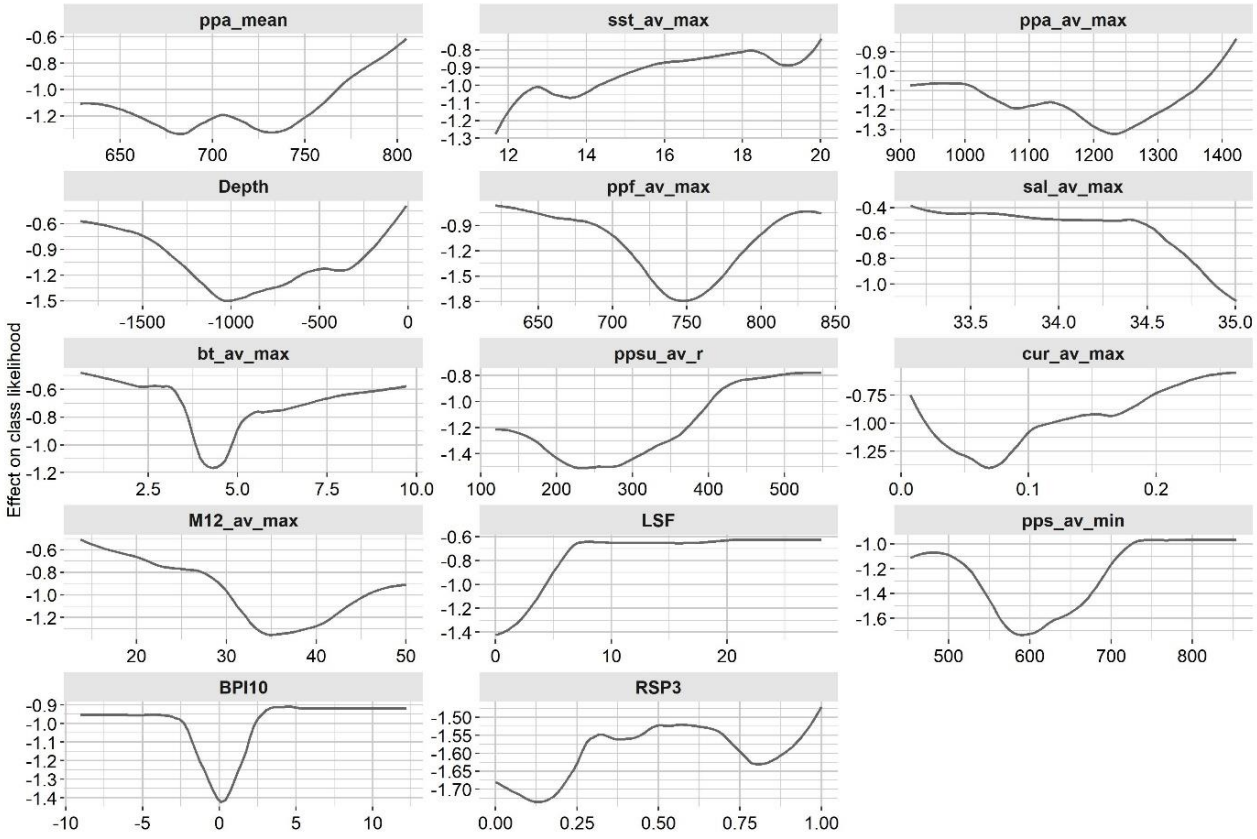

Figure 4. Response curves for the full random forest models for Erect Bryozoans. Explanations of the variables are given in Tables 5 and 6.

Review of Significant Concentrations of Large-sized Sponges

Significant concentrations of *Large-sized Sponges* have been determined previously in the NRA using kernel density analyses and an evaluation of the expansion of the area covered by successive density polygons (NAFO, 2013). These analyses have been updated using all available data from the RV trawl surveys. Specifically, data from the Spanish 3NO survey (2002-2019), EU Flemish Cap Survey (2003-2019), the Spanish 3L Survey (2003-2019) and the DFO-NL Multi-species Surveys (1995-2019) were assessed. These data sources yielded 4390 sponge records (975 from the Canadian surveys and 3415 from the EU-Spanish surveys); 1797 more data points than were available for the last analysis (NAFO, 2013). As noted previously, there were significant differences among the catch series for each survey and differences in the number of small catch weights, likely due to differences associated with gear type, tow length, survey area and sampling protocol. When all records less than 0.5 kg were removed, there was no significant difference among the catch distributions (NAFO, 2013). Therefore the analyses were performed on 1825 catches ≥ 0.5 kg (618 Canadian records and 1207 EU-Spanish records). Following previously established methods and assessment criteria, a kernel density surface was created and the area of successive density polygons calculated. KDE parameters were: Search Radius = 25 km; Contour Interval = 0.01; Cell size default = 3097.9 m. The biomass surface is shown in Figure 5 compared with the surface created from the 2013 analysis. The overall picture is the same and the largest density estimates are also very similar (~ 40 kg km^{-2}).

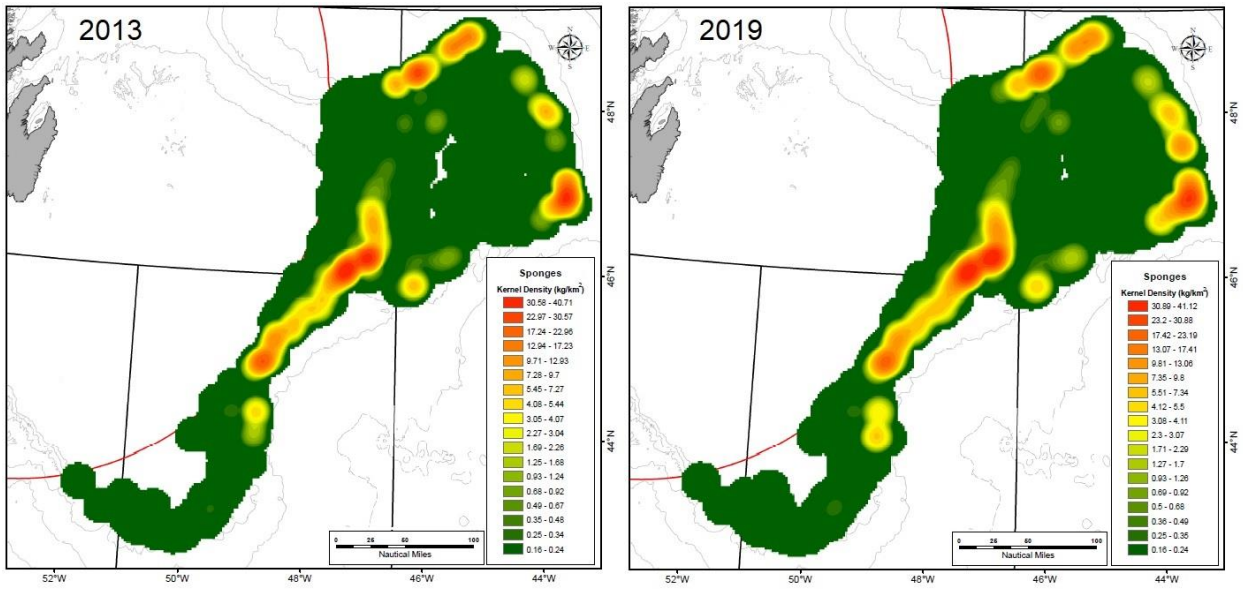

Figure 5. Kernel density biomass surface of sponges in the NAFO Regulatory Area. Left Panel: Surface created in 2013 for closed area assessments; Right Panel: Surface created in 2019 for current closed area re-assessments.

The kernel density distribution identified sponge grounds on the southern portion of Flemish Pass to southwestern Grand Bank, Beothuk Knoll, Sackville Spur and the east and southeast Flemish Cap (Figure 5). Following previously articulated procedures for identifying thresholds (NAFO, 2013), the 100 kg/RV tow density threshold emerged as defining significant concentrations of large-sized sponges (i.e., sponge ground VME) as it is the first catch level where there is a large increase in area once the initial sponge grounds are delineated (Table 9, Figure 6). The VME polygons established with this threshold cover an area of 27,314.6 km^2 and were determined by an additional 20 trawl set observations ≥ 100 kg (see Table 9).

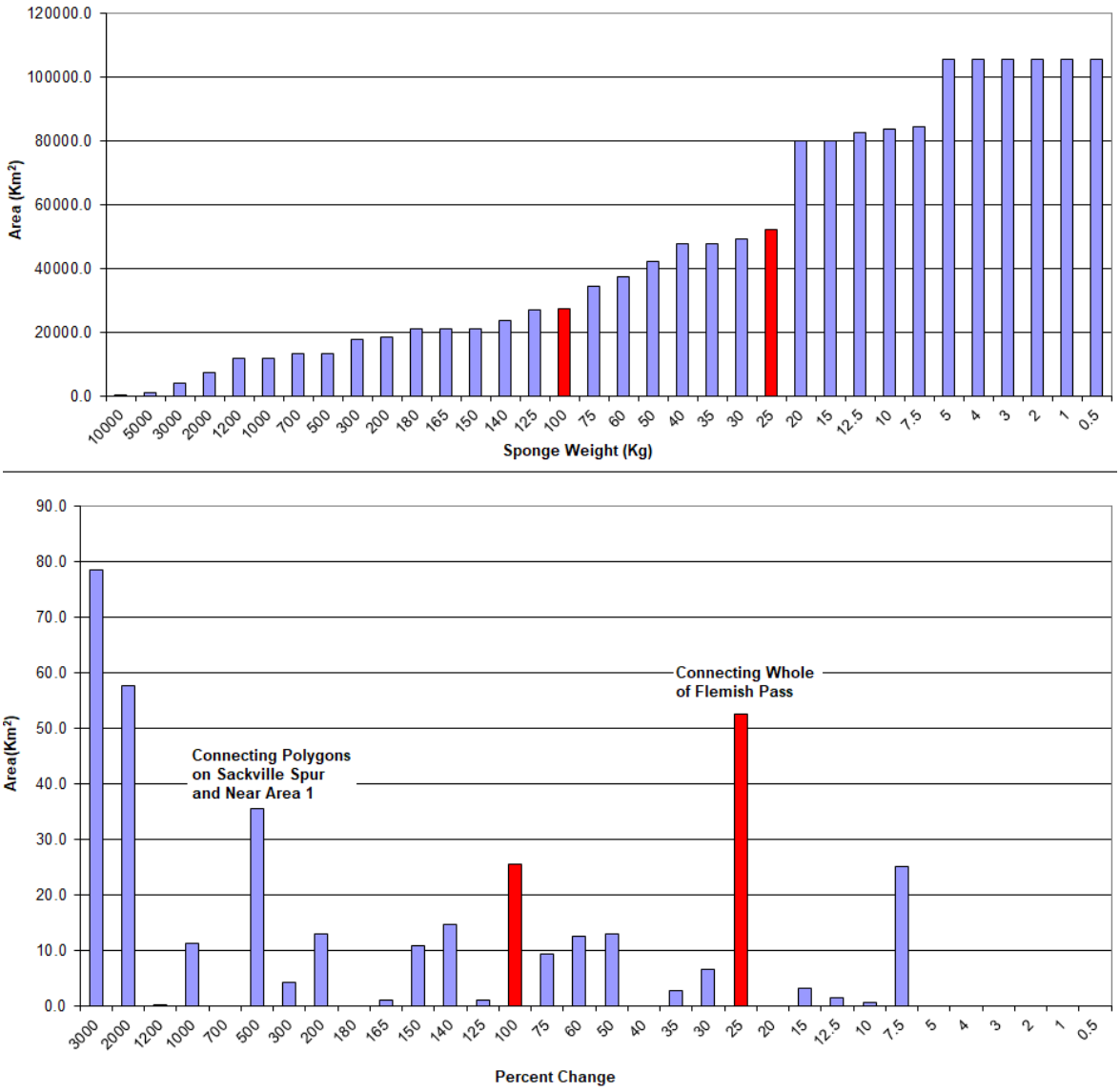

Figure 6. Bar graphs of the polygon area established by successively smaller research vessel sponge catch weight thresholds (upper panel) and of the percent change in area created between successively smaller research vessel catch weight thresholds (lower panel). Red bars indicate potential VME polygon thresholds examined.

Table 9. The number of points attributing to the delineation of sponge VME polygons based on successively smaller research vessel catch weight thresholds (kg). The area and number of observations used to define each polygon and the percent change in area and the number of additional observations between successive thresholds are provided. The shaded rows represent catch thresholds investigated as potential VMEs.

Sponge Catch Threshold (Kg)	Number of Observations in Polygon	Additional Observations Per Interval	Area of Polygon (km^2)	Percent Change in Area Between Successive Thresholds
10000	2		34.7	3234.6
5000	9	7	1156.2	262.2
3000	23	14	4187.5	78.6
2000	37	14	7480.5	57.7
1200	53	16	11797.6	0.2
1000	67	14	11821.7	11.3
700	83	16	13162.2	0.0
500	104	21	13162.2	35.6
300	128	24	17851.1	4.3
200	157	29	18619.6	13.0
180	163	6	21032.0	0.0
165	165	2	21032.0	1.0
150	168	3	21244.0	10.9
140	170	2	23564.6	14.6
125	175	18	27010.5	1.1
100	195	20	27314.6	25.6
75	214	19	34318.4	9.4
60	229	15	37554.3	12.5
50	248	19	42244.5	13.1
40	272	24	47758.6	0.0
35	288	16	47758.6	2.8
30	303	15	49087.6	6.7
25	325	22	52373.4	52.7
20	354	29	79952.9	0.0
15	403	49	79952.9	3.1
12.5	439	36	82450.8	1.5
10	505	66	83706.1	0.7
7.5	586	81	84269.4	25.2
5	726	140	105521.8	0.0
4	818	92	105521.8	0.0
3	933	115	105521.8	0.0
2	1116	183	105521.8	0.0
1	1435	319	105521.8	0.0
0.5	1778	343	105521.8	

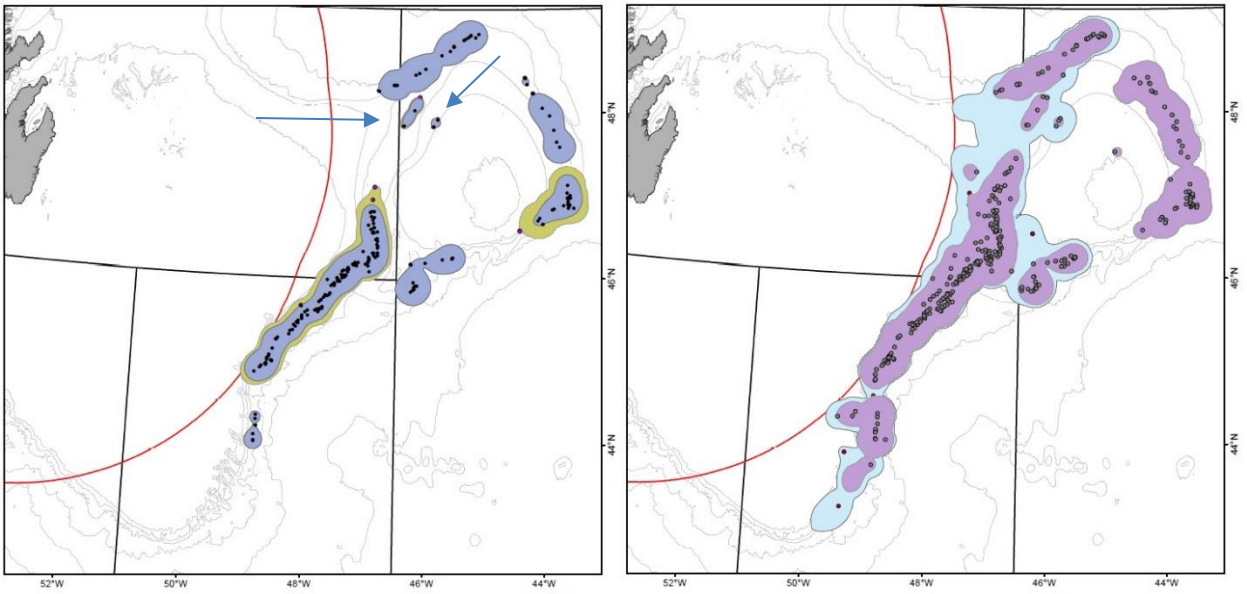

Figure 7. Comparison of the area covered by catches ≥ 100 kg (blue) and catches ≥ 75 kg (olive) (left panel); the area covered by catches ≥ 25 kg (purple) and catches ≥ 20 kg (blue) (right panel). The location of trawl sets ≥ the lowest threshold in each panel are shown. Arrows highlight small VME polygons discussed in the text.

Another potential threshold is 25 kg/RV tow (Table 9, Figure 6). However, this was created by connecting the whole of Flemish Pass including areas up on the shelf (Figure 7, right panel) which have different sponge composition than the *Geodia* grounds present on the slope. The 100 kg/RV tow catch threshold was therefore selected to define the VMEs. This threshold is larger than the 75 kg threshold value that was established previously (NAFO, 2009; NAFO, 2013). This is not surprising given the 6 years of data added to the analyses. In fact, in 2009, using a combination of KDE and the cumulative catch weight curve, the threshold was identified between 75 and 125 kg, indicating consistency between years and methodologies. When superimposed on the 2019 kernel density surface (Figure 7), the 100 kg density polygon captures all of the high density areas from the kernel analysis (Figure 5, right panel).

Figure 8 compares the sponge VME polygons created in the current analysis using the 100 kg threshold with the VME polygons established previously with the 75 kg threshold (NAFO, 2013). The VME areas are very similar and identical in some instances. The 2019 polygons near Area 2 in Flemish Pass are somewhat smaller and it can be seen that the difference between the two analyses is largely created to the north of the polygons where the previous boundary was determined by a single data point. Examination of the 2019 data shows that the gap is occupied by sponge catches, but they are all less than 100 kg (not shown). However, as this zone is within the closed area, this change is not likely due to thinning of the sponge habitat by fishing. Further to the south on the slope of the Tail of Grand Bank, 2019 data around Area 1 redistributes the polygon size from the previous analysis. The area to the north is reduced while the area to the south is expanded (Figure 8 arrow). On Sackville Spur (Area 6) the 2019 analysis connects the three separate polygons from the 2013 analyses. A similar joining of polygons is seen in Area 5.

In the northwestern part of the Flemish Cap, around 1200 m depth, three isolated catches are present (Figure 8, see arrows). They are surrounded by lower catches (Figure 9), and in some cases include species characteristic of *Geodia* grounds. Another sponge VME is located south of the Sackville Spur closed area (Area 6) in what appears to be a lightly fished area (Figure 8). This is a small area, but it can have special environmental or physical conditions enhancing sponge biomass, that could

constitute VMEs. To the southeast of that polygon, there is an area with only two significant catches (Figures 7, 9). These likely have another sponge species composition, which may include *Asconema foliata*, also a VME indicator taxon which has been shown to increase biodiversity. On the eastern slope of the Flemish Cap there is another isolated area which seems to belong to the same sponge VME defined to the north and it is included in the Closed Area 5. Although the smaller polygons may represent small contributions to the total sponge biomass in the NRA, these areas may represent important habitat features and therefore are considered VME based on the criteria previously accepted by NAFO. Gaps in the distribution, which set these smaller polygons apart, may be the result of limited data coverage from the surveys or from previous fishing activity.

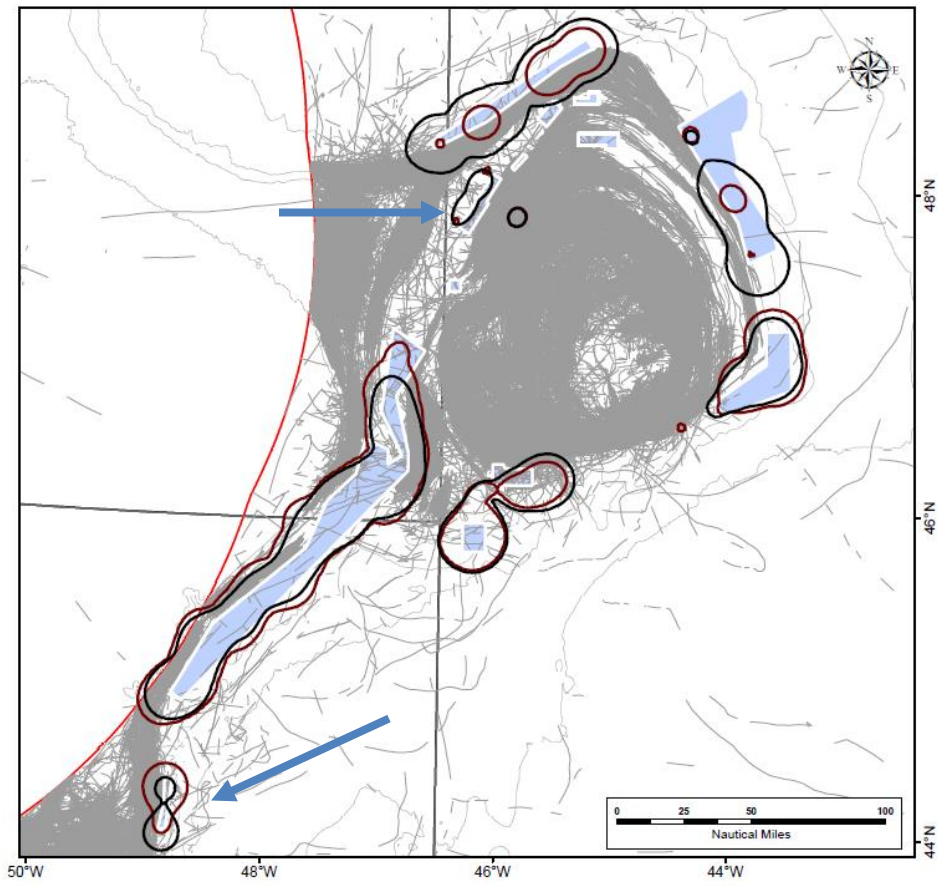

Figure 8. Comparison of the 2019 sponge VME polygons using the 100 kg threshold (black outline) with the sponge VME polygons established previously with the 75 kg threshold (red outline) (NAFO, 2013). Closed areas are outlined in white with blue shading. VMS tracks from 2009-2018 are shown in grey. Arrows indicates VME polygons on the Tail of Grand Bank and south of Area 6 (Sackville Spur) discussed in the text.

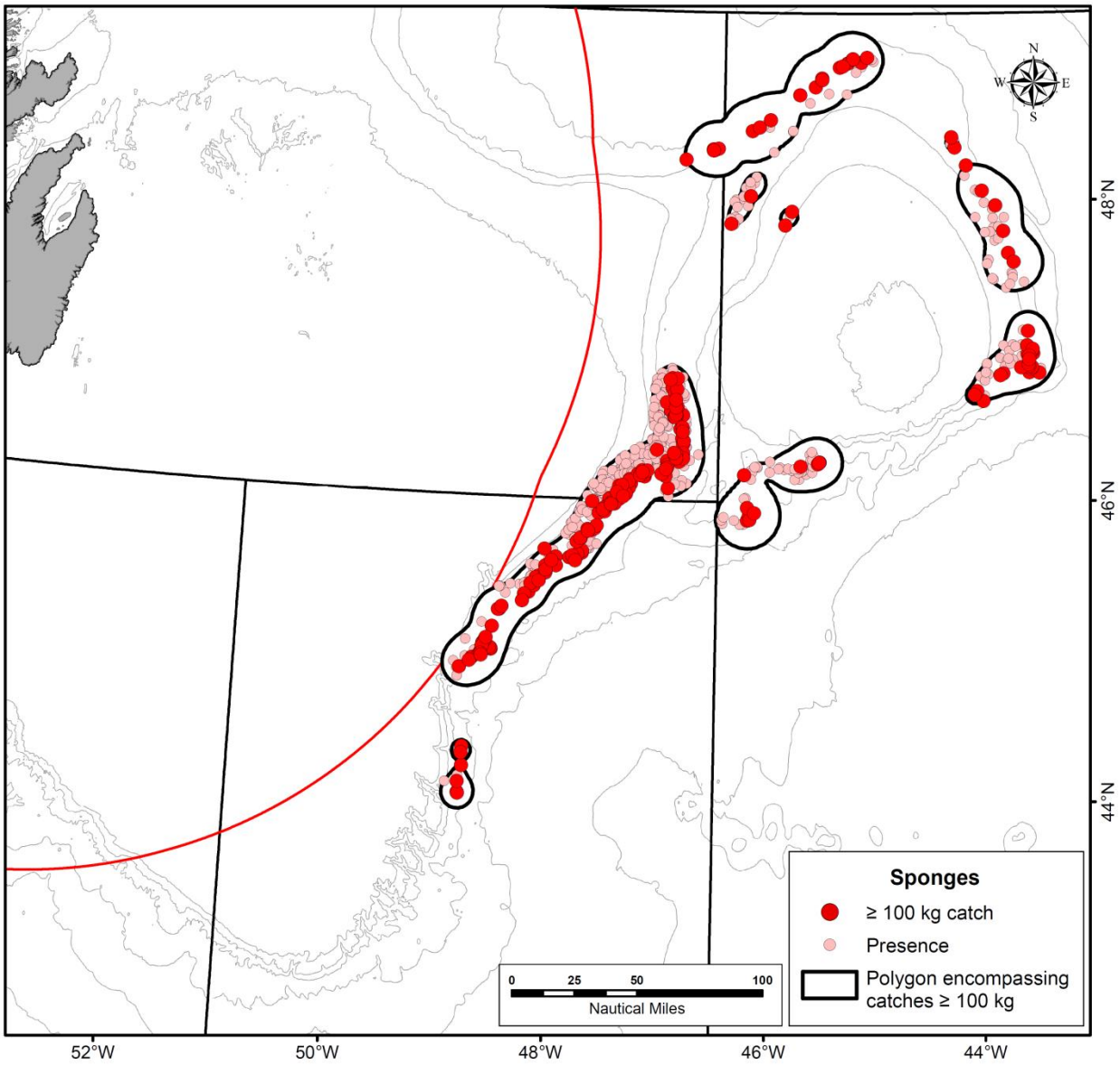

Figure 9. Illustration of the sponge VME polygons (black outline), catches ≥ 100 kg (solid red circles) and catches within the VME polygons but at lower catch weights (solid pink circles).

Modified VME Polygon Boundaries for Large-sized Sponges

Following previously established procedures (NAFO, 2015) the KDE polygons determined above were overlain on species distribution models and trimmed in some instances using the prevalence threshold for sponge grounds (Knudby et al., 2013a) to guide the process. Areas 1 and 3 were entirely within the predicted distributions and so were not trimmed further. Areas 2, 4, 5 and 6 were modified as follows:

Area 2. The 2019 KDE polygon was trimmed in the northern part and along the western boundary (Figure 10, left panel). However, there was a new significant catch outside the previous polygon in the northeast and therefore the boundary was made larger around that area than the boundary from the earlier analysis (NAFO, 2015).

Area 4. The KDE polygon was trimmed (Figure 10, right panel) to the same western boundary as done previously (NAFO, 2015).

Area 5. Area 5 was not trimmed in 2014 (NAFO, 2015). However, the 2019 KDE polygon is larger than that of the 2013 analysis (NAFO, 2013) and extends into shallower water where the sponge grounds are not predicted to occur. The new significant catches are aligned in bathymetry with the previous ones and all are inside the closed areas (Figure 11, left panel). The modified KDE polygon follows the prevalence boundary, leaving some buffer outside the closure in some areas of its length along the shallower boundary (Figure 11, left panel).

Area 6. Area 6 was not trimmed in 2015 (NAFO, 2015). However, as for Area 5, the new 2019 KDE polygon is larger than the previous one (Figure 11, right panel). The bathymetric contour and prevalence map were used to modify the shallow boundary of the 2019 polygon.

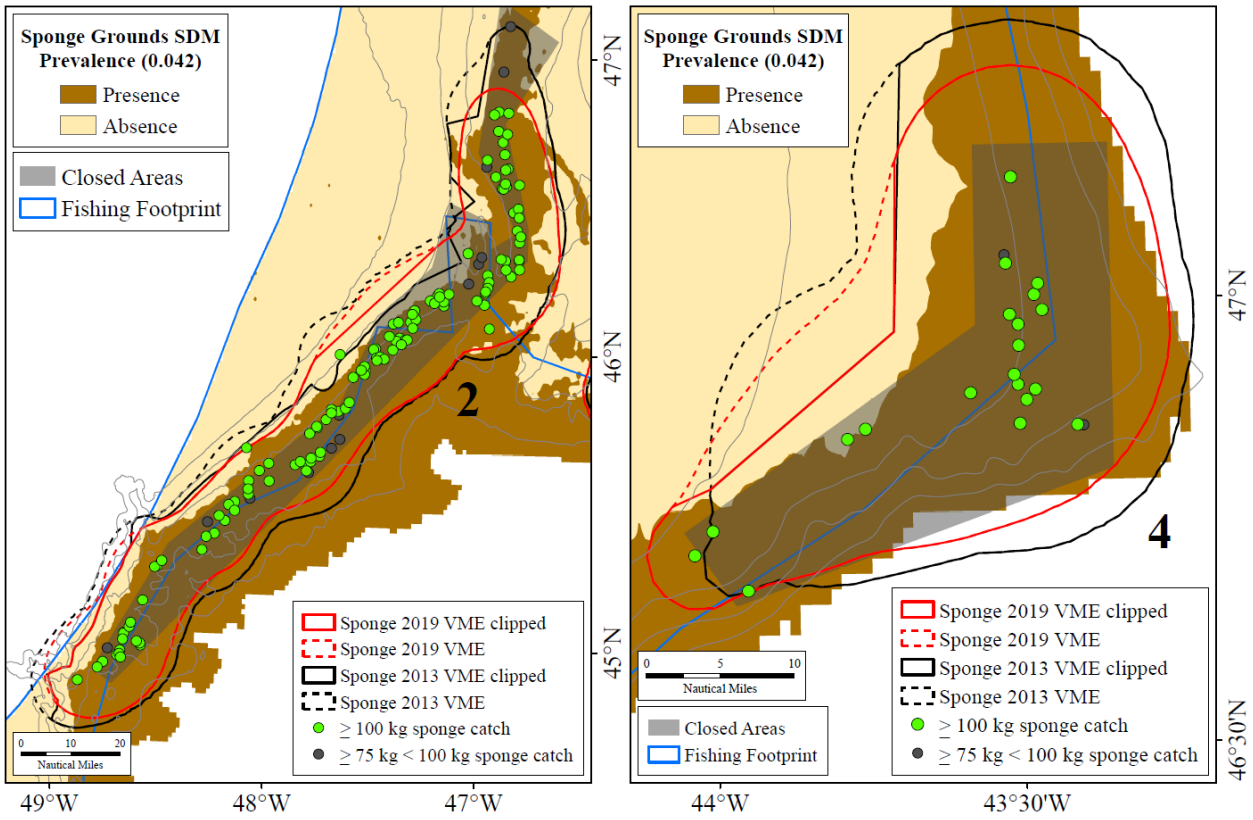

Figure 10. Illustration of the modification (solid red line) of the 2019 KDE polygon (red dashed lines) for Area 2 (left panel) and Area 4 (right panel) in relation to previous modifications (solid black line) and KDE polygons (black dashed lines) and showing the underlying SDM prevalence map (brown area showing predicted presence of sponge grounds). Closed areas are indicated in grey shading. Catches of ≥ 75 kg but < 100 kg are shown in dark grey as they were considered above the threshold in the 2013 analysis (NAFO, 2013).

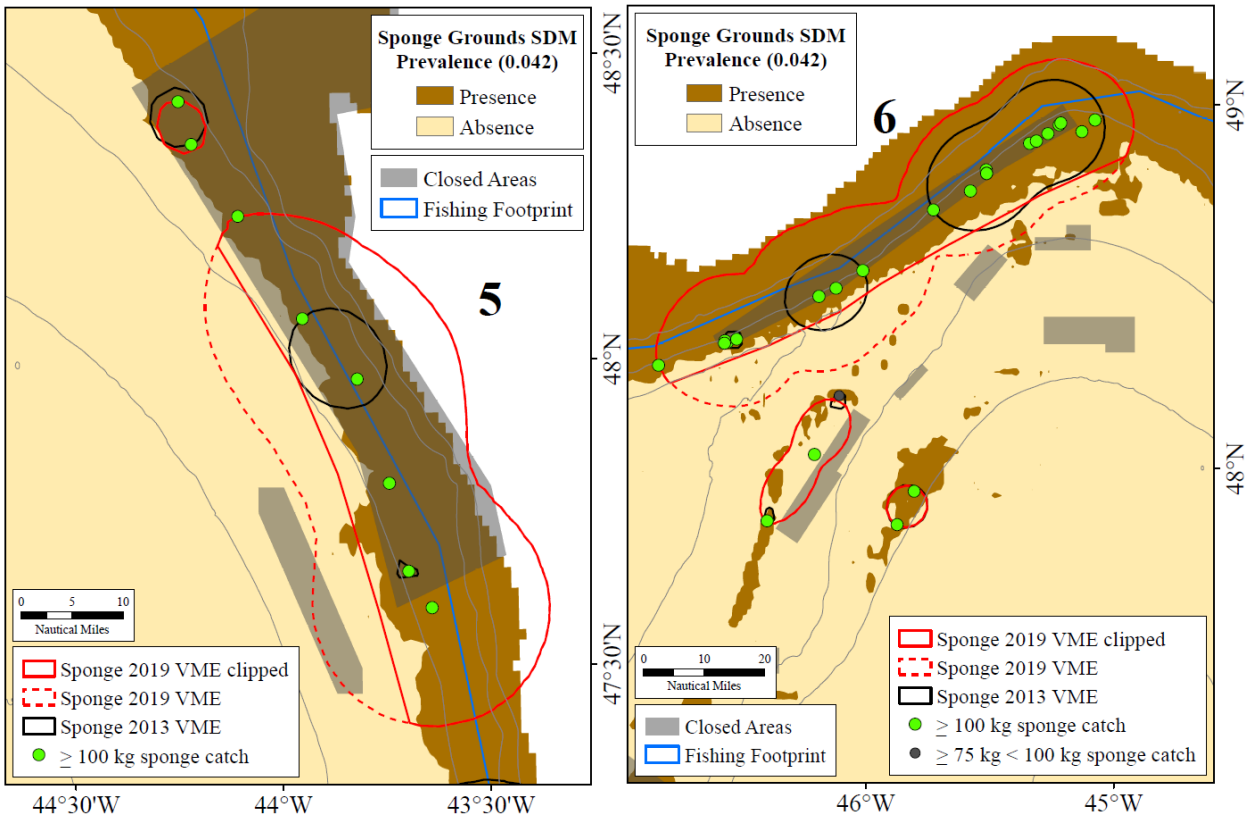

Figure 11. Illustration of the modification (solid red line) of the 2019 KDE polygon (red dashed lines) for Area 5 (left panel) and Area 6 (right panel) in relation to previous modifications (solid black line) and KDE polygons (black dashed lines) and showing the underlying SDM prevalence map (brown area showing predicted presence of sponge grounds). Closed areas are indicated in grey shading. Catches of ≥ 75 kg but < 100 kg are shown in dark grey as they were considered above the threshold in the 2013 analysis (NAFO, 2013).

Review of Significant Concentrations of Sea Pens

Significant concentrations of *Sea Pens* have been identified previously in the NRA using kernel density analyses and an evaluation of the expansion of the area covered by successive density polygons (NAFO, 2013; 2017). These analyses have been updated using all available data from the RV trawl surveys. Specifically, data from the Spanish 3NO survey (2002-2019), EU Flemish Cap Survey (2003-2019), the Spanish 3L Survey (2003-2019) and the DFO-NL Multi-species Surveys (1995-2019) were assessed. As for sponges, there were significant differences among the catch series for each survey with the Campelen catches being more similar to one another than to the Lofoten catches (NAFO, 2013). These dissimilarities were driven by differences in the number of small catch weights. When all records less than 0.2 kg were removed, there was no significant difference among the catch distributions. Therefore, as for previous analyses, the 2019 analyses were performed on catches ≥ 0.2 kg (376 catch records, 54 Canadian records and 430 EU-Spanish records), which included 114 additional observations over the 2013 analysis. Following previously established methods and assessment criteria, a kernel density surface was created and the area of successive density polygons calculated (NAFO, 2013). KDE parameters were: Search Radius = 21.6 km; Contour Interval = 0.00005; Cell size default = 2589.39 m.

The 2019 KDE biomass surface differs from the 2013 KDE surface (NAFO, 2013) (Figure 12), with the same general areas being shown but with steeper gradients between the high and low density

areas around areas of high concentration.

The large increase in area (Table 10, Figure 13) observed when comparing the area captured with catches ≥ 1.3 kg and ≥ 1.2 kg clearly establishes the threshold of 1.3 kg for the sea pen VME. The biomass surface is shown in Figure 14 along with the KDE polygons established with catches ≥ 1.3 kg and ≥ 1.2 kg, illustrating the increase in area in going from the former to the latter. The equivalent threshold established in 2017 (NAFO, 2017) was 1.4 kg and as shown in Figure 15; there is little to no change in the KDE polygons from the previous analysis with the exception of one VME on the Tail of Grand Bank in 3N, which is larger in the 2019 analysis (Figure 15) (NAFO, 2017). The location of catches ≥ 1.3 kg and smaller catches within the KDE polygons is shown in Figure 16. Most of the areas have smaller catches associated with the VME and in part represent different species mixes (NAFO, 2013).

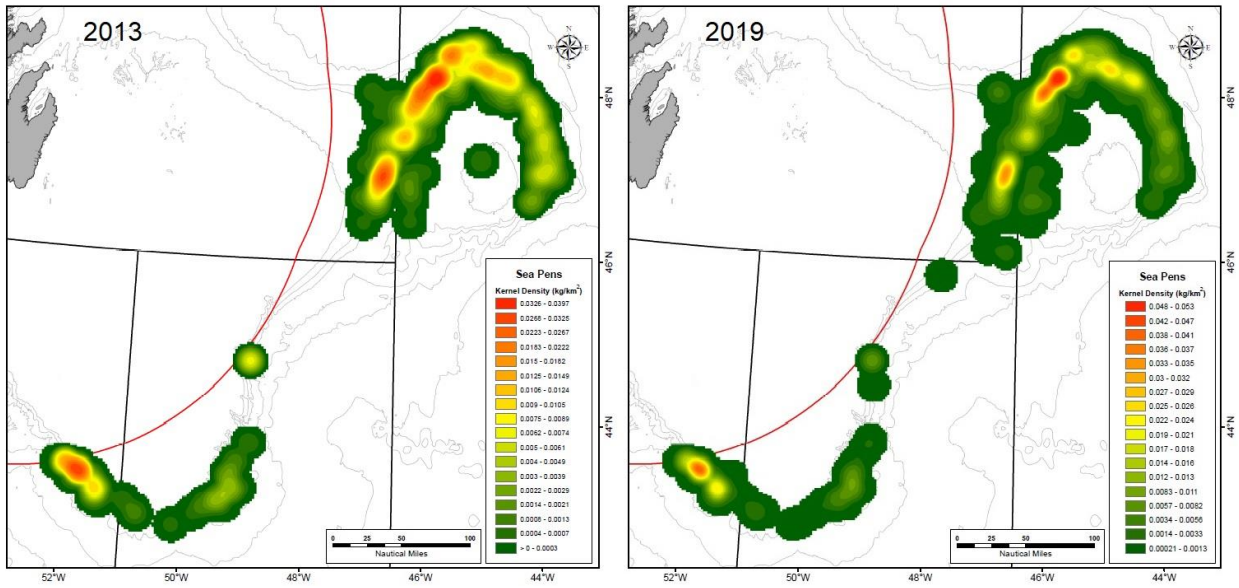

Figure 12. Kernel density biomass surface of sea pens in the NAFO Regulatory Area. Left Panel: Surface created in 2013 for closed area assessments; Right Panel: Surface created in 2019 for current closed area re-assessments.

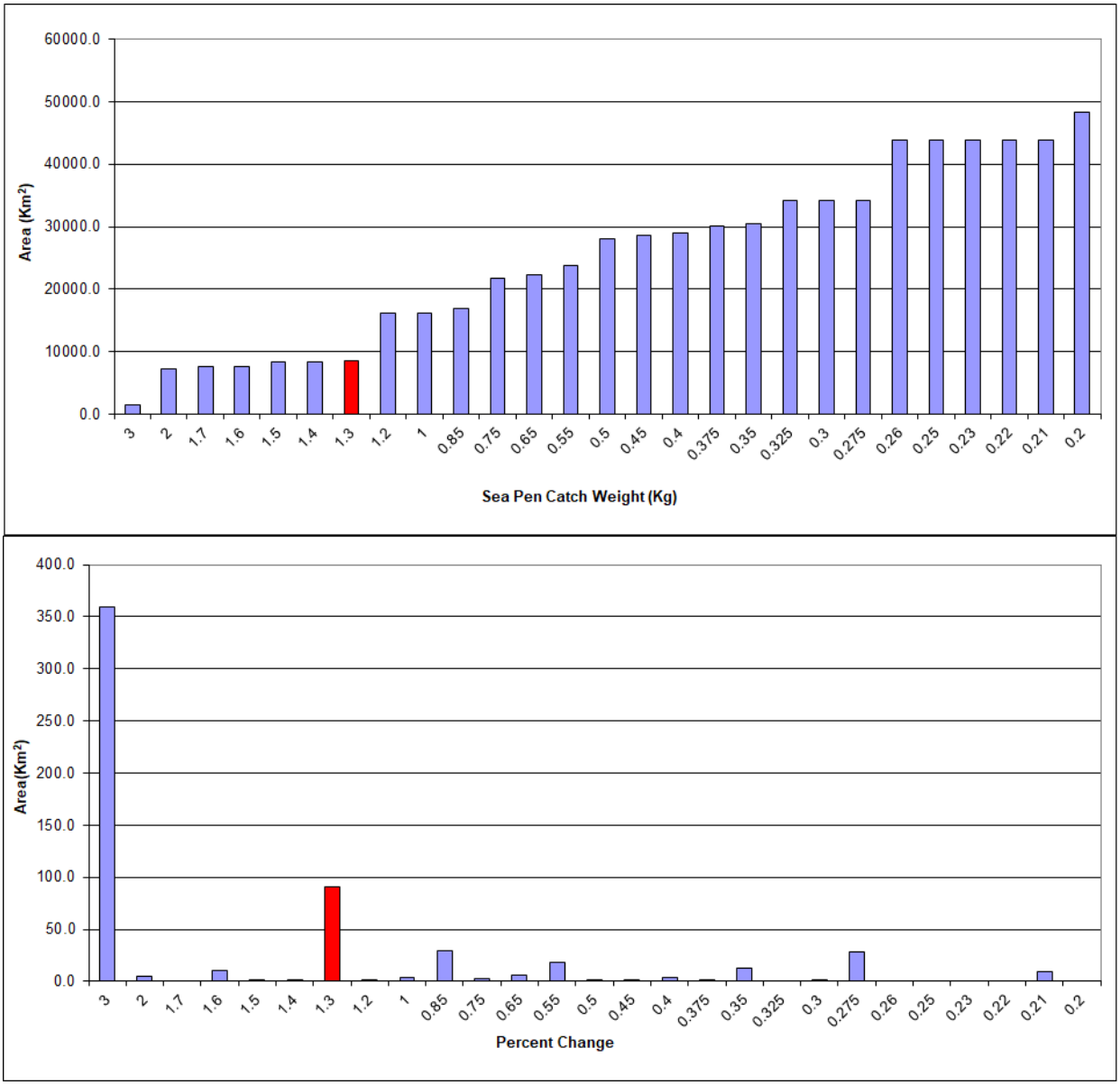

Figure 13. Bar graphs of the polygon area established by successively smaller research vessel sea pen catch weight thresholds (upper panel) and of the percent change in area created between successively smaller research vessel catch weight thresholds (lower panel). The red bar indicates the potential VME polygon threshold.

Table 10. The number of points attributing to the delineation of sea pen VME polygons based on successively smaller research vessel sea pen catch weight thresholds (kg). The area and number of observations used to define each polygon and the percent change in area and the number of additional observations between successive thresholds are provided. The shaded row represents the threshold used to define the VMEs.

Sea Pen Catch Threshold (Kg)	Number of Observations in Polygon	Additional Observations Per Interval	Area of Polygon (km^2)	Percent Change in Area Between Successive Thresholds
3	12		1597.7	359.4
2	22	10	7340.7	4.7
1.7	33	11	7686.7	0.0
1.6	35	2	7686.7	10.3
1.5	43	8	8477.2	0.1
1.4	46	3	8484.0	0.2
1.3	50	4	8497.6	90.6
1.2	56	6	16193.2	0.3
1	75	19	16239.2	4.0
0.85	93	18	16887.1	29.2
0.75	107	14	21820.0	2.5
0.65	126	19	22374.6	6.3
0.55	142	16	23774.4	18.0
0.5	159	17	28042.0	2.0
0.45	175	16	28607.4	1.5
0.4	199	24	29039.3	3.8
0.375	214	15	30134.8	0.9
0.35	239	25	30395.2	12.4
0.325	262	23	34163.2	0.0
0.3	283	21	34163.2	0.2
0.275	302	19	34247.9	28.2
0.26	326	24	43921.7	0.0
0.25	350	24	43921.7	0.0
0.23	374	24	43921.7	0.0
0.22	390	16	43921.7	0.0
0.21	407	17	43921.7	9.8
0.2	430	23	48224.0	

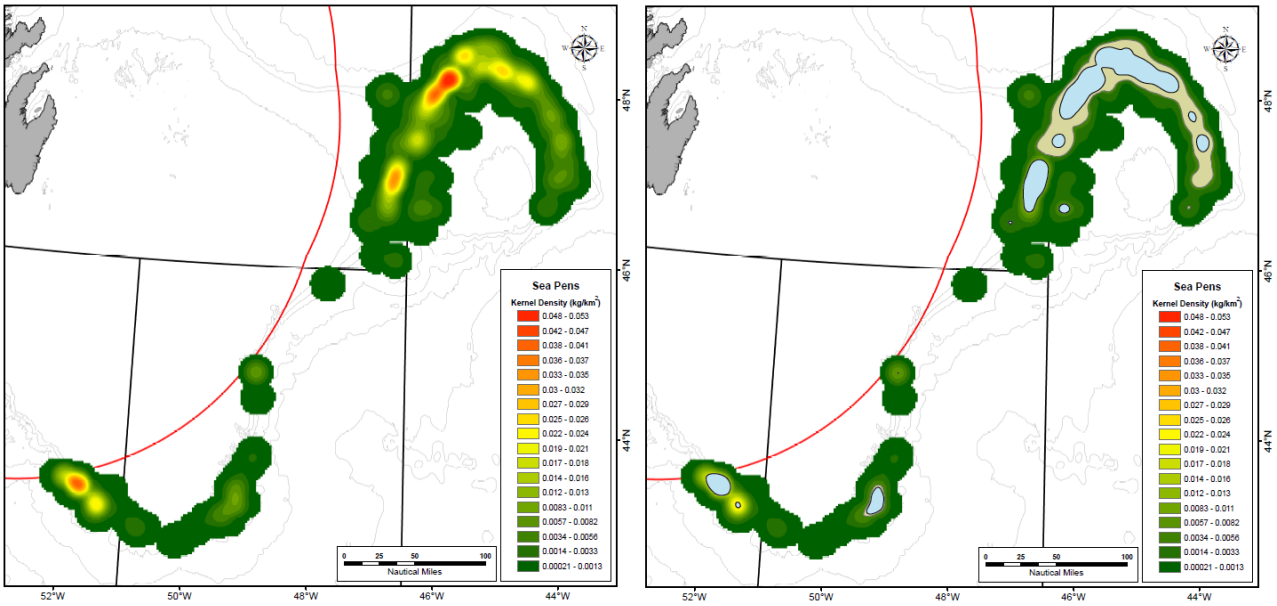

Figure 14. Left panel: The 2019 kernel density distribution of sea pens in the NAFO Regulatory Area. The green areas represent low sea pen densities while the red areas indicate high sea pen densities. Right panel: Comparison of the area covered by catches ≥ 1.3 kg (blue) and catches ≥ 1.2 kg (olive). The blue areas indicate the sea pen VMEs.

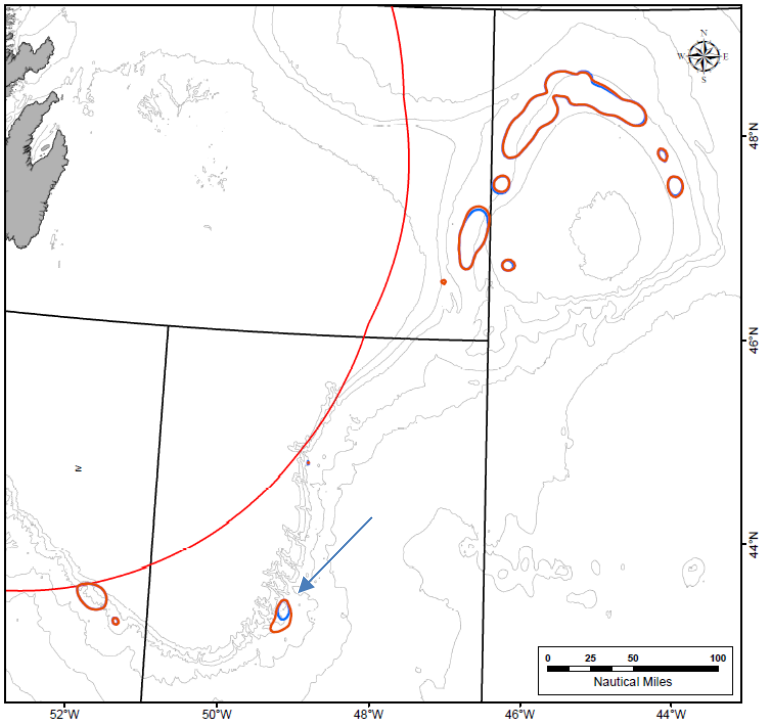

Figure 15. Comparison of the 2019 sea pen VME polygons using the 1.3 kg threshold (orange outline) with the sea pen VME polygons established previously with the 1.4 kg threshold (blue outline) (NAFO, 2017). All polygons completely overlap except for the polygon on the southeast slope of the Tail of Grand Bank (indicated by the arrow).

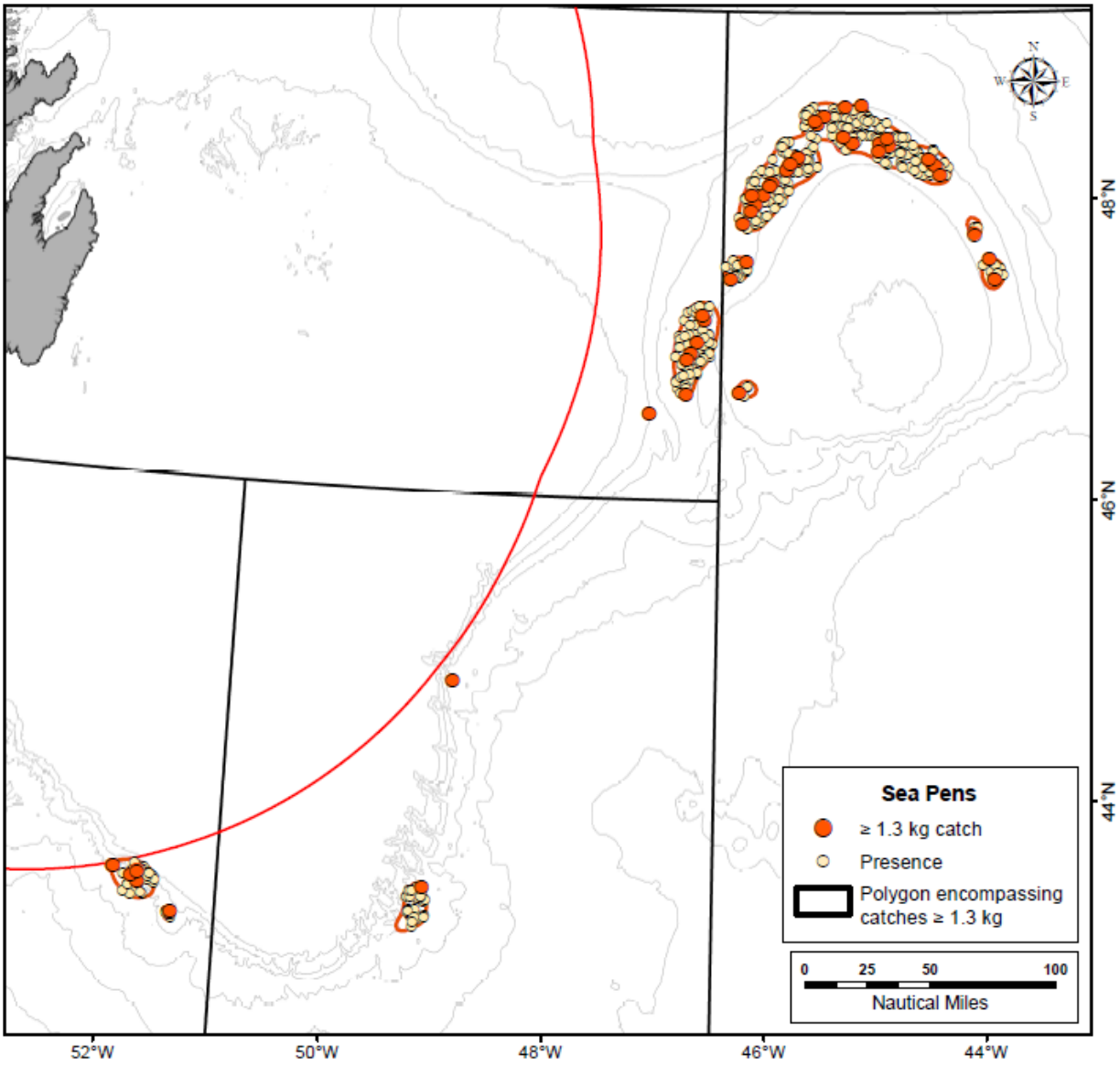

Figure 16. Illustration of the 2019 sea pen VME polygons (orange outline), catches ≥ 1.3 kg (solid orange circles) and catches within the VME polygon but at lower catch weights (solid light orange circles).

Modified VME Polygon Boundaries for Sea Pens

The 2019 sea pen KDE polygons were overlain on the presence-absence prevalence threshold from the sea pen SDM (Knudby et al., 2013c) that was used previously to evaluate whether the KDE polygons should be modified (NAFO, 2015). Most of the KDE area falls within the area of predicted presence (Figure 17), and consequently no modifications were made to the KDE polygons.

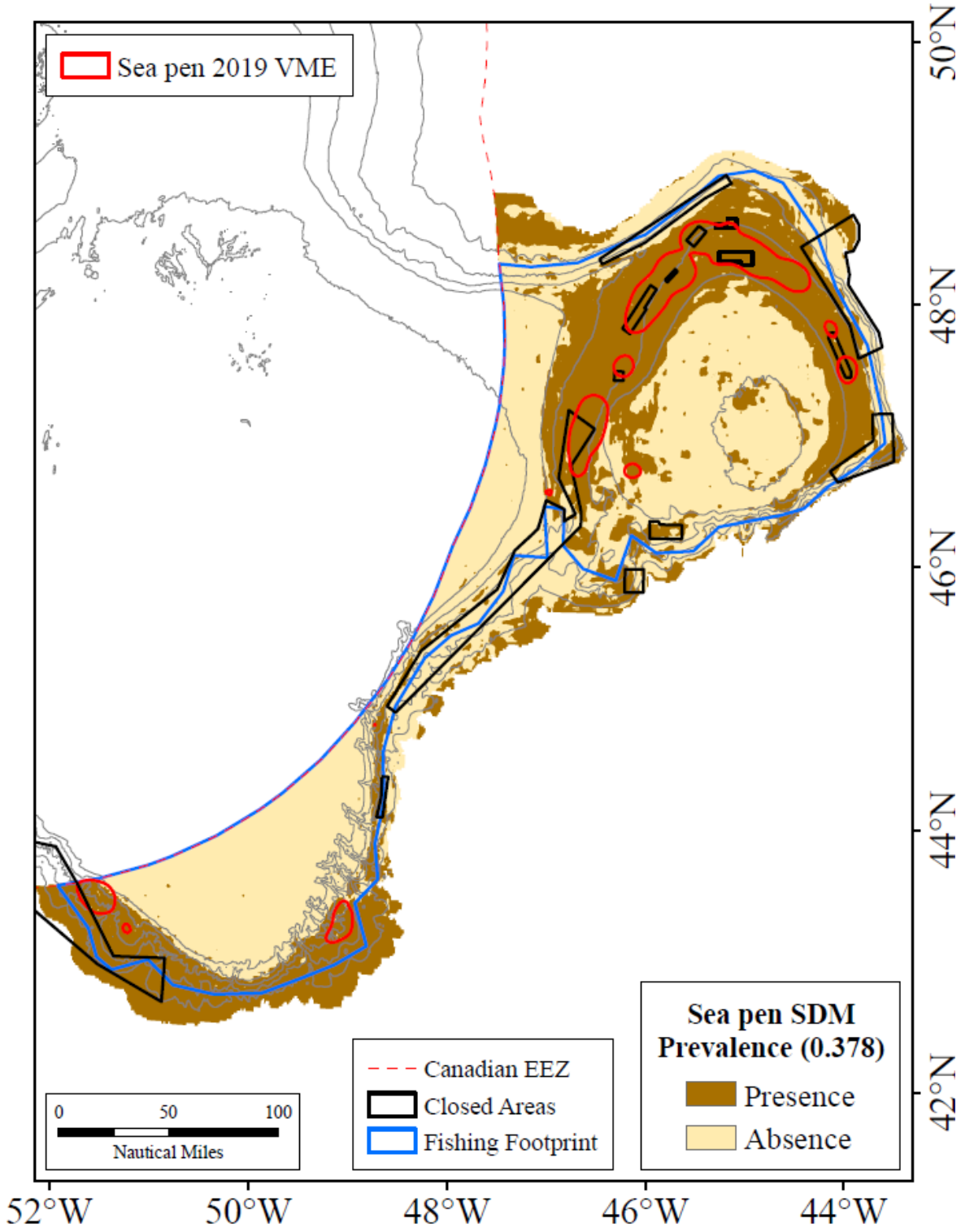

Figure 17. Position of the sea pen KDE polygons in relation to the sea pen SDM prevalence map (Knudby et al., 2013c). The 2019 KDE polygons (red outline) fall within the predicted presence (brown areas) of these species and so there was no need to modify them. Closed areas are outlined in black. The fishing footprint is outlined in blue.

Review of Significant Concentrations of Small Gorgonian Corals

Significant concentrations of *Small Gorgonian Corals* have been determined previously in the NRA using kernel density analyses. As for sponges and sea pens, there were significant differences among the catch series for each survey (NAFO, 2013). However, unlike those VME indicators, previously there was no weight threshold above which these differences were non-significant until the 0.1 kg threshold was reached, at which there were insufficient data to perform the analyses (NAFO, 2013). Consequently separate analyses were run for Divisions 3NO and for Division 3M in order to maximize the amount of data that could be used (NAFO, 2013). The data for 3M included mostly small catches that were not highly aggregated and no clear threshold emerged with sufficient support (Kenchington et al., 2014) so were not reported further. However, with the additional data that has been collected since the 2013 assessment the catches can be combined across divisions for biomass values ≥ 0.02 kg (Table 11). In total 218 records were available for the assessment (62 from Canada and 156 from EU-Spain).

Table 11. Nonparametric statistical tests (Kolmogorov–Smirnov (K-S) statistic) for the equality of the small gorgonian coral catch distributions obtained with different trawl gears (Campelen and Lofoten) and with different tow duration for the Campelen gear.

Comparison Groups	Data (Source)	P- value (K-S test)
Campelen 15 min trawl vs. Campelen 30 min trawl	> 0 kg (N_{Canada}= 106, $N_{EU\text{-}Spain}$ = 337)	< 0.001
	≥ 0.01 kg (N_{Canada} = 102, $N_{EU\text{-}Spain}$ = 159)	< 0.001
	≥ 0.02 kg (N_{Canada} = 62, $N_{EU\text{-}Spain}$ = 104)	0.1285
Combined Campelen trawls vs. Lofoten trawl	≥ 0.02 kg ($N_{Campelen}$= 166, $N_{Lofoten}$ = 52)	0.2218

Following previously established methods and assessment criteria, a kernel density surface was created (Figure 18) and the area of successive density polygons calculated (Table 12, Figure 19). KDE parameters were: Search Radius = 22.1 km; Contour Interval = 0.0000025; Cell size default = 2656.7 m. The default Search Radius was larger in 2019 (previously 12.5 km in 2013) due to the increased spatial extent of the analyses.

The threshold that emerged from the 2019 analysis is ≥ 0.2 kg/tow (Table 12, Figures 19, 20). However there are two areas that are found on Flemish Cap with the ≥ 0.15 kg/tow threshold (Figure 20). The procedures for selecting the appropriate threshold would normally accept the ≥ 0.15 kg/tow threshold as the analysis is identifying new areas. However, in doing that, the merging of the ≥ 0.2 kg/tow areas on the Tail of Grand Bank based on only a few data points would result. Consequently in this particular case we recommend the ≥ 0.2 kg/tow threshold but highlight the potential for small gorgonian coral VME habitat on Flemish Cap from the ≥ 0.15 kg/tow threshold.

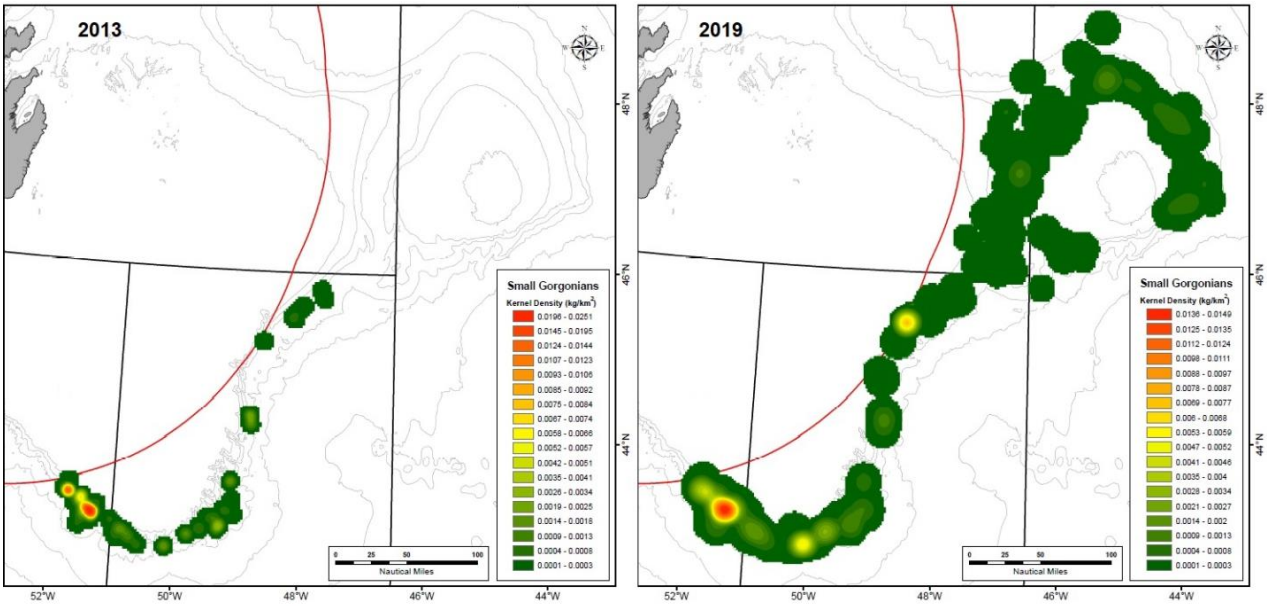

Figure 18. Kernel density biomass surface of small gorgonian corals in the NAFO Regulatory Area. Left Panel: Surface created in 2013 for closed area assessments; Right Panel: Surface created in 2019 for current closed area re-assessments.

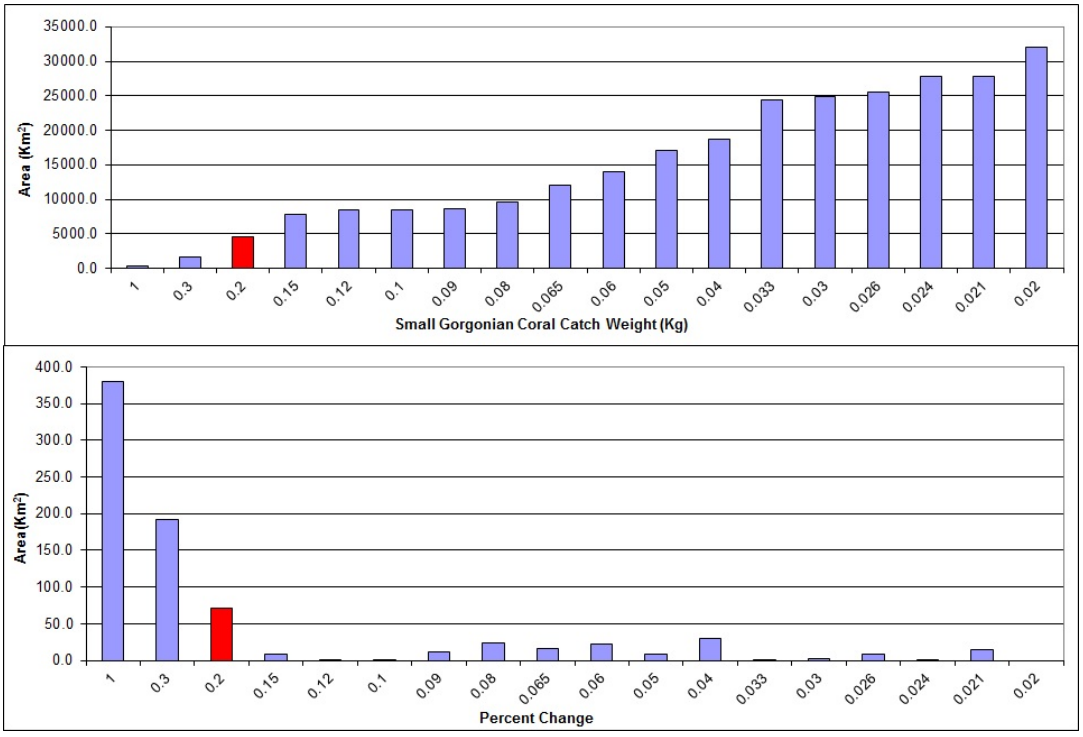

Figure 19. Bar graphs of the polygon area established by successively smaller research vessel small gorgonian coral catch weight thresholds (upper panel) and of the percent change in area created between successively smaller research vessel catch weight thresholds (lower panel). Red bar indicates the potential VME polygon threshold.

Table 12. The number of points attributing to the delineation of small gorgonian coral VME polygons based on successively smaller research vessel small gorgonian coral catch weight thresholds (kg). The area and number of observations used to define each polygon and the percent change in area and the number of additional observations between successive thresholds are provided. The shaded row represents the threshold used to define the VMEs.

Small Gorgonian Coral Catch Threshold (Kg)	Number of Observations in Polygon	Additional Observations Per Interval	Area of Polygon (km^2)	Percent Change in Area Between Successive Thresholds
1	6	6	324.4	380.3
0.3	15	9	1558.0	191.4
0.2	27	12	4540.2	70.7
0.15	39	12	7748.2	8.3
0.12	50	11	8388.5	1.6
0.1	61	11	8520.2	1.2
0.09	66	5	8622.8	11.8
0.08	76	10	9637.9	24.6
0.065	87	11	12012.9	16.5
0.06	97	10	14001.0	22.2
0.05	110	13	17107.5	9.4
0.04	125	15	18714.4	30.5
0.033	137	12	24416.0	1.8
0.03	150	13	24849.2	2.8
0.026	164	14	25553.4	8.8
0.024	175	11	27801.5	0.0
0.021	185	10	27814.7	15.0
0.02	218	33	31977.1	

The 2019 small gorgonian KDE polygons based on catches ≥ 0.2 kg/tow are compared with the 2013 small gorgonian KDE polygons in Figure 21. The polygons on Flemish Cap are new as this area was not included in the previous analysis (see above). On the Tail of Grand Bank the same general areas are depicted. However, with the additional data since 2013, the 2013 VME polygons in 3O have been amalgamated into one larger VME polygon in the 2019 assessment (Figure 21). It can be seen that there are a number of smaller catches as well as significant catches in that area, justifying the linkage.

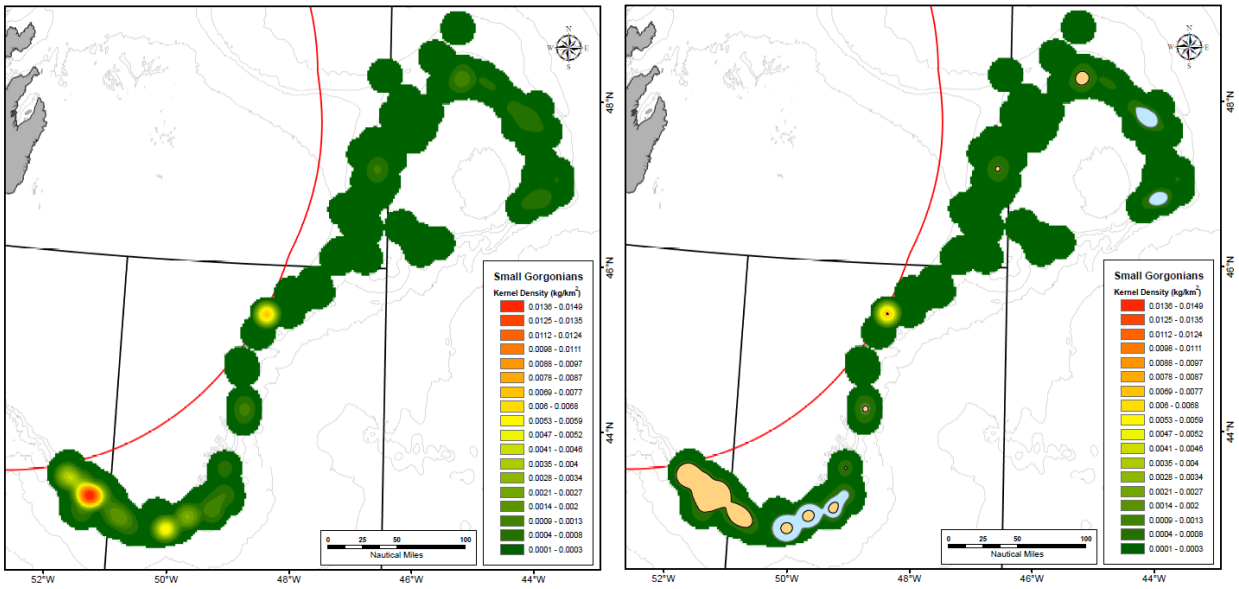

Figure 20. Left panel: Kernel density distribution of small gorgonian corals (primarily *Acanella arbuscula*) in the NAFO Regulatory Area. The green areas represent low small gorgonian coral densities while the red areas indicate high small gorgonian coral densities. Right panel: The location of KDE polygons with thresholds of ≥ 0.2 kg/tow (orange polygons) and ≥ 0.15 kg/tow (blue polygons) showing change in area. The orange KDE polygons define the small gorgonian coral VMEs.

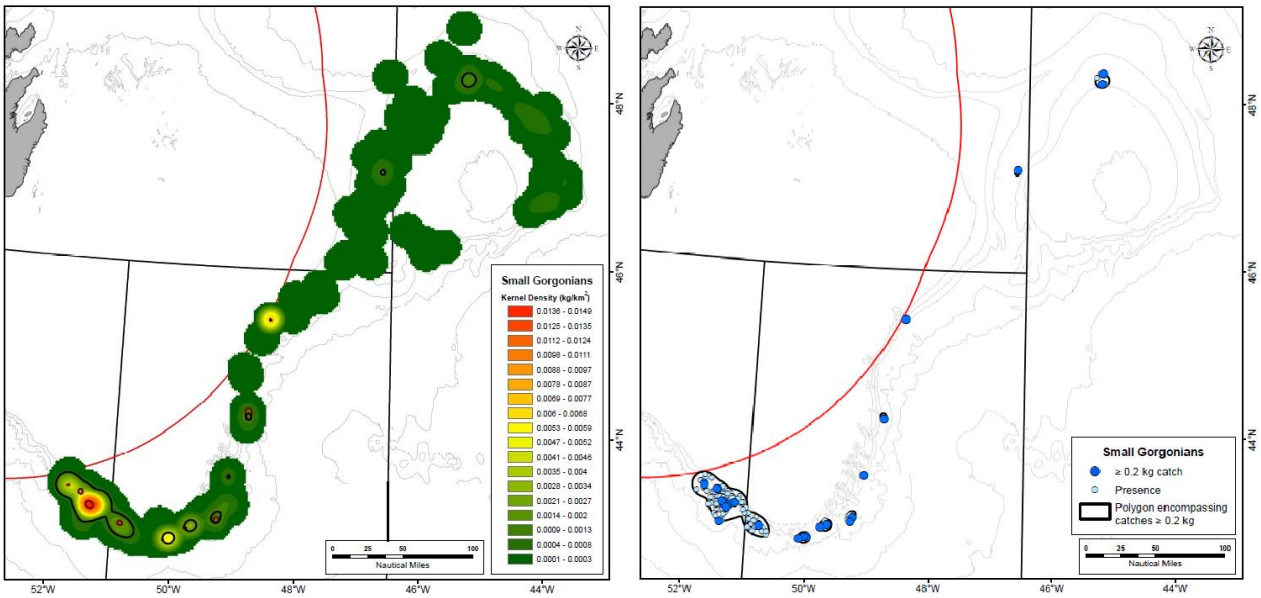

Figure 21. Left Panel. Kernel density distribution of small gorgonian corals (primarily *Acanella arbuscula*) in the NAFO Regulatory Area with the 2013 kernel density polygons defining the small gorgonian coral VMEs superimposed in red and the new 2019 polygons superimposed in black. Right panel. RV Catches ≥ 0.2 kg of small gorgonian corals and all other catches are displayed within the 2019 KDE polygons.

Species distribution models were not previously generated for small gorgonian corals in the NRA (NAFO, 2013). However, Gullage et al. (2017) predicted the distribution of small gorgonian corals on the east coast of Newfoundland and much of the NRA using MaxEnt modelling techniques, and predicted a high probability of occurrence along the slopes of Grand Bank, particularly at the location of the large VME north of the 3O closure delineated in the current assessment. As part of a process to identify significant concentrations of cold-water corals and sponges in eastern Canada (DFO, 2017), both kernel density and random forest species distribution modelling techniques were applied to small gorgonian coral catch data collected across the Newfoundland and Labrador Region (Guijarro et al., 2016b; Kenchington et al., 2016). Several KDE significant concentration polygons were identified north of the 3O closure within Canada's EEZ. The boundary between suitable versus unsuitable habitat defined by thresholding the random forest presence probability surface using model prevalence followed a strong depth gradient, with areas of suitable habitat predicted to occur below 400 m depth. As a result, the significant concentration polygons inside the Canadian EEZ in this region were clipped to both the 400 m contour and prevalence boundary (Kenchington et al., 2016). The presence of non-significant small gorgonian catches above the 400 m contour in the large KDE polygon identified in the 2019 assessment of the NRA indicates that no modifications should occur to the northern boundary of this polygon.

Review of Significant Concentrations of Large Gorgonian Corals

Significant concentrations of *Large Gorgonian Corals* in the NRA were previously identified using kernel density analyses and associated evaluation of the kernel surface (NAFO, 2013). That analysis has been updated using all available data from the RV trawl surveys (Table 1). These data sources yielded 283 large gorgonian coral records (83 from the Canadian surveys and 200 from the EU-Spanish surveys). However as shown previously, there were significant differences among the catch series for each survey (NAFO, 2013). When all records less than 0.1 kg were removed, there was no significant difference among the catch distributions and therefore the analyses here were performed on 89 large gorgonian coral catches ≥ 0.1 kg (29 Canadian records and 60 EU-Spanish records), 31 more observations than in the 2013 analysis (NAFO, 2013). Following previously established methods and assessment criteria, a kernel density surface was created and the area of successive density polygons calculated. KDE parameters were: Search Radius = 19.2 km; Contour Interval = 0.000025; Cell size default = 2298.7 m.

The KDE surfaces from the 2019 analysis are compared with that produced in 2013 (Figure 22). There is some change in the density recorded in Flemish Pass (note differences in scales) but the same general areas of higher density are seen in both assessments. The kernel density distribution identified high concentrations of large gorgonian coral VME in Flemish Pass (Figure 22).

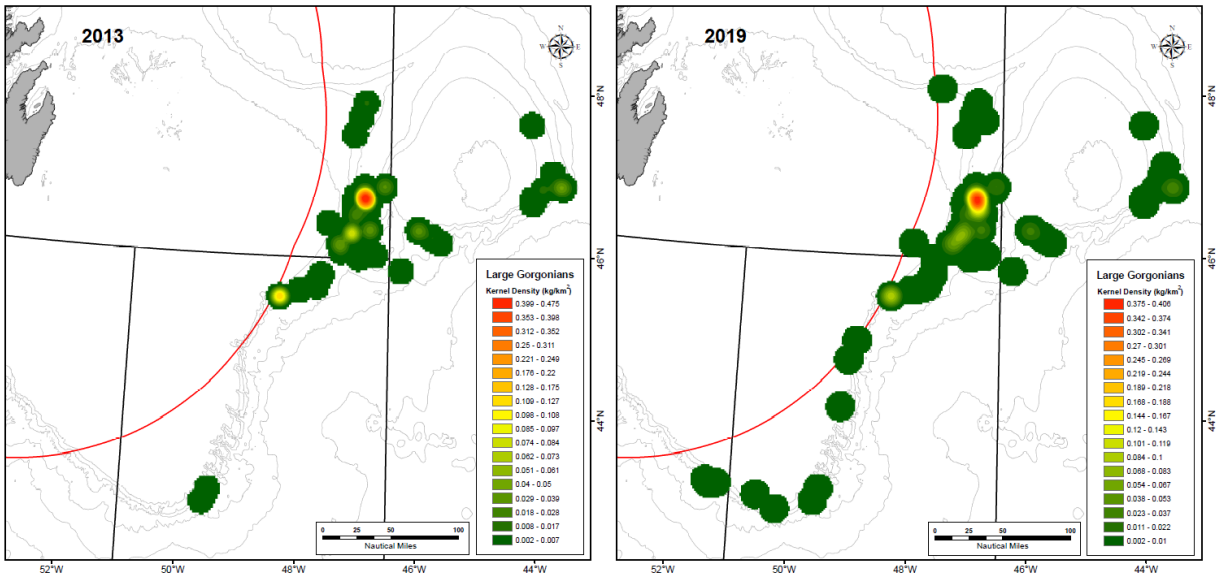

Figure 22. Kernel density biomass surface of large gorgonian corals in the NAFO Regulatory Area. Left Panel: Surface created in 2013 for closed area assessments; Right Panel: Surface created in 2019 for current closed area re-assessments.

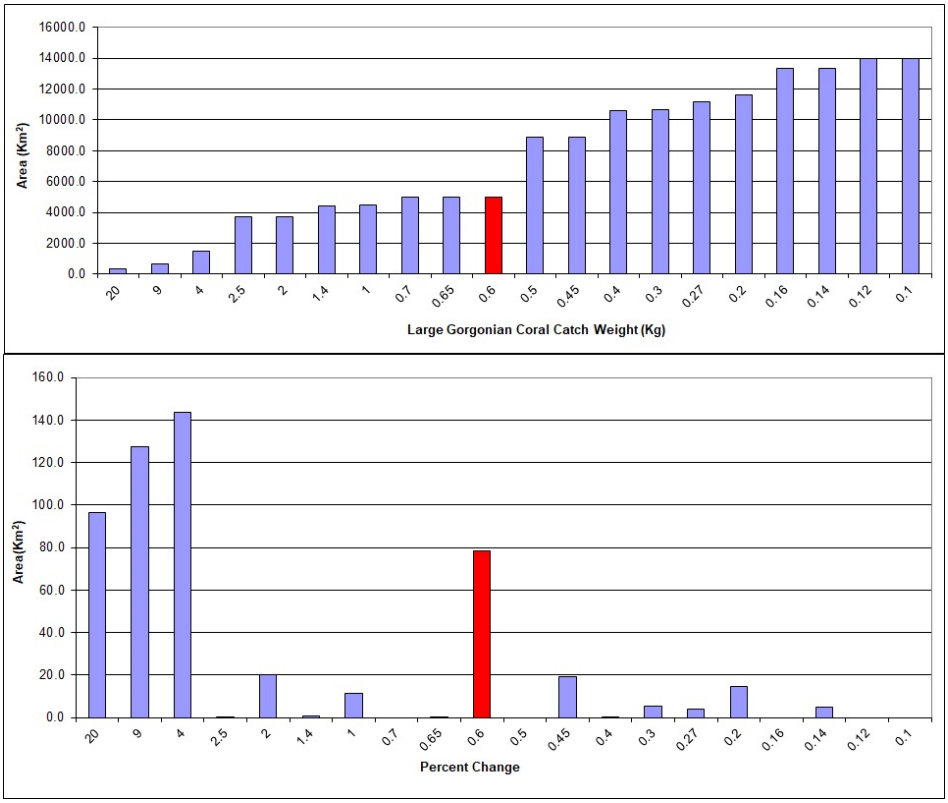

Figure 23. Bar graphs of the polygon area established by successively smaller research vessel large gorgonian coral catch weight thresholds (upper panel) and of the percent change in area created between successively smaller research vessel catch weight thresholds (lower panel). The red bar indicates the potential VME polygon threshold.

The 0.6 kg/RV tow density threshold emerged as defining significant concentrations of large gorgonian corals (i.e., large gorgonian coral VME) (Table 13, Figures 23 and 24), which was the same threshold identified in the previous analysis (NAFO, 2013). When superimposed on the kernel density surface, the 0.6 kg density polygon captures all of the highest density area (red colour on Figure 22) from the kernel analysis and other smaller catches are found within the large KDE polygon in Flemish Pass (Figure 24).

Table 13. The number of points attributing to the delineation of large gorgonian coral VME polygons based on successively smaller research vessel large gorgonian coral catch weight thresholds (kg). The area and number of observations used to define each polygon and the percent change in area and the number of additional observations between successive thresholds are provided. The shaded row represents the threshold used to define the VMEs.

Large Gorgonian Coral Catch Threshold (Kg)	Number of Observations in Polygon	Additional Observations Per Interval	Area of Polygon (km^2)	Percent Change in Area Between Successive Thresholds
20	5		340.1	96.4
9	10	5	668.1	127.5
4	14	4	1519.6	143.8
2.5	20	6	3704.2	0.1
2	26	6	3706.9	20.1
1.4	31	5	4452.6	0.5
1	36	5	4474.8	11.2
0.7	41	5	4977.0	0.0
0.65	43	2	4977.0	0.2
0.6	44	1	4986.9	78.6
0.5	47	3	8905.8	0.0
0.45	47	0	8905.8	19.3
0.4	53	6	10624.4	0.1
0.3	58	5	10639.5	5.1
0.27	65	7	11186.9	3.9
0.2	70	5	11620.6	14.5
0.16	76	6	13306.8	0.0
0.14	81	5	13306.8	4.8
0.12	85	4	13946.3	0.0
0.1	89	4	13946.3	

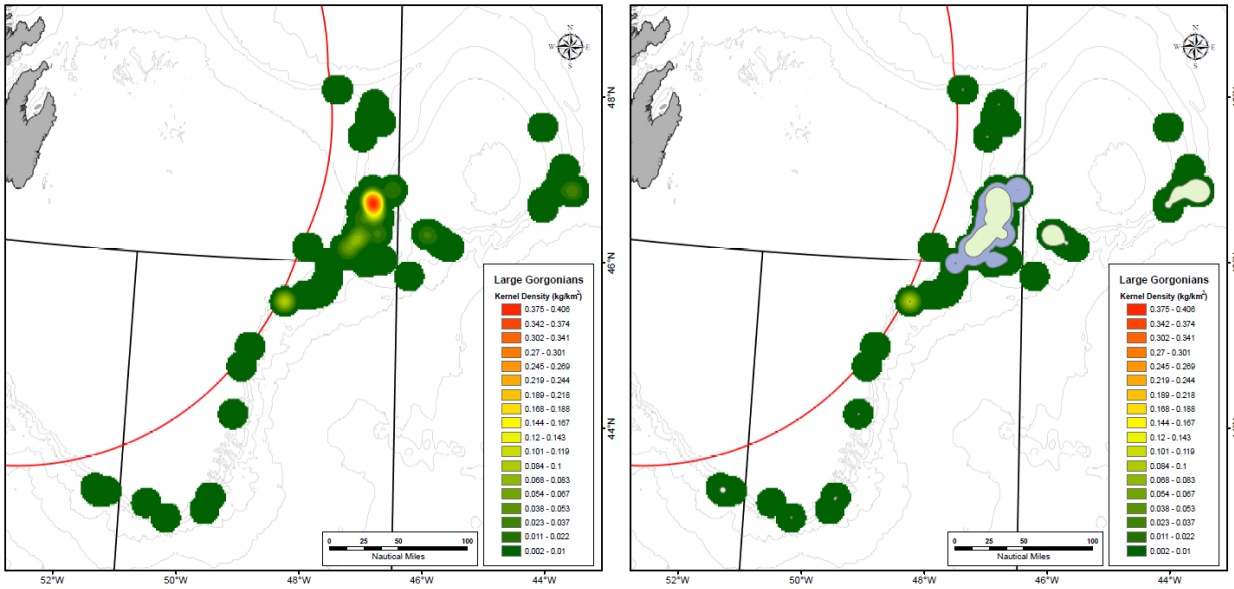

Figure 24. Left panel: The 2019 kernel density distribution of large gorgonian corals in the NAFO Regulatory Area. The green areas represent low coral densities while the red areas indicate high coral densities. Right panel: Comparison of the area covered by catches ≥ 0.6 kg (light green) and catches ≥ 0.5 kg (purple). The light green areas indicate the large gorgonian coral VMEs.

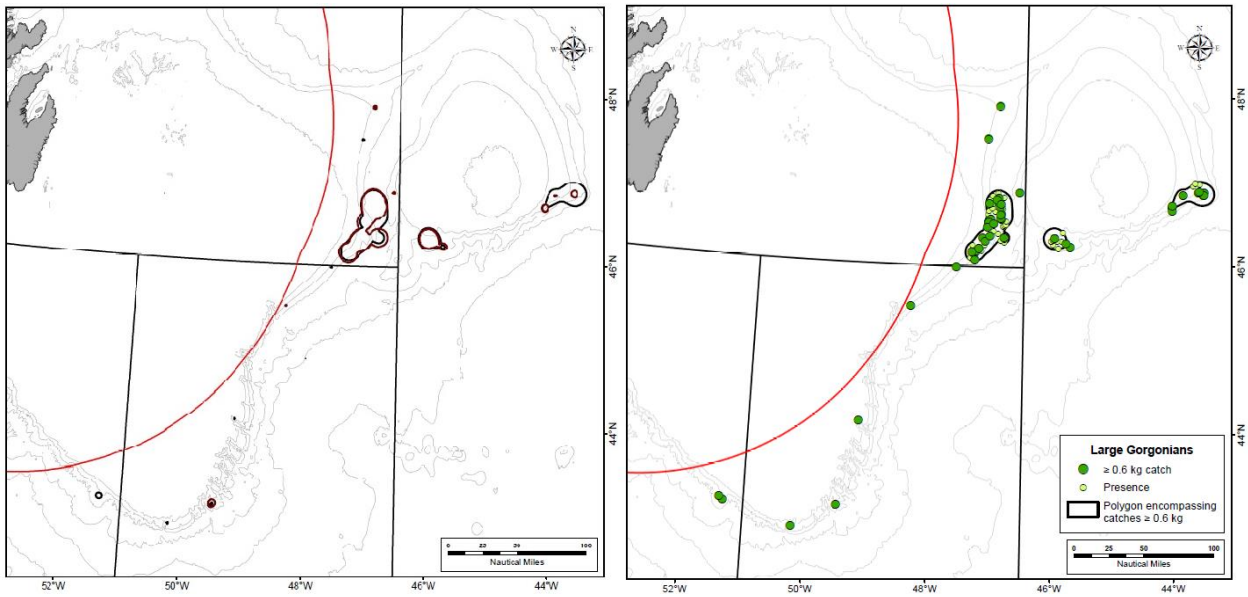

Figure 25. Left Panel. Kernel density distribution of large gorgonian corals in the NAFO Regulatory Area with the 2013 kernel density polygons (red) and the new 2019 polygons (black). Right panel. RV Catches ≥ 0.6 kg of large gorgonian corals and all other catches are displayed within the 2019 KDE polygons.

Modified VME Polygon Boundaries for Large Gorgonian Corals

The species distribution model (SDM) previously generated using presence/absence data of large gorgonian corals from the RV surveys, NEREIDA benthic imagery and rock and scallop dredge samples (Knudby et al., 2013c) was used to determine whether modification to the KDE polygons generated in the current assessment was required. Previously, WGESA modified the large polygon in Flemish Pass (NAFO, 2015) (Figure 26); however, given the uncertainty associated with the SDM, only a small modification to Area 2 was made in the 2019 analyses as the new KDE polygons lie mainly inside the area of predicted large gorgonian presence (Figure 26, right panel, arrow). In that area the boundary for the closed area was used as the notching was driven by a single significant catch on the VME threshold boundary.

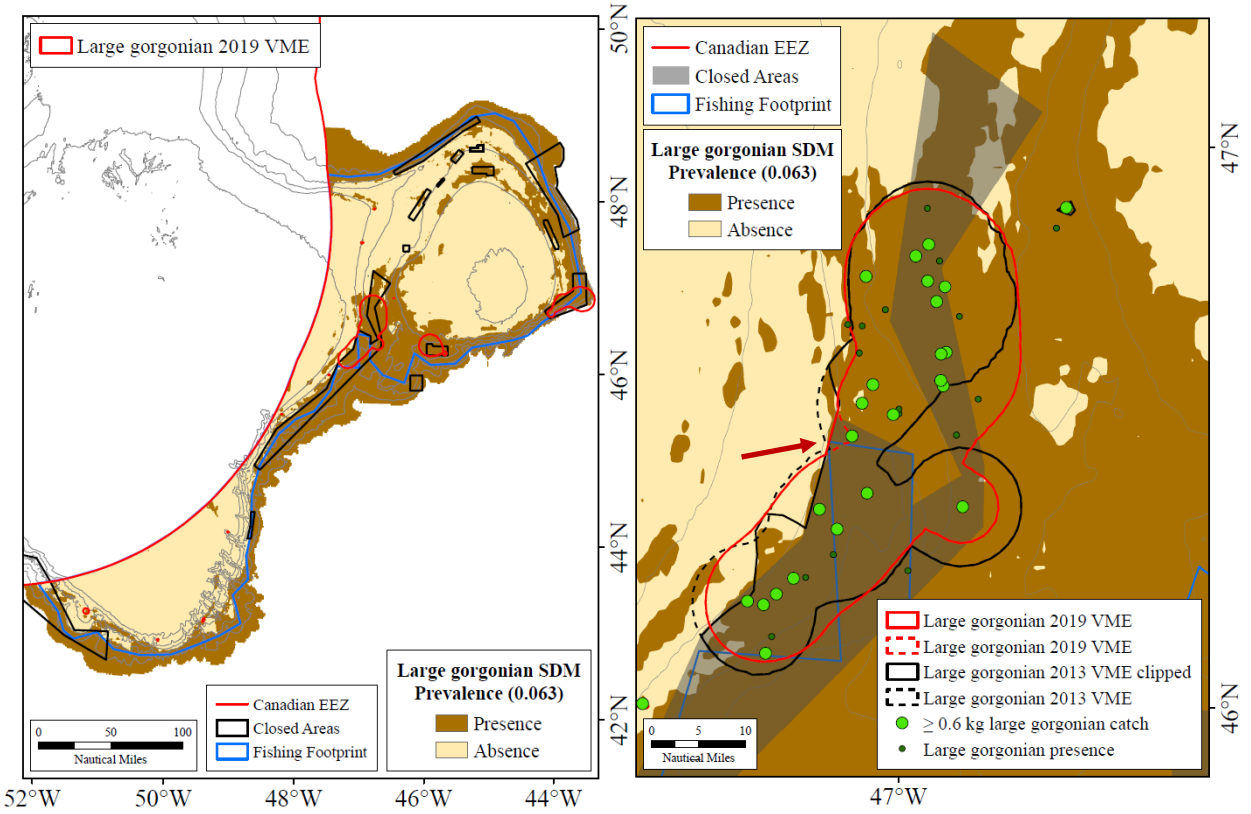

Figure 26. Left panel. Large gorgonian coral KDE polygons overlain on the prevalence map of predicted presence/absence. Closed areas in shown in black outline; fishing footprint in blue. Right panel. Close up of the Large gorgonian coral KDE polygon (red outline) in Flemish Pass showing the outline of the previous 2013 large gorgonian coral KDE polygon, its modification (NAFO, 2015), and the prevalence map of predicted presence/absence. The location of RV catches ≥ 0.6 kg are indicated in green with smaller catches in black. The Area 2 closure is indicated in grey shade. Arrow indicates the 2019 KDE polygon modification discussed in the text.

Review of Significant Concentrations of Tube-dwelling Anemones

Tube-dwelling anemones were observed on several *in situ* photographic transects across the Flemish Cap (Figure 27). The lack of taxonomic details from the photographs and video prevented the identification of these organisms past the subclass level (Ceriantharia). However, these cerianthids were not large, erect species, and do not appear to be the VME indicator species listed in NAFO (2011). These cerianthids formed dense fields (Beazley et al., 2013b) on the southern Flemish Cap

slope that may indicate VMEs, particularly if their bioturbation activities significantly affect infaunal community structure. Elsewhere they have been shown to enhance local species diversity and abundance in featureless soft-bottom areas (Shepard et al., 1986). Similarly the data from the RV surveys and NEREIDA rock and scallop dredge samples were mostly identified to subclass (Ceriantharia) and may contain non-VME cerianthid species, although data from the 2007 RV survey on the Grand Bank confirmed the presence of *Pachycerianthus borealis* at 140 m depth (Murillo et al., 2016).

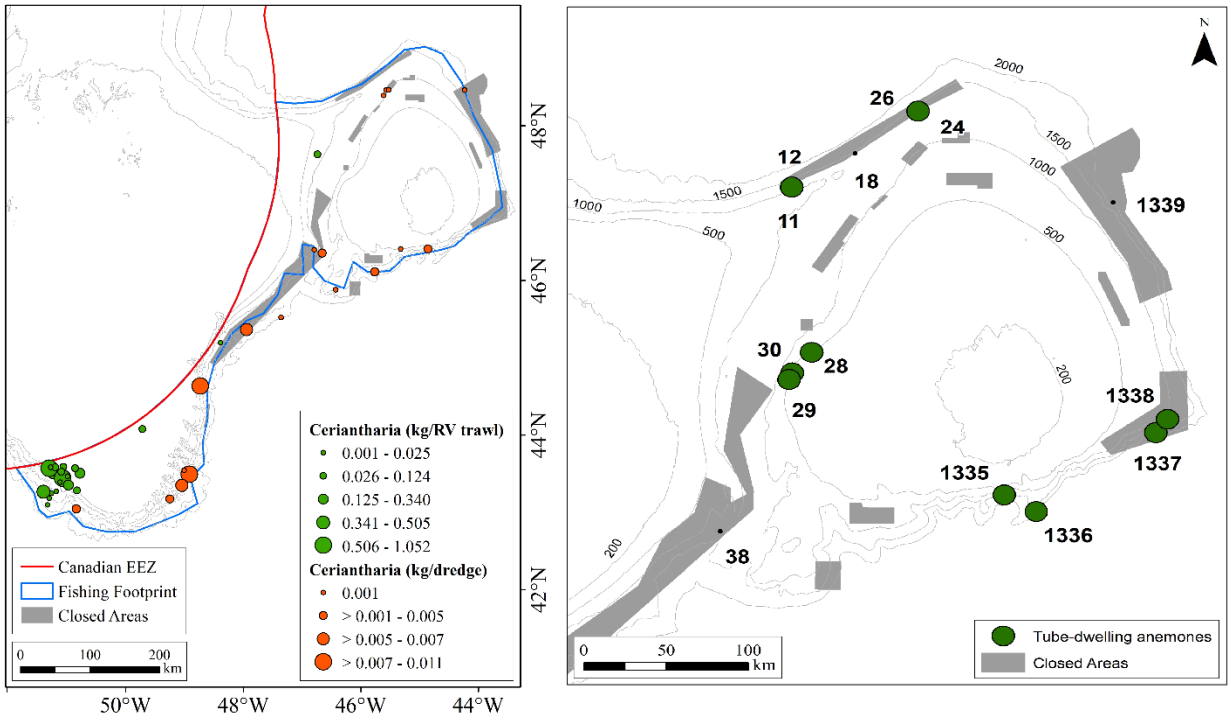

Figure 27. Left panel. Relative biomass of *Ceriantharia* collected in the NRA during the NEREIDA surveys between 2009-2010 using a rock dredge (orange) and EU-Spain research trawl surveys between 2006-2015, 2017-2019 (green). Right panel. Presence of tube-dwelling anemones (Ceriantharia) on video and photographic transects collected from the Flemish Cap area in 2009 and 2010.

Review of Significant Concentrations of Erect Bryozoans

Significant concentrations of *Erect Bryozoans* in the NRA were previously identified using kernel density analyses and associated evaluation of the kernel surface (NAFO, 2013). An updated kernel analysis is presented here for Erect Bryozoans on the Tail of Grand Bank using all available data from the RV trawl surveys (Table 1). Previous analyses only considered data from the EU-Spanish 3NO and 3L surveys (NAFO, 2013). However, with the additional data that have been collected since the 2013 assessment the catches can be combined for biomass values ≥ 0.02 kg. Consequently only catches ≥ 0.02 kg (N=174) were analyzed (12 Canadian records and 162 records from EU-Spain).

Following previously established methods and assessment criteria, a kernel density surface was created and the area of successive density polygons calculated. KDE parameters were: Search Radius = 12.4 km; Contour Interval = 0.00005; Cell size default = 1488.6 m. These parameters are the default parameters and result in a smaller search radius in the 2019 analysis than in the 2013 assessment (2013 Search Radius = 25 km; compare the relative size of the single catches in Figure 28). With the additional data available in 2019, continuous areas could be formed on the KDE surface without

increasing the search radius. This will help to refine the KDE polygons by reducing the area of data interpolation around each data record.

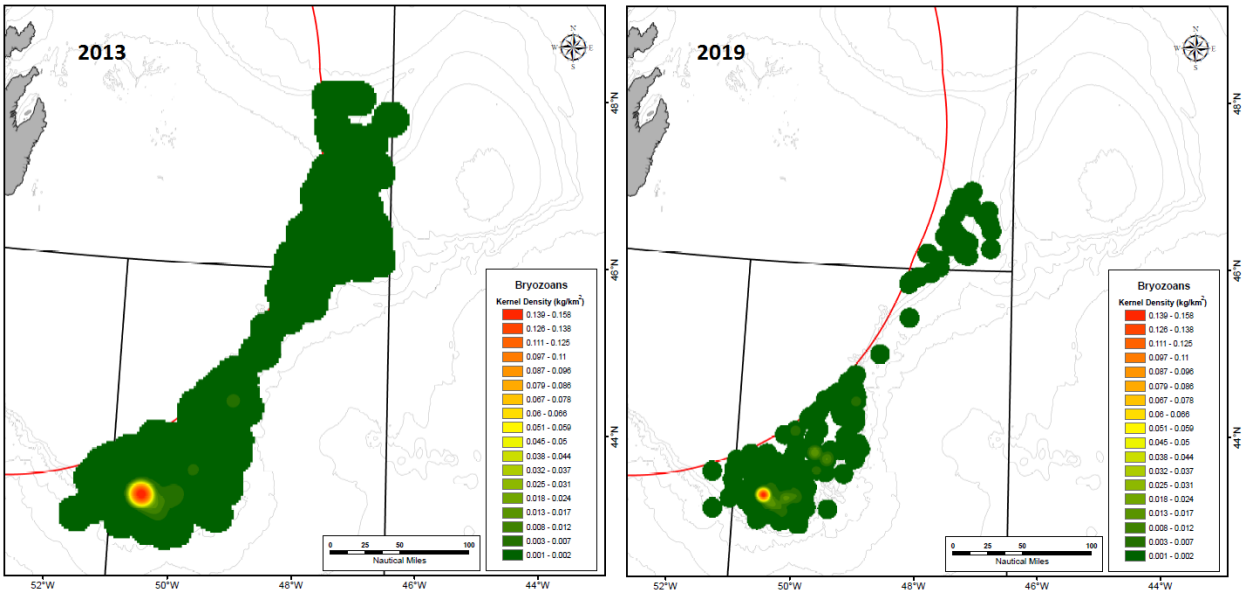

Figure 28. Kernel density biomass surface of erect bryozoans in the NAFO Regulatory Area. Left Panel: Surface created in 2013 for closed area assessments; Right Panel: Surface created in 2019 for current closed area re-assessments.

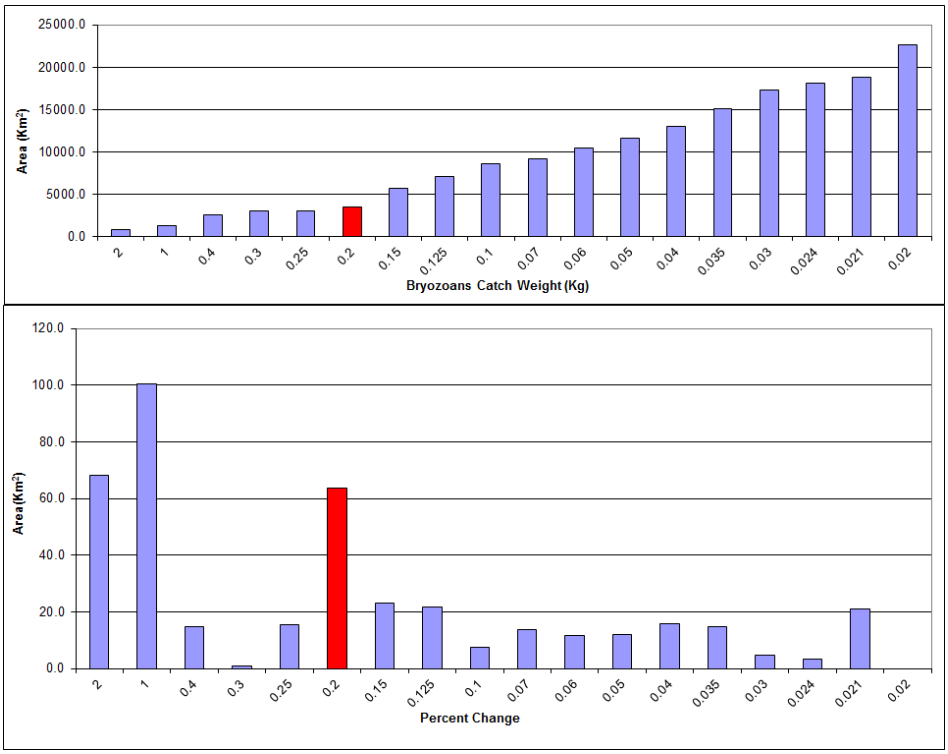

Figure 29. Bar graphs of the polygon area established by successively smaller research vessel *Erect Bryozoan* catch weight thresholds (upper panel) and of the percent change in area created between successively smaller research vessel catch weight thresholds (lower panel). Red bar indicates the potential VME polygon threshold.

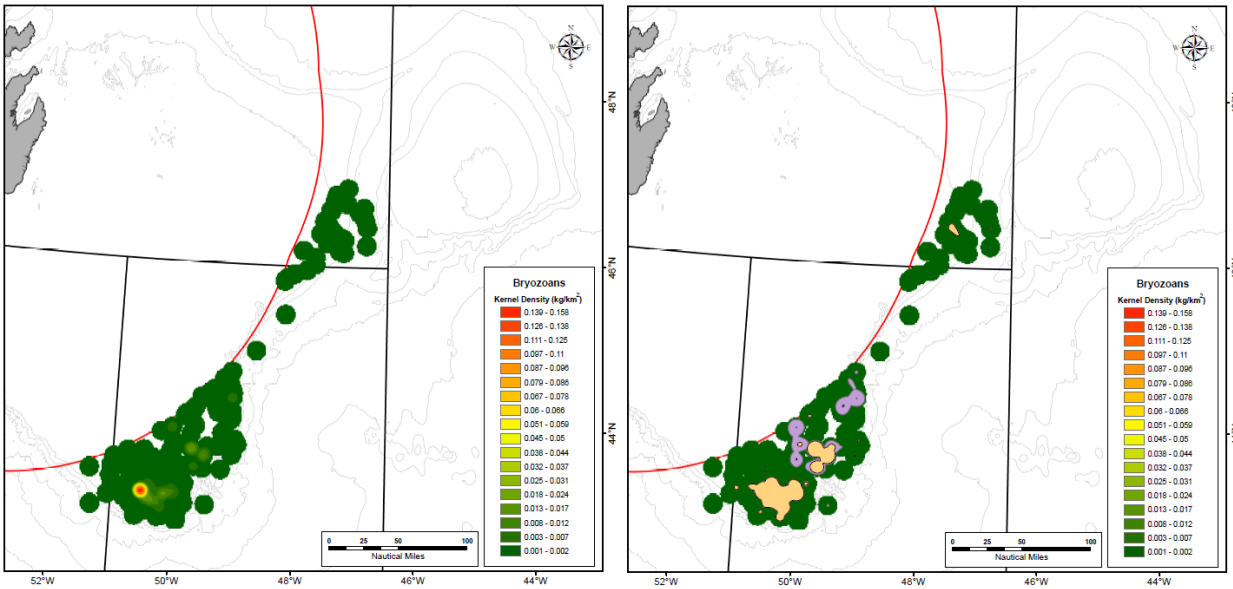

Figure 30. Left panel: The 2019 kernel density distribution of *Erect bryozoans* in the NAFO Regulatory Area. The green areas represent low bryozoan densities while the red areas indicate high densities. Right panel: Comparison of the area covered by catches ≥ 0.2 kg (orange) and catches ≥ 0.15 kg (purple). The orange areas indicate the bryozoan VMEs.

Table 14. The number of points attributing to the delineation of *Erect Bryozoan* VME polygons based on successively smaller research vessel *Erect Bryozoan* catch weight thresholds (kg). The area and number of observations used to define each polygon and the percent change in area and the number of additional observations between successive thresholds are provided. The shaded row represents the threshold used to define the VMEs.

Erect Bryozoan Catch Threshold (Kg)	Number of Observations in Polygon	Additional Observations Per Interval	Area of Polygon (km²)	Percent Change in Area Between Successive Thresholds
2	9		774.4	68.2
1	17	8	1302.8	100.5
0.4	29	12	2611.6	14.7
0.3	35	6	2995.1	0.8
0.25	38	3	3019.7	15.6
0.2	43	5	3491.5	63.7
0.15	50	7	5714.0	23.2
0.125	59	9	7038.9	21.6
0.1	71	12	8558.0	7.3
0.07	83	12	9183.4	13.6
0.06	94	11	10431.4	11.8
0.05	108	14	11658.0	11.9
0.04	119	11	13046.6	15.8
0.035	130	11	15104.9	14.8
0.03	139	9	17342.3	4.7
0.024	150	11	18165.3	3.3
0.021	159	9	18765.4	20.9
0.02	174	15	22693.7	

The 2019 kernel density distribution identified high density areas of erect bryozoans on the Tail and Nose of the Grand Bank similar to the results from 2013 (Figure 28). The 0.2 kg/RV tow density threshold emerged as defining significant concentrations of erect bryozoans (Table 14, Figures 29 and 30). This was the same threshold identified in the 2013 analysis (NAFO, 2013). The main bryozoan species that constitutes the significant concentrations is *Eucratea loricata*. When superimposed on the kernel density surface (Figure 30), the 0.2 kg density polygon captures all of the highest density areas (red colour on Figure 30) from the kernel analysis and other smaller catches are found within the defining polygons (Figure 31).

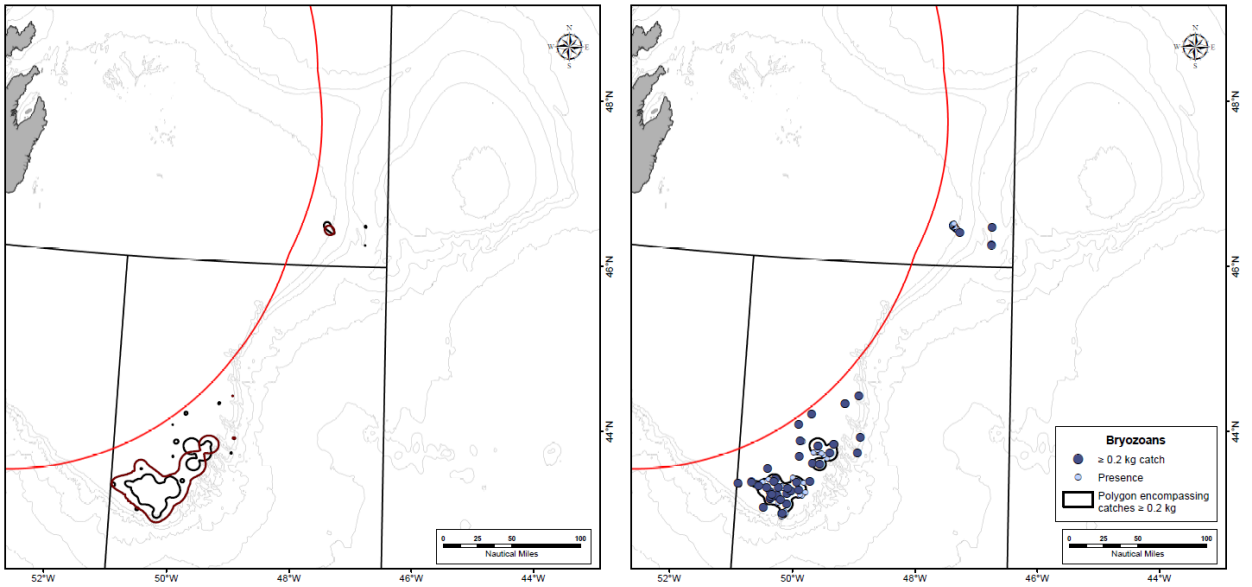

Figure 31. Left Panel. Kernel density distribution of erect bryozoans in the NAFO Regulatory Area with the 2013 kernel density polygons (red) and the new 2019 polygons (black). Right panel. RV Catches ≥ 0.2 kg of erect bryozoans and all other smaller catches are displayed within the 2019 KDE polygons.

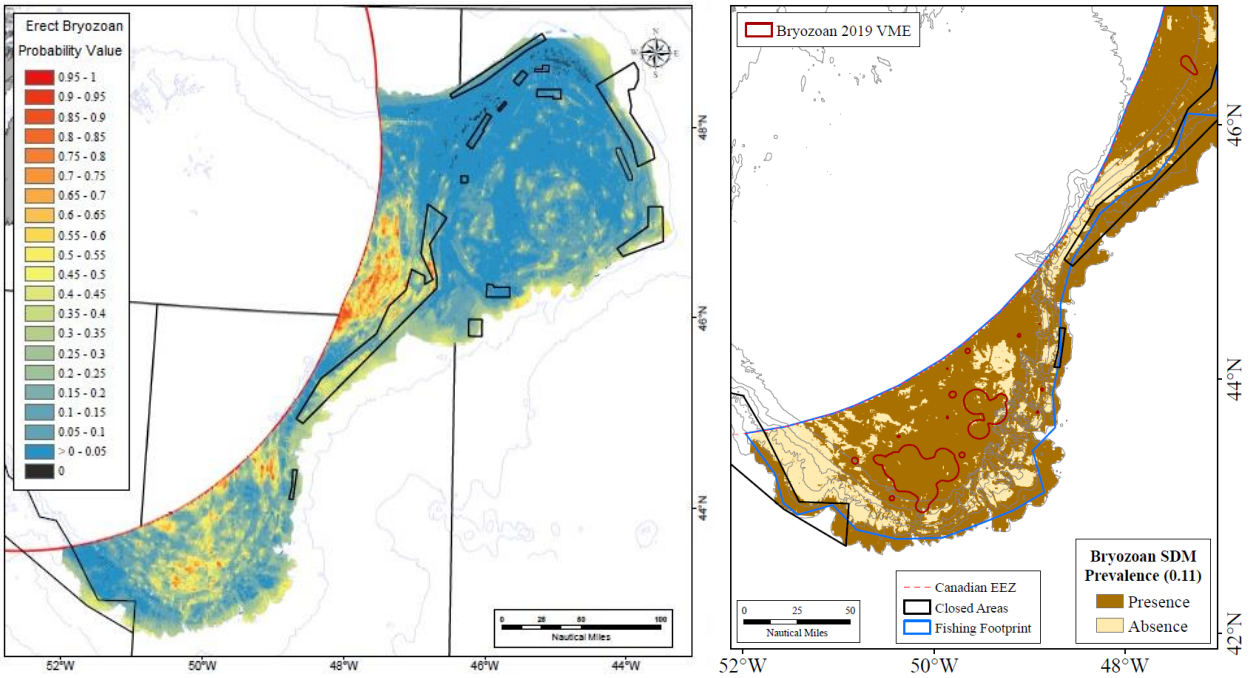

Figure 32. Left Panel. Random forest species distribution model of erect bryozoans showing the high probability of occurrence of these VME indicators on Grand Bank. Closed areas are indicated in black outline. Right panel. Close up of the position of the erect bryozoan KDE polygons in relation to the erect bryozoan SDM prevalence map (see above for details of methodology). The 2019 KDE polygons (red outline) fall within the predicted presence (brown areas) of these species and so there was no need to modify them.

The species distribution model for the probability of occurrence of erect bryozoans is shown in Figure 32. Although this model only showed acceptable performance (Table 7), it did detect higher probability of occurrence inside the large VME polygons (shown in the right panel of Figure 32 using a prevalence threshold over the SDM). The higher presence in the deeper waters can be seen on the slopes (Figure 32, left panel) and suggests that two or more species with different physical niches are found. As all the deeper catches had very low biomass, applying the KDE catch biomass threshold would concentrate the observations on top of Grand Bank. A similar situation occurred with the large-sized sponges which led to the identification of the glass sponge grounds on the top of Flemish Cap (*Asconema foliata*), a light weight species that was not given predominance in the KDE.

Review of Significant Concentrations of Sea Lilies (Crinoids)

Crinoids are delicate organisms that are not well-sampled by trawl nets although they are represented in the catch (NAFO, 2013). The NEREIDA photographic transects provide *in situ* evidence for dense aggregations of this VME indicator (Figure 33). The stalked crinoid *Conocrinus lofotensis*, a VME indicator species, was observed in high abundances on the Sackville Spur, but was completely absent from the Flemish Pass area.

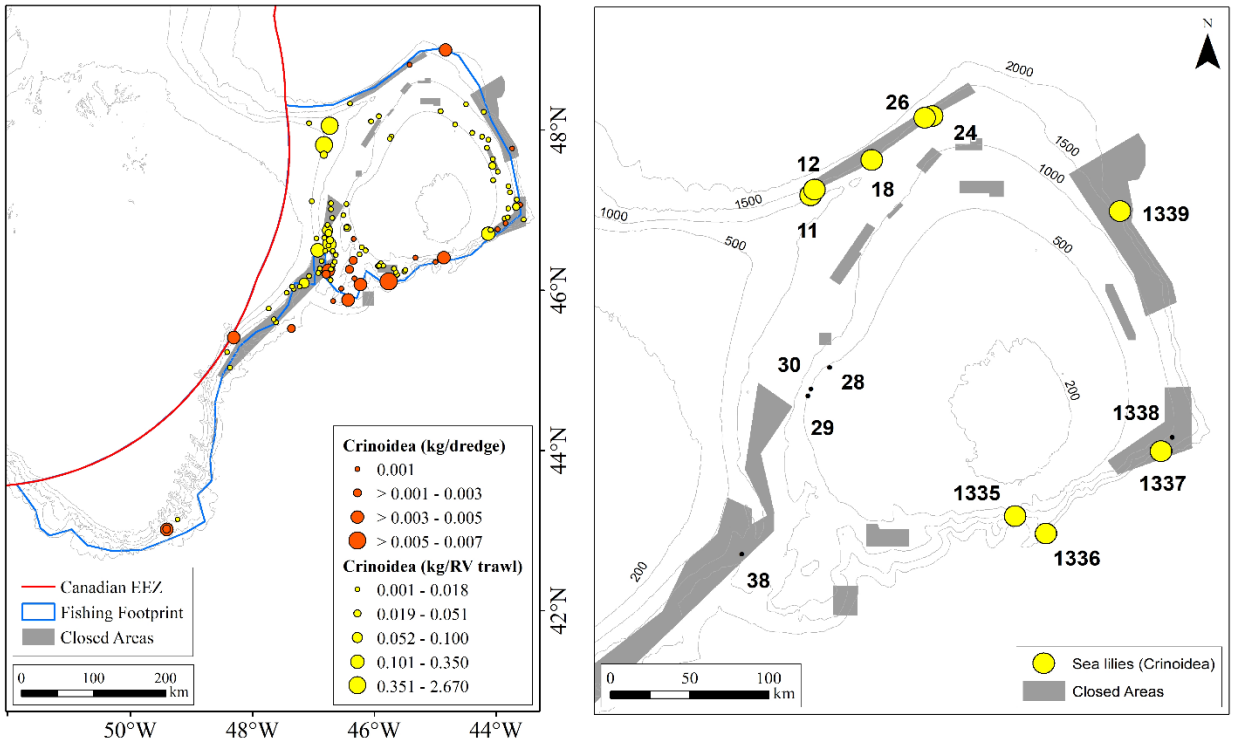

Figure 33. Left Panel. Relative biomass of Crinoidea collected in the NRA during the NEREIDA surveys between 2009-2010 using a rock dredge (orange) and EU-Spain research trawl surveys between 2006-2015, 2017-2019 (yellow). Right Panel. Presence of sea lilies (*Conocrinus lofotensis* and *Gephyrocrinus grimaldii*; Crinoidea) on video and photographic transects collected from the Flemish Cap area in 2009 and 2010.

Video analysis revealed dense fields of the stalked crinoid *Gephyrocrinus grimaldii* on the southern, southeastern, and northeastern slope of the Flemish Cap. This species was completely absent on transects from the Sackville Spur and Flemish Pass area. Unstalked crinoids were not observed in high abundances on any transect analyzed. The data from the RV surveys and NEREIDA rock and scallop dredge samples were mostly identified to class (Crinoidea) but do identify crinoids in Flemish Pass and on Grand Bank that were not seen in the benthic imagery. Data from the 2007 RV survey on Flemish Cap confirmed the presence of *Trichometra cubensis* between 770 and 1242 m depth (Murillo et al., 2016).

Review of Significant Concentrations of Sea Squirts

Sea squirts (specifically stalked tunicates) were identified as VME indicators in Murillo et al. (2011b) and accepted by NAFO as such (NAFO, 2012). There are now 334 records of sea squirts (172 from Canadian surveys, 162 from EU surveys), mainly of *Boltenia ovifera*, a habitat-forming stalked tunicate VME indicator, and all are located on the Tail and Nose of Grand Bank. This represents 247 more observations than were available in the previous KDE analysis (NAFO, 2013). KDE parameters were: Search Radius = 10.1 km; Contour Interval = 0.00005; Cell size default = 2897.8 m.

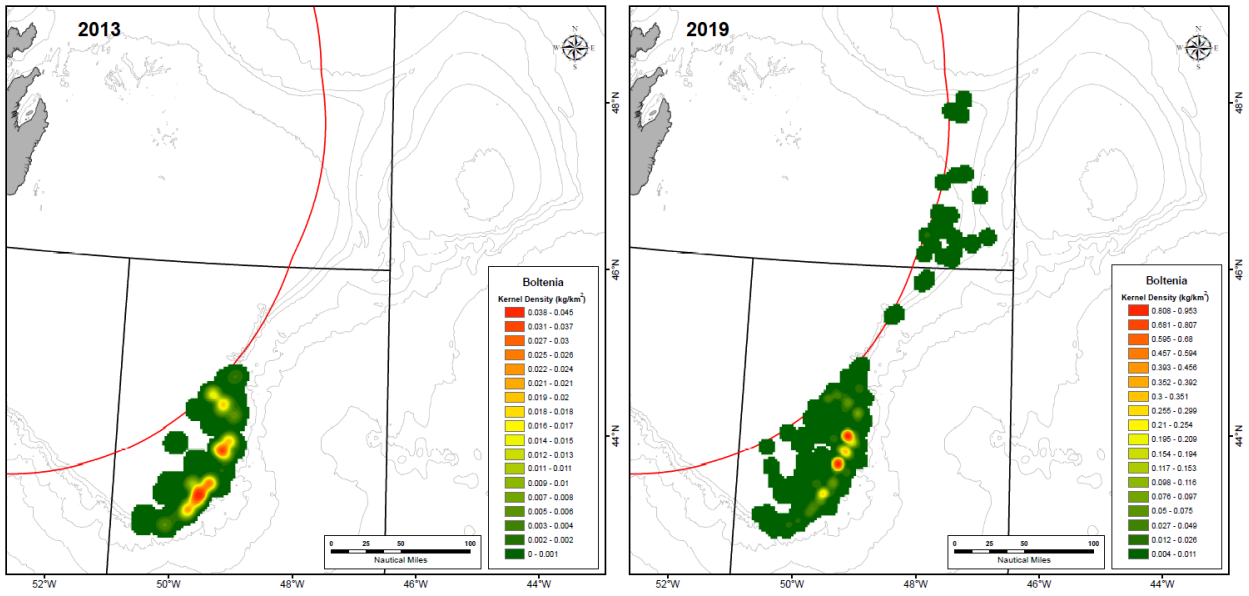

Figure 34. Kernel density biomass surface of sea squirts in the NAFO Regulatory Area. Left Panel: Surface created in 2013 for closed area assessments; Right Panel: Surface created in 2019 for current closed area re-assessments. Note differences in scales: the maximum density in 2013 is 0.045 kg km^2 and in 2019 it is 0.953 kg km^2.

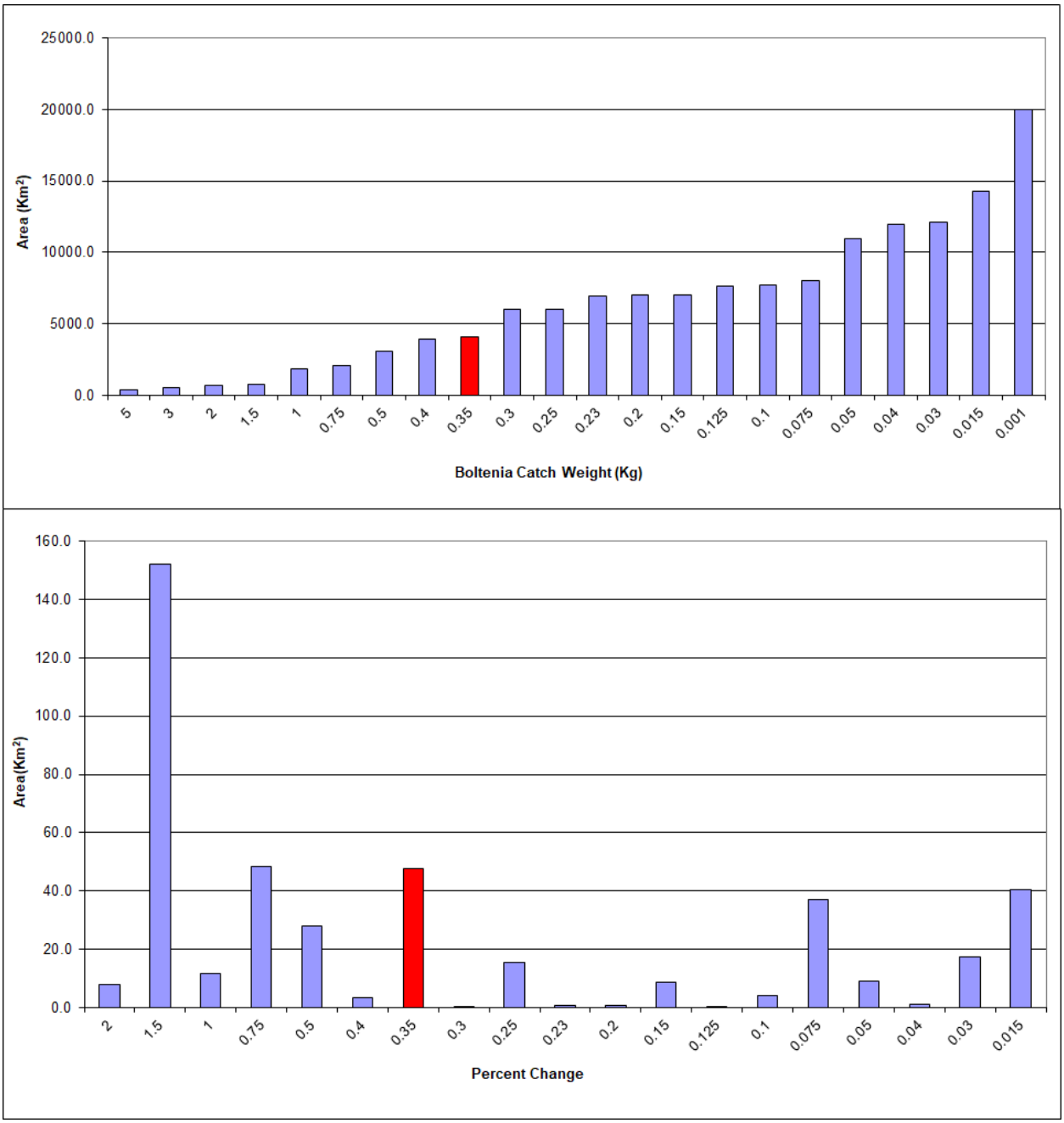

Figure 35. Bar graphs of the polygon area established by successively smaller research vessel sea squirt (*Boltenia ovifera*) catch weight thresholds (upper panel) and of the percent change in area created between successively smaller research vessel catch weight thresholds (lower panel). Red bar indicates the potential VME polygon threshold.

Table 15. The number of points attributing to the delineation of sea squirt (*Boltenia ovifera*) VME polygons based on successively smaller research vessel sea squirt catch weight thresholds (kg). The area and number of observations used to define each polygon and the percent change in area and the number of additional observations between successive thresholds are provided. The shaded row represents the threshold used to define the VMEs.

Boltenia Catch Threshold (Kg)	Number of Observations in Polygon	Additional Observations Per Interval	Area of Polygon (km^2)	Percent Change in Area Between Successive Thresholds
5	10		384.7	45.4
3	22	12	559.3	22.3
2	36	14	684.0	8.0
1.5	50	14	738.6	152.0
1	63	13	1861.2	11.6
0.75	79	16	2076.9	48.5
0.5	95	16	3084.7	27.8
0.4	106	11	3943.5	3.4
0.35	118	12	4076.7	47.6
0.3	132	14	6018.6	0.0
0.25	142	10	6020.0	15.3
0.23	149	7	6944.0	0.7
0.2	168	19	6994.7	0.8
0.15	182	14	7050.3	8.8
0.125	197	15	7674.0	0.2
0.1	214	17	7690.3	4.0
0.075	235	21	8001.7	37.1
0.05	253	18	10968.9	9.3
0.04	269	16	11984.0	1.2
0.03	292	23	12127.2	17.6
0.015	313	21	14257.5	40.3
0.001	334	21	20008.3	

Following previously established methods and assessment criteria (NAFO, 2013), a kernel density surface was created (Figure 34). Much larger densities were observed in the 2019 analysis over those seen in 2013 (Figure 34). The area of successive density polygons was calculated (Table 15). The analysis performed well and a clear threshold value of 0.35 kg was established (Table 15, Figures 35 and 36), which is slightly higher than the previous threshold of 0.3 kg (NAFO, 2013). The next threshold (0.3 kg) linked some of the polygons created at the 0.35 kg and did not create new locations (Figure 36). The locations of significant catches and smaller catches inside the VME polygons are shown in Figure 37. The area linking the 2013 KDE polygons in the 2019 analysis (Figure 37, left panel) is well justified with the occurrence of significant catches (and smaller catches) in that region and throughout the KDE polygon on the Tail of Grand Bank (Figure 37, right panel).

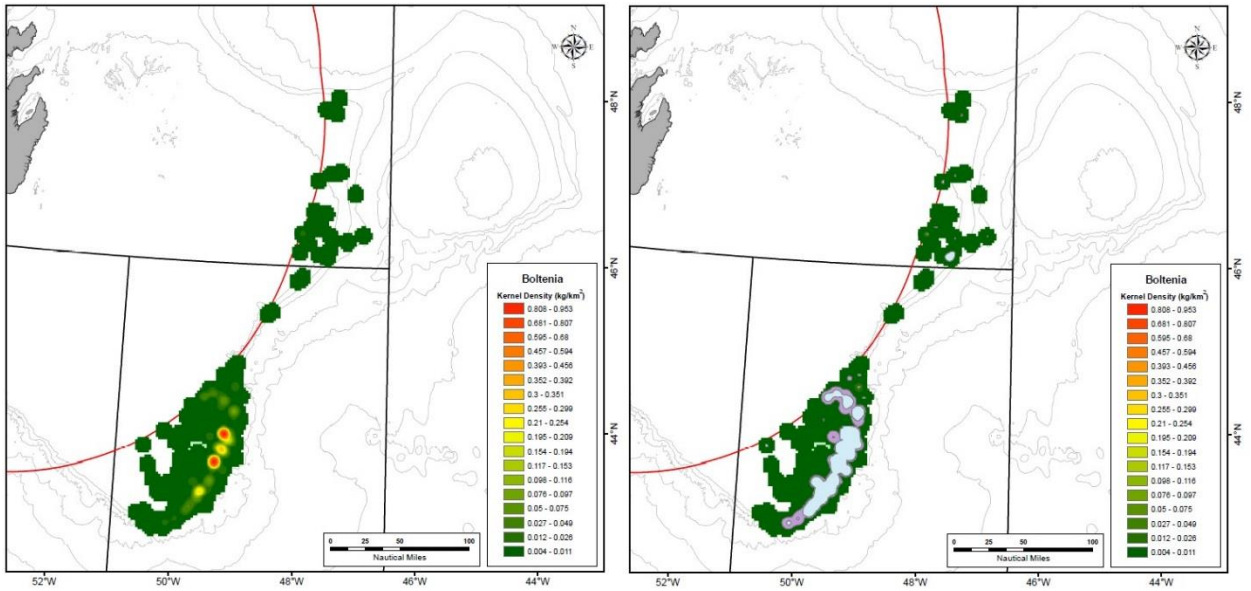

Figure 36. Left panel: The 2019 kernel density distribution of sea squirt (*Boltenia ovifera*) in the NAFO Regulatory Area. The green areas represent low sea squirt densities while the red areas indicate high densities. Right panel: Comparison of the area covered by catches ≥ 0.35 kg (blue) and catches ≥ 0.3 kg (purple). The blue areas indicate the sea squirt VMEs.

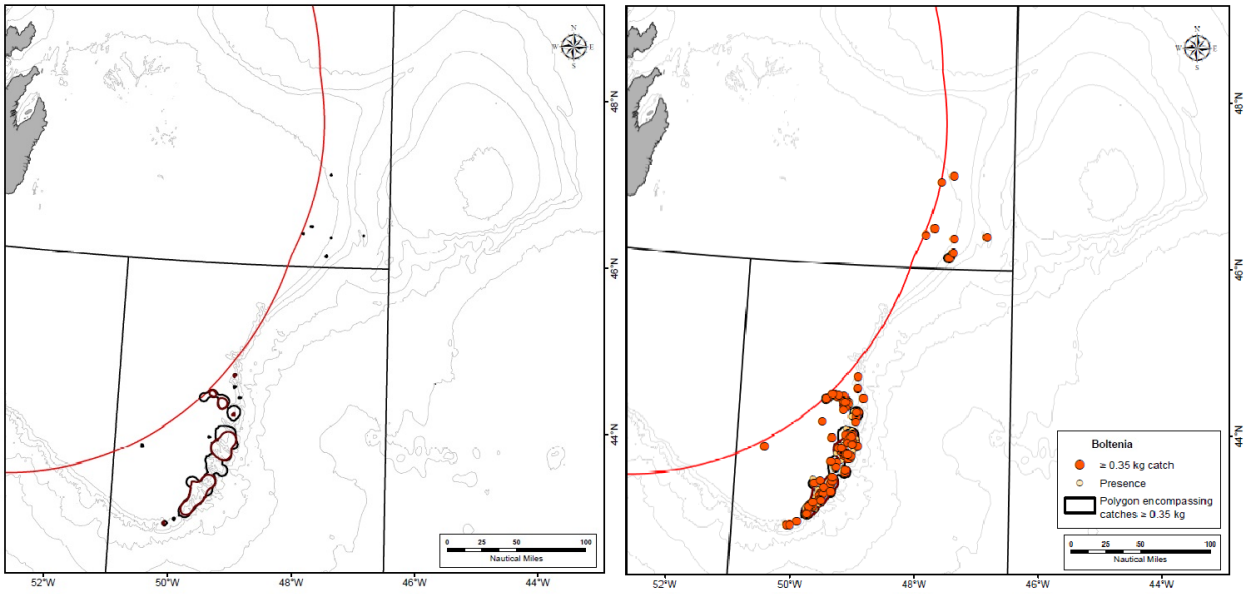

Figure 37. Left Panel. Kernel density distribution of sea squirt (*Boltenia ovifera*) in the NAFO Regulatory Area with the 2013 kernel density polygons (red) and the new 2019 polygons (black). Right panel. RV Catches ≥ 0.35 kg of sea squirts (*Boltenia ovifera*) and all other catches are displayed within the 2019 KDE polygons.

Modified VME Polygon Boundaries for Sea Squirts **(Boltenia ovifera)**

The species distribution model for the sea squirts (Boltenia ovifera) had an outstanding model performance (Table 7) and the model presence prediction aligned well with the location of the KDE

polygons (Figure 38). Most of the KDE area falls within the area of predicted presence (Figure 38), and consequently no modifications were made to the KDE polygons.

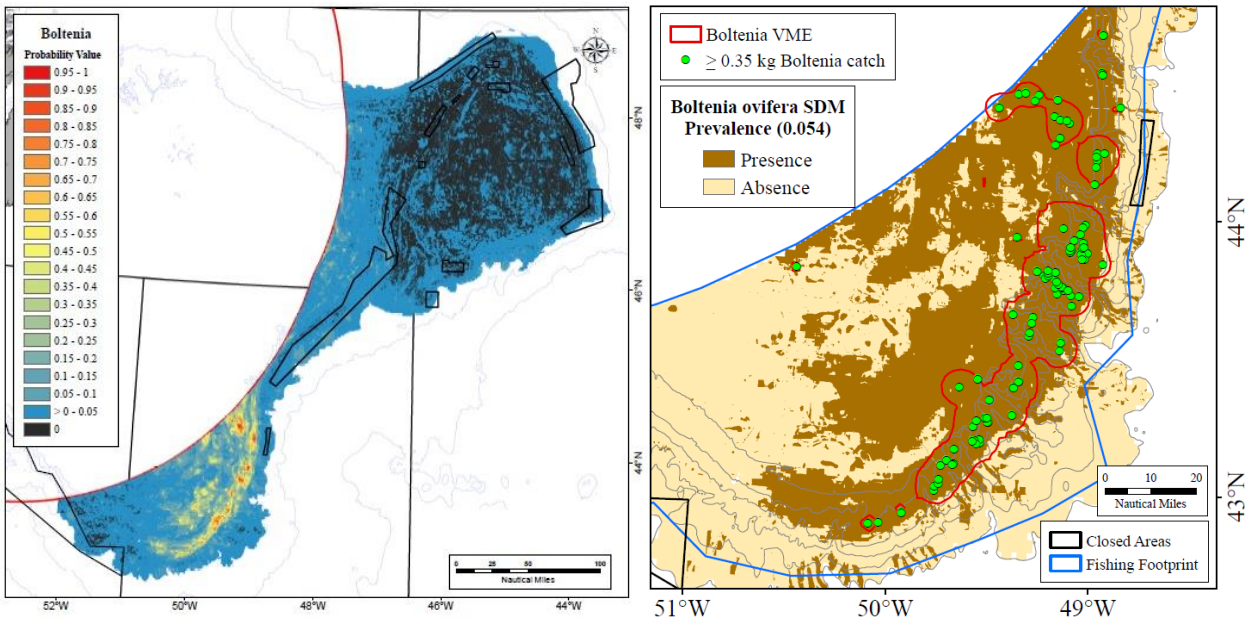

Figure 38. Left Panel. Random forest species distribution model of sea squirts (*Boltenia ovifera*) showing the high probability of occurrence of these VME indicators on the Tail of Grand Bank. Closed areas are indicated in black outline. Right panel. Close up of the position of the sea squirt KDE polygons in relation to the sea squirt SDM prevalence map (see above for details of methodology). The 2019 KDE polygons (red outline) fall within the predicted presence (brown areas) of these species and so there was no need to modify them.

Review of Black Coral Biology, Distribution, and Functional Significance

Members of the order Antipatharia, commonly known as black corals, are considered some of the longest living organisms on the planet, with longevity estimates reaching up to 4265 years for some species (Etnoyer et al., 2018; Wagner et al., 2012). In certain locations where environmental conditions are deemed favourable for the growth and settlement of black corals, such as the deep-water seamounts (550-1150 m) in the eastern North Pacific, some antipatharian species achieve high population densities (up to 20 individuals per m^2) and form monospecific aggregations that extend over large areas (reviewed in Wagner et al. (2012)). However, information on the functional significance of these aggregations is largely unknown. Wagner et al. (2012) reviewed the known associations of demersal fauna with black corals and noted that many fish and motile invertebrates are thought to utilize the structure provided by black corals in an opportunistic or transient way, but do not form obligate associations with them. One exception is the ophiuroid *Astrobrachion constrictum*, which has only been observed on the colonies of antipatharians, and never in a free-living state (Grange, 1991). Similarly, some species of fish in the shallow waters of Indonesia and in the Mediterranean were found to lay eggs on colonies of black corals (Tazioli et al., 2007; Bo, 2008), suggesting they could be important nursery grounds. Recently, De Clippele et al. (2019) have described the role that some non-scleractinian corals play on cold-water mounds in the northeast Atlantic, suggesting that areas with high diversity of both gorgonians and antipatharians offer food and are important habitat for other invertebrates.

In the NAFO Regulatory Area, a total of nine species of black coral have been reported from a combination of research vessel trawl catch data and *in situ* observations (Table 16) (Waller et al., 2007; Shank, 2010; Murillo et al., 2011a; Wareham et al., 2012; Beazley et al., 2013b; MacIsaac et al., 2013; NAFO, 2014), with five occurring in the fishing footprint: *Stauropathes arctica*, *Sticopathes* sp., *Leiopathes* cf. *expansa*, *Leiopathes* sp., and the recently described black coral species *Telopathes magnus* (Beazley et al., 2013b; MacIsaac et al., 2013).

Table 16. Black coral taxa known to occur in the NAFO Regulatory Area (including seamounts).

Known Taxon	Family	Location
Stichopathes sp.	Antipathidae	NRA (Divs. 3KM)
Leiopathes cf. *expansa*	Leiopathidae	NRA (Divs. 3KM)
Leiopathes sp.	Leiopathidae	NRA (Divs. 3KLM)
Plumapathes sp.	Myriopathidae	Corner Rise Seamounts (Div. 6G)
Bathypathes cf. *patula*	Schizopathidae	NRA (Div. 3K)
Parantipathes sp.	Schizopathidae	Corner Rise Seamounts (Div. 6G)
Stauropathes arctica	Schizopathidae	NRA (Divs. 3LMN)
Stauropathes cf. *punctata*	Schizopathidae	Orphan Knoll (Div. 3K)
Telopathes magnus	Schizopathidae	New England and Corner Rise Seamounts, NRA (Divs. 3M)

Black corals were previously considered VME indicators by NAFO due to their fragility and vulnerability (Grigg, 1989; Fuller et al., 2008), and were the only group considered to have met the criterion of uniqueness/rarity based on the available information on their distribution in the NRA (Murillo et al., 2011b). However, subsequent occurrence data on black corals collected from *in situ* camera surveys, rock dredges, and trawl surveys revealed a relatively widespread occurrence at low densities across the NRA and the slopes of Labrador (NAFO, 2013). Isolated colonies of the most common species in the area, *Stauropathes arctica*, were observed over kilometer scales during *in situ* camera surveys of the Flemish Pass in 2009 (NAFO, 2013). This non-aggregating distribution negated the application of kernel density estimation techniques (NAFO, 2013); however, given their long-lived nature and 'iconic', over rare status, efforts have been made to map the occurrences of black corals in relation to the other VME indicators and the closed areas. As an alternative to KDE, Knudby et al. (2013c) applied the random forest species distribution modelling technique to black coral presence and absence data to identify areas of suitable habitat based on environmental preferences and to evaluate the potential presence of black corals within the closed areas (NAFO, 2013). A total of 163 presences and 4185 absences from three different sources were modelled: EU-Spanish and Canadian research vessel trawl surveys to 2013 (155 presences, filtered to 148 presences/4097 absences), the NEREIDA rock dredge and scallop gear surveys from 2009 to 2010 (7 presences and 88 absences), and NEREIDA benthic imagery surveys from 2009-2010 (8 presences). The model predicted a ring of higher black coral presence probability around the Cap between 500 and 1000 m depth, with smaller pockets of higher-quality habitat along the eastern and northeastern slopes.

Since 2013, additional data on the distribution of black corals in the NRA has been collected through the EU-Spanish and Canadian RV trawl surveys, bringing the total number of RV tow sets from 155 to 280. Examination of the cumulative catch weight distribution curve applied to these data (Figure 39, left panel) revealed a highly skewed weight distribution - many small catches, and few large that may be indicative of significant concentrations. The spatial distribution of these data revealed that some aggregation of these larger catches was occurring (Figure 39, right panel), suggesting that the additional data may now allow for the application of KDE techniques.

Kernel Density Analysis of Black Corals

As for other VME indicators it was necessary to exclude some of the smaller catches in order to combine the data from the different gear types (Table 17). Only catches ≥ 0.2 kg were included in the

analysis. This left 44 records from the original 280 (6 from Canada and 38 from EU-Spain). Previously established methods and assessment criteria were followed for the analysis (NAFO, 2013), and the KDE parameters were: Search Radius = 19.8 km; Contour Interval = 0.000005; Cell size default = 2386.0 m. A kernel density surface was created (Figure 40) and the area of successive density polygons calculated (Table 18). The analysis performed well and a weight threshold value of 0.4 kg was identified (Table 18, Figures 41 and 42).

Table 17. Nonparametric statistical tests (Kolmogorov–Smirnov (K-S) statistic) for the equality of the black coral catch distributions obtained with different trawl gears (Campelen and Lofoten) and with different tow duration for the Campelen gear.

Comparison Groups	Data (Source)	P- value (K-S test)
Campelen 15 min trawl vs. Campelen 30 min trawl	> 0 kg (N_{Canada}= 20, $N_{EU\text{-}Spain}$ = 20)	0.55960
Combined Campelen trawls vs. Lofoten trawl	> 0 kg ($N_{Campelen}$=40, $N_{Lofoten}$ = 240)	0.01774
	≥ 0.01 kg ($N_{Campele}$=35, $N_{Lofoten}$ = 177)	0.02761
	≥ 0.02 kg ($N_{Campele}$=28, $N_{Lofoten}$ = 152)	0.00528
	≥ 0.05 kg ($N_{Campele}$=25, $N_{Lofoten}$ = 109)	0.01959
	≥ 0.1 kg ($N_{Campele}$=16, $N_{Lofoten}$ = 68)	0.00209
	≥ 0.2 kg ($N_{Campele}$=15, $N_{Lofoten}$ = 29)	0.38790

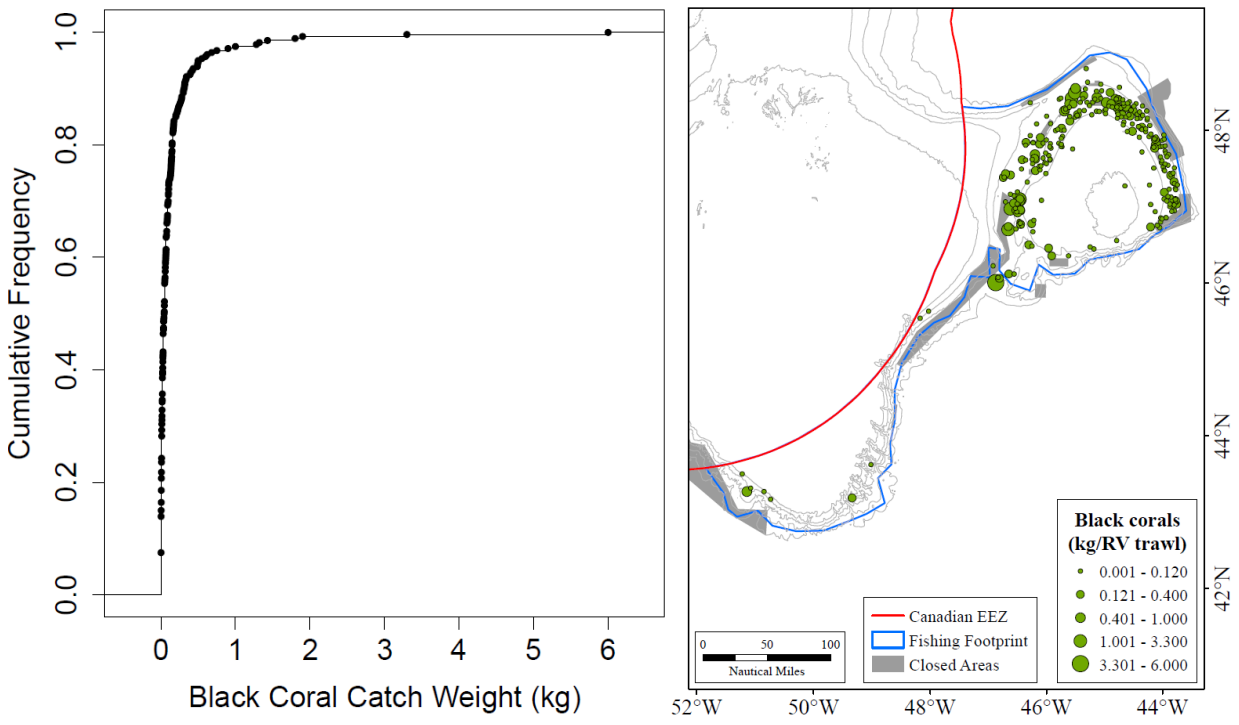

Figure 39. Left panel. Cumulative distribution of black coral in research vessel (RV) catches (kg/tow). Right panel. Biomass distribution (kg/tow) of RV catches with black coral in the NRA. Areas closed to protect coral and sponge VMEs are indicated in grey shaded areas. Blue line indicates the NAFO Fishing Footprint.

Table 18. The number of points attributing to the delineation of black coral VME polygons based on successively smaller research vessel black coral catch weight thresholds (kg). The area and number of observations used to define each polygon and the percent change in area and the number of additional observations between successive thresholds are provided. The shaded row represents the threshold used to define the VMEs.

Black Coral Catch Threshold (Kg)	Number of Observations in Polygon	Additional Observations Per Interval	Area of Polygon (km^2)	Percent Change in Area Between Successive Thresholds
1.5	4	4	44.6	1667.2
1	8	4	787.7	89.2
0.5	15	7	1490.3	76.5
0.4	21	6	2631.1	25.4
0.32	26	5	3300.1	5.0
0.3	32	6	3463.5	6.8
0.25	37	5	3699.5	48.3
0.2	44	7	5487.8	

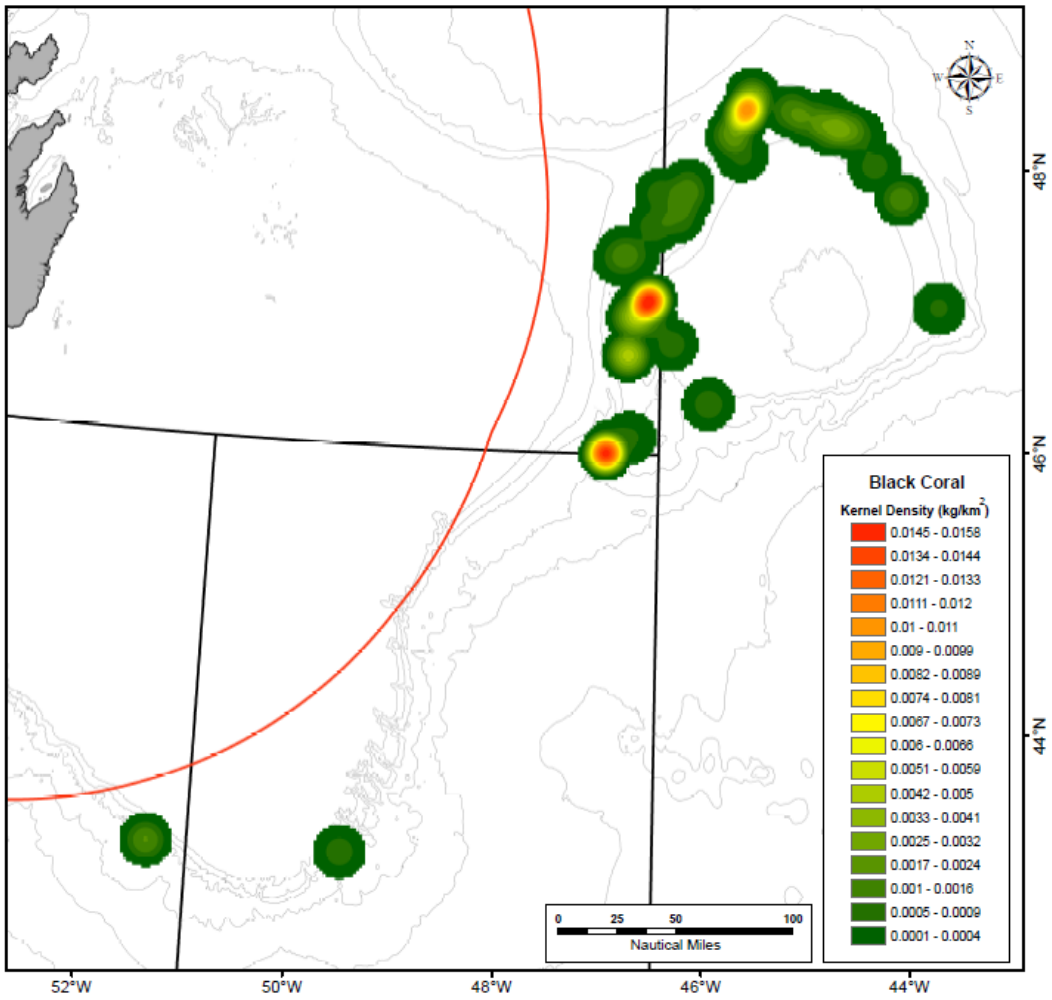

Figure 40. Kernel density biomass surface of black corals in the NAFO Regulatory Area.

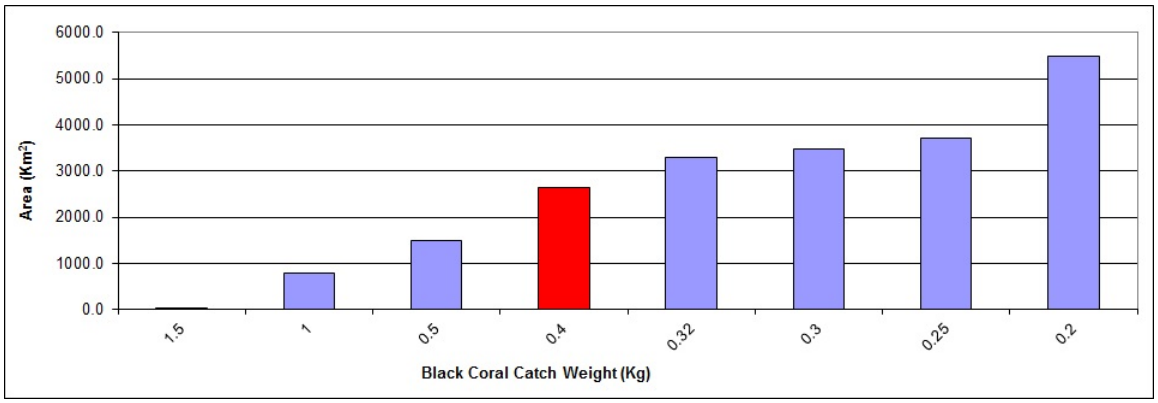

Figure 41. Bar graphs of the polygon area established by successively smaller research vessel black coral catch weight thresholds. Red bar indicates the potential VME polygon threshold.

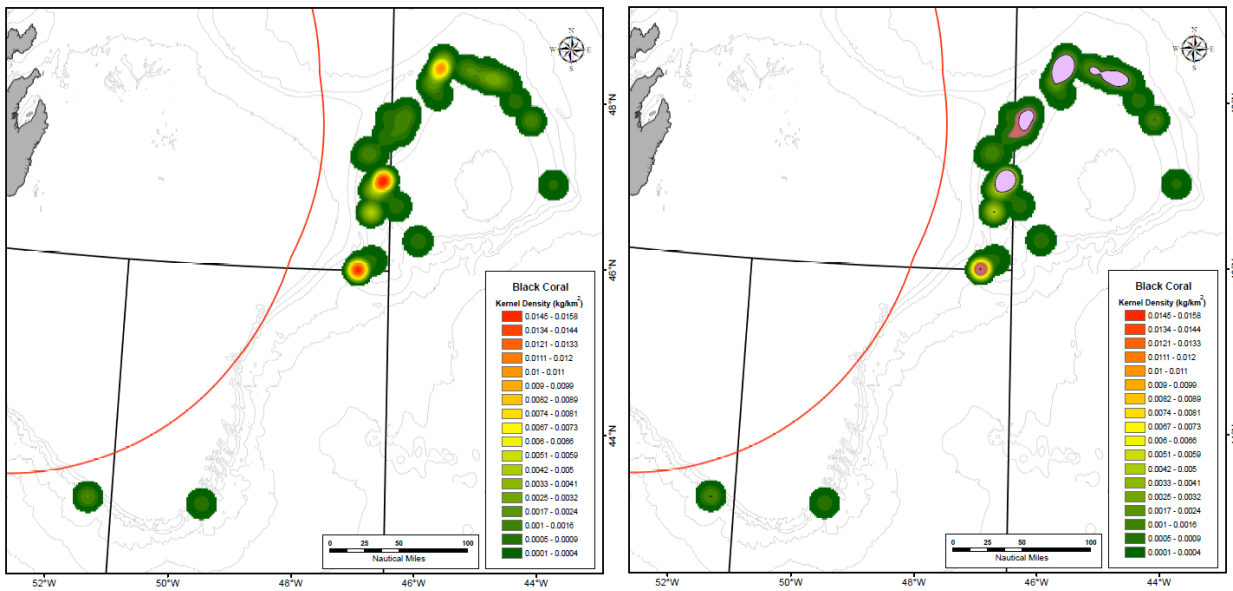

Figure 42. Left panel: The 2019 kernel density distribution of black corals in the NAFO Regulatory Area. The green areas represent low black coral densities while the red areas indicate high densities. Right panel: Comparison of the area covered by catches ≥ 0.4 kg (mauve) and catches and catches ≥ 0.32 kg (purple).

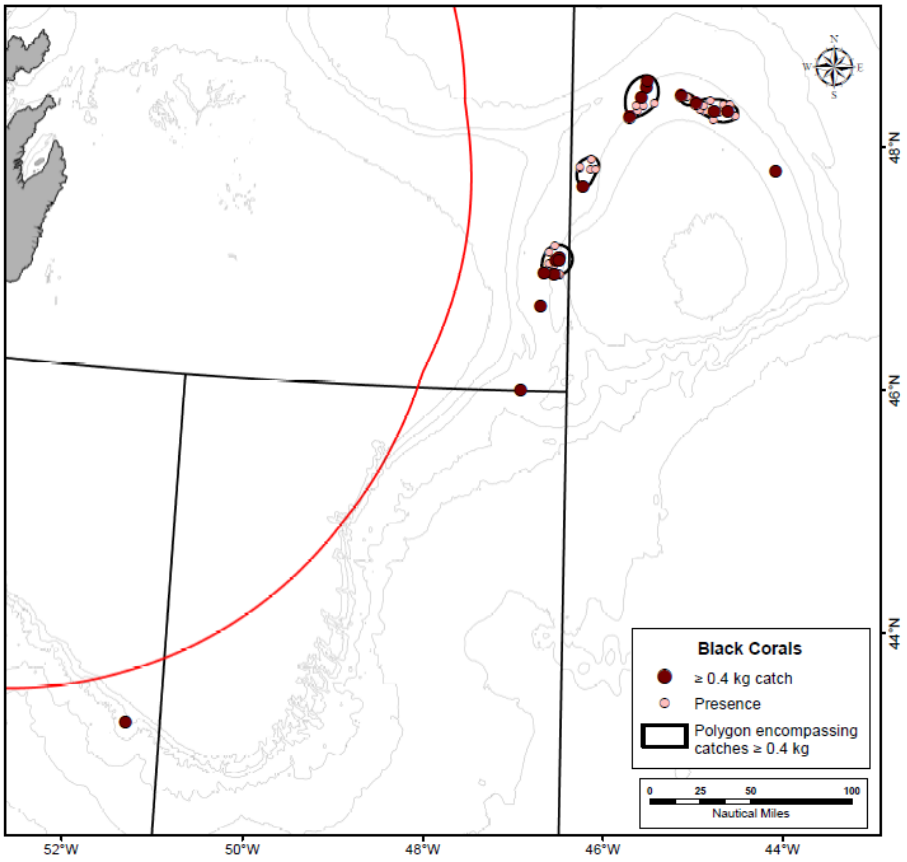

Figure 43. RV Catches ≥ 0.4 kg of black corals and all other catches are displayed within the 2019 KDE polygons.

Modified VME Polygon Boundaries for Black Corals

The 2019 black coral KDE polygons were overlain on the presence-absence prevalence threshold from the black coral SDM generated in 2013 (Knudby et al., 2013c). Most of the KDE area falls within the area of predicted presence (Figure 44). Consequently, no modifications were made to the KDE polygons.

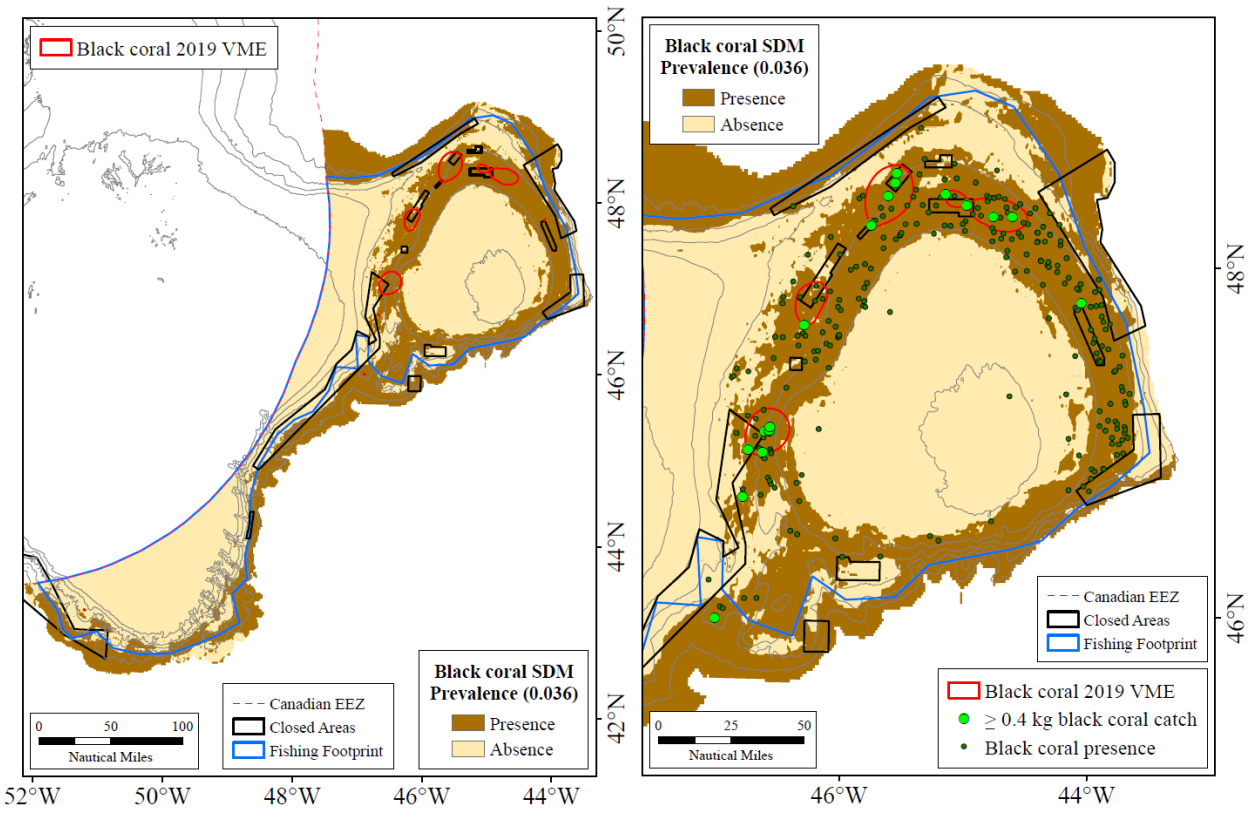

Figure 44. Left panel. Position of the black coral 2019 KDE polygons in relation to the black coral SDM prevalence map (Knudby et al., 2013c) for the full NRA. Right panel. Close up of Flemish Cap. The 2019 KDE polygons (red outline) fall within the predicted presence (brown areas) of these species and so were not modified. Closed areas are outlined in black. The fishing footprint is outlined in blue.

The black coral KDE polygons are shown in Figure 45 along with the location of black corals recorded from *in situ* benthic imagery transects collected from the Flemish Cap area as part of the NEREIDA program in 2009 and 2010 (orange circles; summarized in Beazley et al., 2013b). Transects that were considered null for the presence of black corals are shown as black circles. The final KDE polygons show good spatial congruence with the location of sea pen closure areas 7, 9, 10, and 12 on the north and northwest Flemish Cap. The KDE polygon overlapping with the northern portion of Area 2 is congruent with anecdotal observations of an antipatharian hotspot previously noted by Dr. Antonio Vázquez (known colloquially as "Antonio's Point") based on the occurrence of black corals in RV trawl survey catch from the area (NAFO, 2010). Examination of the *in situ* data collected from Transect 29 inside this KDE polygon revealed the presence of *Stauropathes arctica* in low densities (2 colonies; Figure 45).

Although the evidence to date indicates that black corals occur as solitary colonies across the NRA, the results of this analysis suggests some aggregating properties of this taxonomic group, possibly reflecting a preference for certain oceanographic conditions and/or geomorphic features. Although the ecosystem function of these higher density areas remains poorly studied (but see De Clippele et al., 2019), the longevity, fragility, and vulnerability of this iconic group warrants consideration of these areas for future protection measures.

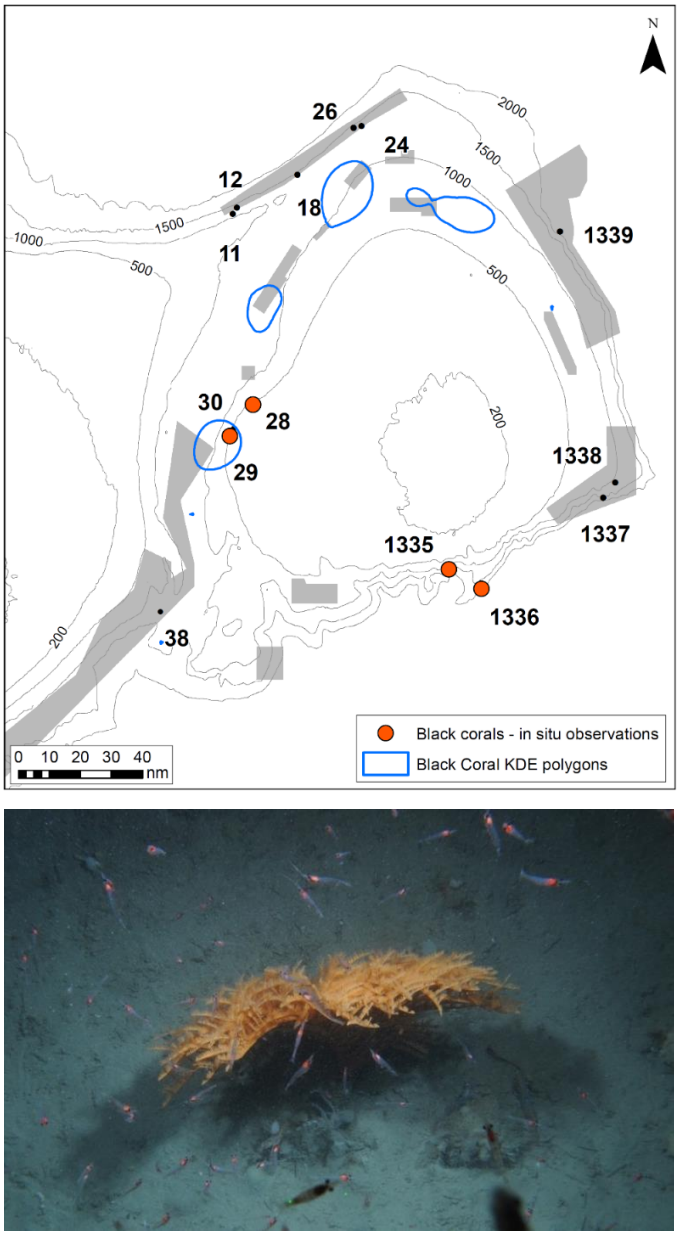

Figure 45. Top panel: Black coral KDE polygons (blue outline) with location of *in situ* observations of black corals (orange circles), which are labelled by transect number. Bottom panel: Colony of *Stauropathes arctica* observed on Transect 29, inside the KDE significant concentration polygon.

Conclusions of the 2019 Analyses of VME Indicator Taxa

Since the 2013 assessment of the closed areas, 3,989 additional data records from the RV surveys, including the 2019 surveys, were collected (Table 19). Most of those catches were small and could not be included in the KDE analyses. Nevertheless, 1,114 new records were used in the KDE analyses, with 60% of those being records of sponge catches (Table 19). In 2013 the fewer data required the search radii in the KDE analyses to be adjusted so that continuous biomass surfaces could be created. However, in 2019 the default parameters (determined from the spatial extent of the data) were used, which in future will create even further stability to the results.

Table 19. Number of records from the Canadian and EU-Spanish research vessel (RV) surveys used in the 2019 and 2013 assessments of the closed areas, by VME indicator group. Records used for the kernel density analyses are indicated in columns showing records above the RV catch threshold where data could be combined. Sponge=large-sized sponges; SGC=small gorgonian corals; LGC=large gorgonian corals; Bryozoan=erect bryozoan.

VME Indicator	Year	Canadian Records	EU-Spain Records	Total Records	RV Catch Threshold for Combining Data	Canadian Records above Threshold	EU-Spain Records above Threshold	Total Records Above Gear Threshold
Sponge	2019	975	3,415	4,390	0.5 kg	618	1,207	1,825
Sponge	2013	553	2,040	2,593	0.5 kg	391	763	1,154
Sea Pen	2019	259	1,954	2,213	0.2 kg	54	376	430
Sea Pen	2013	183	1,172*	1,355	0.2 kg	35	227	262
SGC	2019	106	582	688	0.02 kg	62	156	218
SGC**	2013	87	317	404	0.02 kg	40	45	85
LGC	2019	83	200	283	0.1 kg	29	60	89
LGC	2013	42	153	195	0.1 kg	13	45	58
Bryozoan	2019	21	768	789	0.02 kg	12	162	174
Bryozoan	2013	-	353***	353	none	-	353	353
Sea Squirts	2019	172	162	334	none	172	162	334
Sea Squirts	2013	-	88	88	none	-	88	88
Black Coral	2019	20	260	280	0.2 kg	6	38	44
Total	2019	1,636	7,341	8,977		953	2,161	3,114
Total	2013	865	4,123	4,988		479	1,521	2,000

*Misreported as 1127 in NAFO (2013). Totals corrected here. **In 2013 KDE analyses were performed for Divisions 3NO and in 2019 the areas 3LMNO were combined. *** Misreported as 344 records in NAFO (2013). Totals corrected here.

In general there was good spatial congruence between the 2013 and 2019 analyses which is most evident in the comparison of the VME polygons from those years (Figure 46). The same general areas were identified and the RV catch threshold defining the VME polygons were similar between assessments (Table 20). However, with the new data most VMEs increased in area (Table 20; see below section on 'Indicators for the Effectiveness of the NAFO Closed Areas' for details on how area and biomass of the VMEs was calculated), the exception being erect bryozoans where the new data and analyses reduced the VME area. The reduction of area for the erect bryozoans, despite maintaining the same threshold (Table 20) is due to the smaller search radius used in the 2019 analyses which draws tighter bounds around each data point. The large increase in area of the small gorgonian coral VME can be seen on the Tail of Grand Bank near the 3O closure where the new data expanded the significant concentrations identified in 2013 (Figure 46). This increase in area was created through additional data points linking the 2013 polygons (Figure 21) and through an increase in the search radius of 9.6 km in the KDE analysis as a result of performing the analysis on the full spatial extent of the data (3LMNO). Similarly the increase in area for the sea squirt (*Boltenia ovifera*) VME was created through additional data linking two polygons identified in 2013 (Figure 37) on the Tail of Grand Bank. Like area, the total biomass inside the VME increased for all VME indicator types between 2013 and 2019 (Table 20).

Table 20. Change in significant concentration threshold (kg) from research vessel catches and total area (km^2) and KDE biomass (kg) of VME polygons derived from kernel density estimation and species distribution modelling techniques between 2019 and 2013. Also shown is the percent change in polygon area and biomass between 2019 and 2013. SGC=small gorgonian corals; LGC=large gorgonian corals.

VME Indicator	Research Vessel Catch Threshold (kg) for Identifying VME Polygons		Area of VME (km^2)		Change in Area between 2019 & 2013 (%)	KDE biomass of VME (kg)		Change in KDE biomass between 2019 & 2013 (%)
	2019	2013	2019	2013		2019	2013	
Large-sized sponges	100	75	24,218	19,824	22	199,640	156,671	27
Sea pens	1.3	1.4	8,498	6,983	22	167	107	57
SGC	0.2	0.15*	4,540	307	1,377	16	3	508
LGC	0.6	0.6	5,007	3,506	43	292	213	37
Sea squirts	0.35	0.3	4,077	2,193	86	396	41	876
Erect bryozoans	0.2	0.2	3,491	6,587	-47	122	103	18
Black corals**	0.4	-	2,631	-	-	14	-	-

*In 2013 KDE analyses were performed for Divisions 3NO and in 2019 the areas 3LMNO were combined. ** KDE analyses on black coral catches were performed for the first time in 2019.

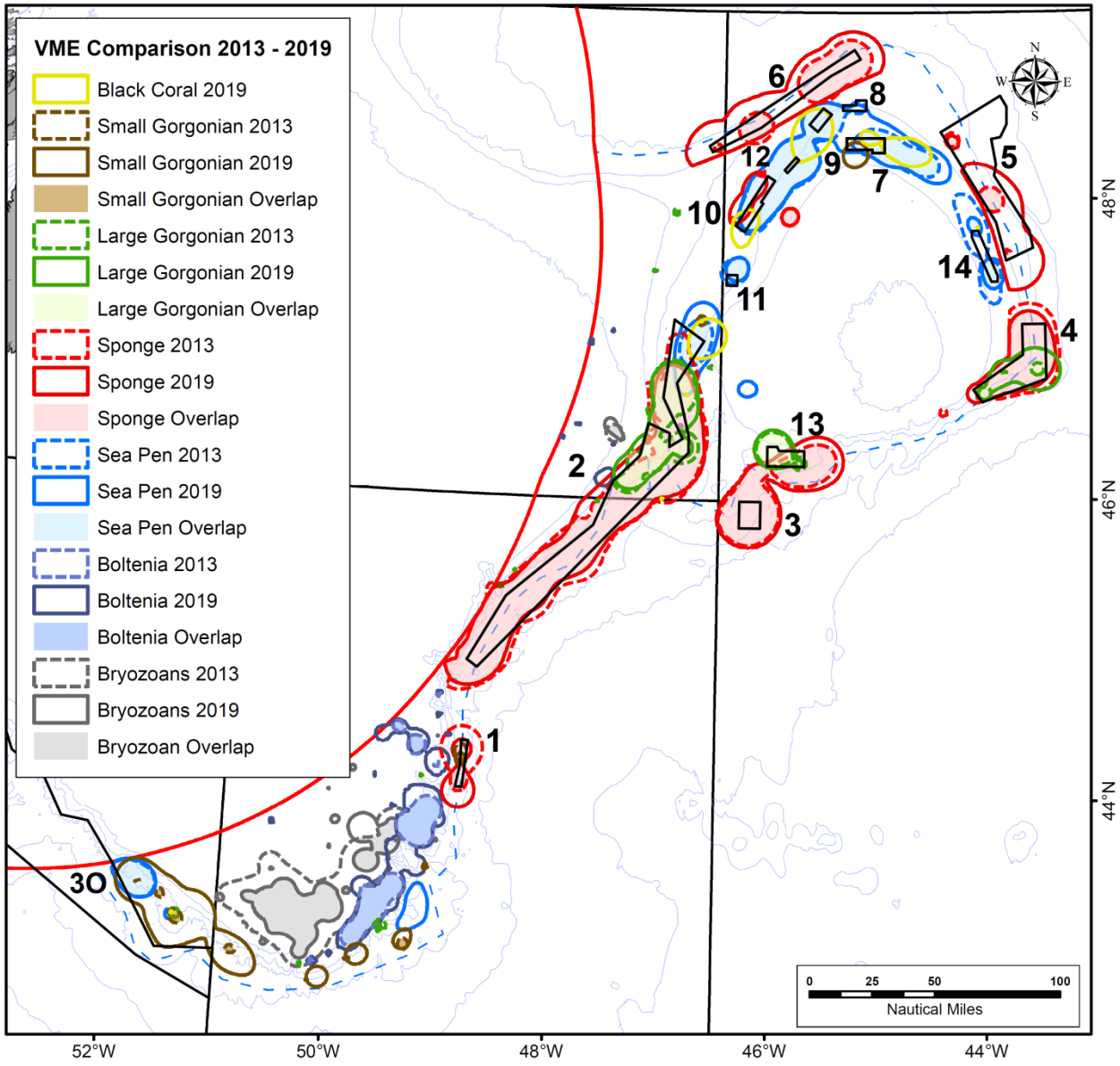

Figure 46. Overview map of the location of VME taxa (large-sized sponges, sea pens, small gorgonian corals, large gorgonian corals, erect bryozoans, sea squirts (*Boltenia ovifera*), and black corals) in the NRA, colour coded by taxon. For all taxa the polygons determined from the 2013 analysis are shown in dashed line and compared with those from the 2019 analyses in solid lines. Areas of overlap between the polygons produced in each year are shaded. The closed areas are indicated in black outline and their numbers shown near the closure. Dashed blue line is the fishing footprint.

Indicators for the Effectiveness of the NAFO Closed Areas

In order to evaluate the effectiveness of the closed areas, the proportion of total area and biomass of VME within and outside the closed areas were examined for VMEs delineated in the 2013 and 2019 assessments. Area and biomass were calculated for each VME indicator type, using the current closed areas defined in the NAFO CEM (NAFO, 2019), but with Area 14 included (NAFO, 2018b). For sponges

and large gorgonian corals, the KDE polygons that were modified by the prevalence boundary of their respective random forest species distribution models were used in this assessment (see above). The total area encompassed by these polygons will be smaller than that defined by the unmodified KDE significant concentration threshold.

All area and biomass calculations were done in ArcMap version 10.7 with layers projected using the NAD 1983 UTM Zone 23N projection coordinate system. The area of the 2019 and 2013 VME polygons was calculated using the 'Calculate Geometry' function in ArcMap, with units in square kilometres.

The biomass encompassed by the VME polygons of each indicator type was derived from the output kernel density raster surfaces, which measure biomass as kg per unit area (in this case, per km^2) for each raster cell across the data range, and is therefore more accurately referred to as a biomass density rather than a true biomass. The 'Extract by Mask' tool in ArcMap 10.7 was used to extract the cells of the KDE density surfaces that fall within the VME polygons. The resulting raster layer was converted to points representing the value of each cell, and the total biomass density was summed across all points within the VME polygons of each VME indicator type. The biomass density of each raster cell and subsequently the points representing them, provide biomass density as kg/km^2. However, the underlying cell size of the density raster is not 1 km^2, but is the default cell size of the kernel density function, which is the shorter distance of the height or width extent of the dataset divided by 250. In order to convert biomass density to true biomass, the biomass density values summed across the VME polygons of each VME indicator type was multiplied by the default cell size identified by the KDE function. Also, the 'Extract by Mask' tool extracts only whole raster cells from the KDE density surface, but as the VME boundaries are smooth and undulate across the gridded raster cells of the underlying KDE surfaces (illustrated in the centre panel of Figure 47), this resulted in some raster cells and their modelled biomass extending beyond the VME polygon in some areas of the VME, while other areas of the VME were not fully populated. Given that both under- and over-extension of the KDE biomass raster surface in relation to the VME boundaries occurred, efforts to clip the underlying raster surfaces exactly to the boundaries of the VME and re-calculate the biomass of the clipped cells were not undertaken here.

The decision to use the KDE biomass surfaces to represent VME indicator biomass was made knowing that it was not the most accurate way to estimate true biomass. However, KDE surfaces were available for seven of the nine VME indicator taxa and so allowed for the effectiveness of the closed areas to be compared in the current assessment. In a separate study, Pham et al. (2019) used two separate approaches to estimate sponge biomass in the NRA: (1) biomass calculated from a random forest regression model to predict the distribution of the sponge biomass using environmental predictors, the "modelling approach"; and (2) gridded biomass surface based on individual RV survey records, the "grid-cell approach" (Figure 47). The modelling approach produces a continuous biomass surface and allows predictions in areas beyond the sampled locations based on environmental variables, thereby capturing the full extent of the sponge grounds, which in this area includes deep waters where there are relatively few RV trawls (Figure 47). In contrast, the gridded biomass surface (Figure 47) used only the actual RV catch data to populate cells and so relies less on spatial interpolation/extrapolation. Details of the method used to create the surface are outlined in Cogswell et al. (2011), where for each 5 km x 5 km grid cell the mean biomass was calculated based on all of the sponge RV catch data in each cell applied to the total cell area. The value for cells with no RV trawl data is a function of the values of all the input cells that are in a specified neighborhood around that location. Both approaches assume 100% catchability which is unlikely and so are expected to underestimate true biomass. Ideally these two approaches for estimating biomass would be applied to all VME indicators in the NRA; however there was insufficient time to complete that work for the 12th meeting of the NAFO Working Group on Ecosystem Science and Assessment

(WGESA). In the future, alternative biomass estimates for the VME indicator taxa should be derived in order to determine the best approach for developing indicators of the effectiveness of the protection provided by the closed areas.

In order to compare the values produced from each method we calculated the large-sized sponge biomass for Area 2. This large closed area in Flemish Pass is the least affected by the difference in depth coverage of each of the methods, although some areas of the VME polygon lie outside the grids in the grid cell method (Figure 47), causing the biomass estimated by that approach to be underestimated. The grid cell approach produced a sponge biomass for Area 2 of 58,602 tons, while the SDM biomass prediction was 36,843 tons. The KDE biomass for Area 2 was only 115 tons. It is clear that the KDE biomass is much less than that produced by the other two approaches. This is not unexpected as the KDE method is designed to accentuate high density areas (hotspots) which will have the effect of concentrating high biomass. Further, the method spreads the biomass out over the grid cell, diluting the overall density (explaining why for sponges the KDE density is a maximum of 41.12 kg/km^2 (Figure 5) when 67 catches were over 1 ton/RV tow (Table 9)). Therefore the biomass figures reported here are measures of relative biomass and are not indicative of true biomass.

The proportion of the area and total biomass of VME within the closed areas irrespective of the fishing footprint (referred to as 'Closed Area Protected' hereafter), outside the closed areas and outside the fishing footprint (i.e., 'Conditionally Protected'), and outside the closed areas but within fishing footprint (i.e., 'Unprotected') was calculated for the 2019 and 2013 VME (see Figure 48). Fishing activities, while allowed outside the fishing footprint, are subject to the provisions outlined in 'Article 18 - Exploratory Bottom Fishing Activities' of the NAFO CEM, which requires contracting parties to submit a notice of intent and preliminary assessment of the known and anticipated impacts of exploratory bottom fishing outside the footprint, and is subject to approval by the NAFO Executive Secretary (NAFO, 2019). These provisions afford an additional level of scrutiny of fishing on VME delineated beyond the boundaries of the fishing footprint, warranting their designation as 'Conditionally Protected' in this assessment, although there is no certainty that fishing would not be allowed.

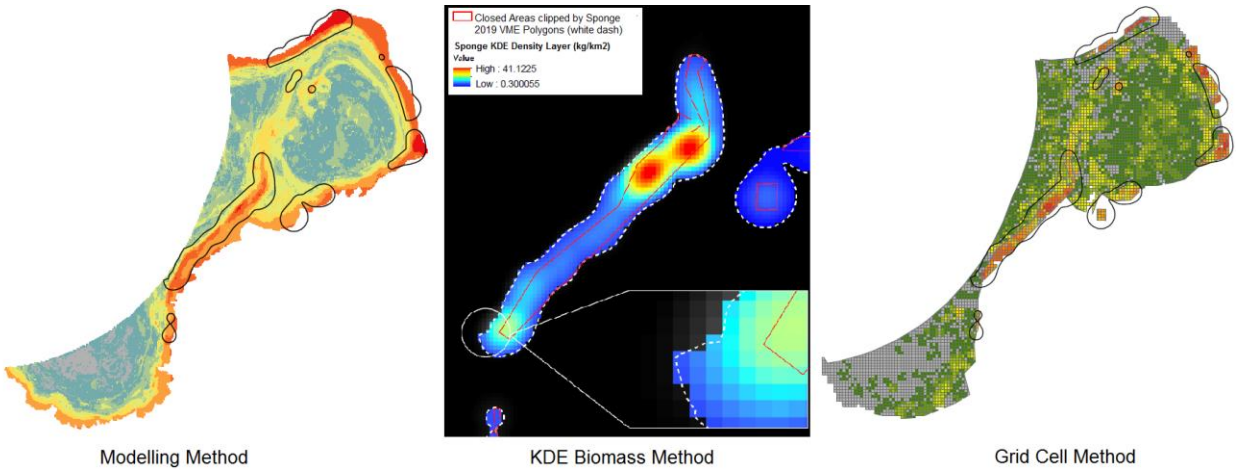

Figure 47. Illustration of three methods used to determine VME biomass in the NRA. Left panel: the species biomass distribution model used here for sponge biomass (Pham et al., 2019); Middle panel: the KDE biomass method used to evaluate the effectiveness of the closed areas in this report with an inset showing the under- and over-extension of the KDE biomass raster surface in relation to the VME boundaries; Right panel: the grid cell method used here for sponge biomass (Pham et al., 2019). The 2019 KDE polygons for large-sized sponges are shown.

For the area-based calculations, the 'Erase' tool in ArcMap was used to erase the area occupied by the closure areas from the VME polygons, when overlap occurred. ArcMap's 'Clip' tool was then used to clip the NAFO closure areas by the VME polygons. The resulting area depicts the proportion of the VME closed to fishing, and represents the 'Closed Area Protected' area of Figure 48. The 'Erase' tool was then used to erase the closed area from the VME, and the Clip tool was used to clip this area by the fishing footprint, resulting in the VME area inside the fishing footprint but outside the closure ('Unprotected'; Figure 48) and outside the fishing footprint and closed areas ('Conditionally Protected'; Figure 48).

For the biomass-based calculations, the area of the VME considered 'Closed Area Protected' was extracted from the kernel density rasters using the 'Extract by Mask' tool, and was converted to a point layer. The point layers representing the closed areas and the VMEs were clipped using the same process as outlined above for the area-based calculations to create the three different levels of protection outlined in Figure 48.

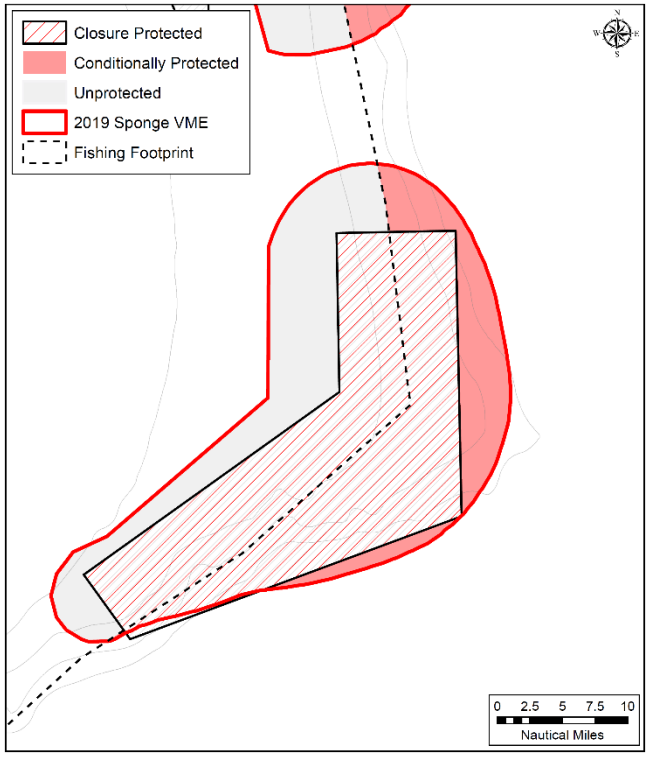

Figure 48. Example of the different levels of protection of VME in the NRA based on the 2019 sponge VME overlapping closed Area 4. The area of VME inside the closure is considered 'Closed Area Protected' (red thatched polygon with black outline); the VME area outside the fishing footprint and closed area 'Conditionally Protected' (red shaded polygon), and the VME area outside the closed area, inside fishing footprint 'Unprotected' (grey shaded polygon). Note that the area outside the VME but inside the closed area (white area in southwest portion of the polygon) is not included in the calculations as it is outside the sponge VME. The boundary of the fishing footprint is represented by the dashed black line.

Tables 21 and 22 show the proportion of VME area delineated in 2013 and 2019 that is Closed Area Protected, Conditionally Protected, and Unprotected for each VME indicator type. Each of these areas are similar between 2013 and 2019 for all VME indicator types. Overall, the level of protected area is low for most VME indicators in 2019, and is near zero for small gorgonian corals, sea squirts and erect bryozoans (Table 22).

Tables 23 and 24 show the proportion of VME biomass delineated in 2013 and 2019 that is Closed Area Protected, Conditionally Protected, and Unprotected for each VME indicator type. The proportion of VME biomass across the different levels of protection is similar between 2013 and 2019 for all VME indicator types. Overall, the level of protected biomass is low for most VME indicators in 2019, and is near zero for small gorgonian corals, sea squirts and erect bryozoans (Table 24).

Table 21. Total area (km^2) of VME polygons generated in 2013 that is Closed Area Protected, Conditionally Protected, and Unprotected in NAFO Divisions 3LMNO. The percentage (%) of total area of each treatment is also shown. Note that Area 14 was included in this calculation.

VME Indicator	Total Area of 2013 VME (km^2)	Closed Area Protected		Conditionally Protected		Unprotected	
		Area (km^2)	Percentage of Total (%)	Area (km^2)	Percentage of Total (%)	Area (km^2)	Percentage of Total (%)
Large-sized sponges	19,824	7,907	40	4,900	25	7,017	35
Sea pens	6,983	1,383	20	0.04	0	5,600	80
Small gorgonian corals*	307	56	18	3	1	249	81
Large gorgonian corals	3,506	1,981	57	0	0	1,524	43
Sea squirts	2,193	0	0	0	0	2,193	100
Erect bryozoans	6,587	0	0	0	0	6,587	100

*In 2013 KDE analyses were performed for Divisions 3NO and for Division 3M for small gorgonian corals and in 2019 the areas were combined.

Table 22. Total area (km^2) of VME polygons generated in 2019 that is Closed Area Protected, Conditionally Protected, and Unprotected in NAFO Divisions 3LMNO. The percentage (%) of total area of each treatment is also shown. Note that Area 14 was included in this calculation.

VME Indicator	Total Area of 2019 VME (km^2)	Closed Area Protected		Conditionally Protected		Unprotected	
		Area (km^2)	Percentage of Total (%)	Area (km^2)	Percentage of Total (%)	Area (km^2)	Percentage of Total (%)
Large-sized sponges	24,218	9,324	39	6,076	25	8,818	36
Sea pens	8,498	1,439	17	1	0	7,057	83
Small gorgonian corals*	4,540	188	4	0	0	4,352	96
Large gorgonian corals	5,007	2,750	55	293	6	1,964	39
Sea squirts	4,077	0	0	18	0	4,059	100
Erect bryozoans	3,491	5	0.14	0	0	3,486	99.86
Black corals**	2,631	456	17	1	0	2,173	83

*In 2013 KDE analyses were performed for Divisions 3NO and for Division 3M for small gorgonian corals and in 2019 the areas were combined. ** KDE analyses on black coral catches were performed for the first time in 2019.

Table 23. Total biomass (kg) VME indicator taxa inside the 2013 VME polygons derived from KDE density surfaces that is Closed Area Protected, Conditionally Protected, and Unprotected in NAFO Divisions 3LMNO. The percentage (%) of total area of each treatment is also shown. Note that the most recent closure areas were used for this calculation, with Area 14 included. SGC=Small gorgonian corals; LGC=Large gorgonian corals.

	Total KDE Biomass of 2013 VME (kg)	Closed Area Protected		Conditionally Protected		Unprotected	
		KDE Biomass (kg)	Percentage of Total (%)	KDE Biomass (kg)	Percentage of Total (%)	KDE Biomass (kg)	Percentage of Total (%)
Large-sized sponges	156,671	96,677	62	17,723	11	42,271	27
Sea pens	107	22	21	0	0	85	79
SGC*	3	0	4	0	0	2	96
LGC	213	132	62	0	0	81	38
Sea squirts	41	0	0	0	0	41	100
Erect bryozoans	103	0	0	0	0	103	100

*In 2013 KDE analyses were performed for Divisions 3NO and for Division 3M for small gorgonian corals and in 2019 the areas were combined.

Table 24. Total biomass (kg) VME indicator taxa inside the 2019 VME polygons derived from KDE density surfaces that is Closed Area Protected, Conditionally Protected, and Unprotected in NAFO Divisions 3LMNO. The percentage (%) of total area of each treatment is also shown. Note that the most recent closure areas were used for this calculation, with Area 14 included. SGC=Small gorgonian corals; LGC=Large gorgonian corals.

VME Indicator	Total KDE Biomass of 2019 VME (kg)	Closed Area Protected		Conditionally Protected		Unprotected	
		KDE Biomass (kg)	Percentage of Total (%)	KDE Biomass (kg)	Percentage of Total (%)	KDE Biomass (kg)	Percentage of Total (%)
Large-sized sponges	199,640	112,788	57	26,731	13	60,122	30
Sea pens	167	30	18	0	0	137	82
SGC*	16	0	1	0	0	16	99
LGC	292	165	57	4	1	123	42
Sea squirts	396	0	0	1	0.14	396	99.86
Erect bryozoans	122	0	0	0	0	122	99.99
Black corals**	14	2	16	0	1	11	83

*In 2013 KDE analyses were performed for Divisions 3NO and for Division 3M for small gorgonian corals and in 2019 the areas were combined. ** KDE analyses on black coral catches were performed for the first time in 2019.

References

Beazley, L.I., Kenchington, E. L., Murillo, F. J. and Sacau M. 2013a. Deep-sea sponge grounds enhance diversity and abundance of epibenthic megafauna in the Northwest Atlantic. ICES J. Mar. Sci. 70: 1471-1490.

Beazley, L.I., Anstey, L.J., and Kenchington, E.R. 2013b. Summary of the Location of VME Indicators on the Flemish Cap Slope Based on *in situ* Benthic Imagery. N6274. NAFO SCR Doc. 13/76, 18 pp.

Bo, A. 2008. Taxonomy and ecology of antipatharians. Ph.D. Dissertation in Marine Biology and Ecology, Universita Politecnica Delle Marche, Ancona, Italy. 212 pp.

Boehner, J., and Selige, T. 2006. Spatial prediction of soil attributes using terrain analysis and climate regionalisation. In: Boehner, J., McCloy, K.R., Strobl, J. (Eds.). SAGA - Analysis and Modelling Applications, Goettinger Geographische Abhandlungen, Goettingen, pp. 13-28.

Boehner, J., and Antonic, O. 2009. Land-surface parameters specific to topo-climatology. In: Hengl, T., Reuter, H. (Eds.). Geomorphometry - Concepts, Software, Applications. Developments in Soil Science, Volume 33, Elsevier, Amsterdam, pp. 195-226.

Breiman, L. 2001. Random Forests. Mach. Learn. 45: 5–32.

Cogswell, A., Kenchington, E., Lirette, C., Murillo, F.J., Campanis, G., Campbell, N., and Ollerhead, N. 2011. Layers Utilized by an ArcGIS Model to Approximate Commercial Coral and Sponge By-catch in the NAFO Regulatory Area. Serial No. N6002, NAFO SCR Doc. 11/72, 50 pp.

Conrad, O., Bechtel, B., Bock, M., Dietrich, H., Fischer, E., Gerlitz, L., Wehberg, J., Wichmann, V., and Böhner, J. 2015. System for Automated Geoscientific Analyses (SAGA) v. 2.1.4. Geosci. Model Devel. 8: 1991-2007. https://doi.org/10.5194/gmd-8-1991-2015

Cutler, D.R., Edwards, T.C., Beard, K.H., Cutler, A., Hess, K.T., Gibson, J., and Lawler, J.J. 2007. Random Forests for classification in ecology. Ecology 88: 2783–2792.

De Clippele, L.H., Huvenne, V.A.I., Molodtsova, T., and Roberts, J.M. 2019. The diversity and ecological role of non-scleractinian corals (Antipatharia and Alcyonacea) on scleractinian cold-water coral mounds. Front. Mar. Sci. https://doi.org/10.3389/fmars.2019.00184

Desmet, P.J.J., and Govers, G. 1996. A GIS procedure for automatically calculating the USLE LS factor on topographically complex landscape units. J. Soil Water Conserv. 51(5): 427-433.

DFO. 2017. Delineation of Significant Areas of Coldwater Corals and Sponge-Dominated Communities in Canada's Atlantic and Eastern Arctic Marine Waters and their Overlap with Fishing Activity. DFO Can. Sci. Advis. Sec. Sci. Advis. Rep. 2017/007.

Etnoyer, P.J., Wagner, D., Fowle, H.A., Poti, M., Kinlan, B., Georgian, S.E., Cordes, E.E. 2018. Models of habitat suitability, size, and age-class structure for the deep-sea black coral *Leiopathes glaberrima* in the Gulf of Mexico. Deep-Sea Res. 150: 218-228.

FAO. 2009. International guidelines for the management of deep-sea fisheries in the high seas, Food and Agriculture Organization of the United Nations, Rome. 92 pp.

Freeman, E. A., and Moisen, G. 2008. PresenceAbsence: An R Package for Presence-Absence Model Analysis. J. Stat. Softw. 23(11): 1-31.

Fuller, S.D., Murillo Perez, F.J., Wareham, V., and Kenchington, E. 2008. Vulnerable Marine Ecosystems Dominated by Deep-Water Corals and Sponges in the NAFO Convention Area. NAFO SCR Doc. 08/22, Serial No. N5524, 24 pp.

Grange, K.R. 1991. Mutualism between the antipatharian *Antipathes fiordensis* and the ophiuroid *Astrobrachion constrictum* in New Zealand fjords. Hydrobiologia 216: 297-303

Grigg, R.W. 1989. Precious coral fisheries of the Pacific and Mediterranean, in J.F. Caddy (Ed.), Marine Invertebrate Fisheries: Their Assessment and Management, Wiley, New York, 637-645.

Guijarro, J., Beazley, L., Lirette, C., Wang, Z., and Kenchington, E. 2016a. Characteristics of environmental data layers for use in species distribution modelling in the Newfoundland and Labrador Region. Can. Tech. Rep. Fish. Aquat. Sci. 3187: viii + 325 pp.

Guijarro, J., Beazley, L., Lirette, C., Kenchington, E., Wareham, V., Gilkinson, K., Koen-Alonso, M., and Murillo, F.J. 2016b. Species Distribution Modelling of Corals and Sponges from Research Vessel Survey Data in the Newfoundland and Labrador Region for Use in the Identification of Significant Benthic Areas. Can. Tech. Rep. Fish. Aquat. Sci. 3171: vi + 126 p.

Gullage, L., Devillers, R., and Edinger, E. 2017. Predictive distribution modelling of cold-water corals in the Newfoundland and Labrador region. Mar. Ecol. Progr. Ser. 582: 57-77.

Kenchington, E., Beazley, L., Lirette, C., Murillo, F.J., Guijarro, J., Wareham, V., Gilkinson, K., Koen Alonso, M., Benoît, H., Bourdages, H., Sainte-Marie, B., Treble, M. and Siferd, T. 2016. Delineation of Coral and Sponge Significant Benthic Areas in Eastern Canada Using Kernel Density Analyses and Species Distribution Models. DFO Can. Sci. Advis. Sec. Res. Doc. 2016/093. vi + 178 p.

Kenchington, E., Murillo, F.J., Lirette, C., Sacau, M., Koen-Alonso, M., Kenny, A., Ollerhead, N., Wareham, V. and Beazley, L. 2014. Kernel density surface modelling as a means to identify significant concentrations of vulnerable marine ecosystem indicators. PLoS ONE 9(10): e109365. doi:10.1371/journal.pone.0109365.

Kenchington, E., Cogswell, A., Lirette, C. and Murillo-Perez, F.J. 2009. The Use of Density Analyses to Delineate Sponge Grounds and Other Benthic VMEs from Trawl Survey Data. Serial No. N5626. NAFO SCR Doc. 09/6, 18 pp.

Knudby, A., Kenchington, E., Cogswell, A.T., Lirette, C.G., Murillo, F.J. 2013a. Distribution modelling for sponges and sponge grounds in the northwest Atlantic Ocean. Can. Tech. Rep. Fish. Aquat. Sci. 3055: v + 73 p.

Knudby, A., Kenchington, E., Murillo, F.J. 2013b. Modeling the Distribution of *Geodia* Sponges and Sponge Grounds in the Northwest Atlantic. PLoSONE 8: e82306. doi:10.1371/journal.pone.0082306.

Knudby, A., Lirette, C., Kenchington, E., and Murillo, F.J. 2013c. Species Distribution Models of Black Corals, Large Gorgonian Corals and Sea Pens in the NAFO Regulatory Area. NAFO SCR Doc. 13/78, Serial No. N6276, 17 pp.

Kursa, M.B., and Rudnicki, W.R. 2010. Feature Selection with the Boruta Package. J. Stat. Softw. 36(11): 1-13.

Liaw, A., Wiener, M. 2002. Classification and Regression by randomForest. R News 2: 18–22.

MacIsaac, K.G., Best, M., Brugler, M.R., Kenchington, E.L.R., Anstey, L.J, Gordan, T. 2013. *Telopathes magna* gen. nov., spec. nov. (Cnidaria: Anthozoa: Antipatharia: Schizopathidae) from deep waters off Atlantic Canada and the first molecular phylogeny of the deep-sea family Schizopathidae. Zootaxa 3700 (2): 237–258.

Mandrekar, J.N. 2010. Receiver operating characteristic curve in diagnostic test assessment. J. Thor. Oncol. 5: 1315-1316.

Murillo, F.J., Kenchington, E., Gonzalez, C., and Sacau, M. 2010. The use of density analyses to delineate significant concentrations of Pennatulaceans from trawl survey data. Serial No. N5753. NAFO SCR Doc. 10/07, 7 pp.

Murillo, F.J., Durán Muñoz, P., Altuna, A., and Serrano, A. 2011a. Distribution of deep-water corals of the Flemish Cap, Flemish Pass and the Grand Banks of Newfoundland (Northwest Atlantic Ocean): interaction with fishing activities. ICES J. Mar. Sci., 68: 319-332.

Murillo, F.J., Sacau, M., Piper, D.J.W., Wareham, V., and Muñoz, A. 2011b. New VME indicator species (excluding corals and sponges) and some potential VME elements of the NAFO Regulatory Area. NAFO SCR Doc. 11/73, Serial No. N6003, 19 pp.

Murillo, F. J., Serrano, A., Kenchington E., and Mora, J. 2016. Epibenthic assemblages of the Tail of the Grand Bank and Flemish Cap (northwest Atlantic) in relation to environmental parameters and trawling intensity. Deep-Sea Res. 109: 99–122.

NAFO. 2009. Report of the NAFO Scientific Council Working Group on Ecosystem Approach to Fisheries Management (WGEAFM). Response to Fisheries Commission Request 9.b and 9.c. NAFO SCS Doc. 09/6, Serial No. N5627, 26 pp.

NAFO. 2010. Report of the NAFO Scientific Council Working Group on Ecosystem Approaches to Fisheries Management (WGEAFM). NAFO SCS Doc. 10/19, Serial No. N5815, 101 pp.

NAFO. 2011. Report of the 4th Meeting of the NAFO Scientific Council Working Group on Ecosystem Approaches to Fisheries Management (WGEAFM). NAFO SCS Doc. 11/22, Serial No. N6006, 126 pp.

NAFO. 2012. Report of Scientific Council Meeting - June 2012. NAFO SCS Doc. 12/19, 192 pp.

NAFO. 2013. Report of the 6th Meeting of the NAFO Scientific Council Working Group on Ecosystem Science and Assessment (WGESA) [Formerly SC WGEAFM]. NAFO SCS Doc. 13/024, Serial No. N6277, 209 pp.

NAFO. 2015. Report of the 8th Meeting of the NAFO Scientific Council (SC) Working Group on Ecosystem Science and Assessment (WGESA) [Formerly SC WGEAFM]. NAFO SCS Doc. 15/29, Serial No. N6549, 176 pp.

NAFO. 2017. Report of the 10th Meeting of the NAFO Scientific Council Working Group on Ecosystem Science and Assessment (WG-ESA). NAFO SCS Doc. 17/21, Serial No. N6774, 166 pp.

NAFO. 2018a. Report of the 11th Meeting of the NAFO Scientific Council Working Group on Ecosystem Science and Assessment (WG-ESA). NAFO SCS Doc. 18/23, Serial No. N6900, 112 pp.

NAFO 2018b. Conservation and Enforcement Measures 2018. NAFO/COM Doc. 18-01, Serial No. N6767, 190 pp.

NAFO. 2019. Northwest Atlantic Fisheries Organization Conservation and Enforcement Measures 2019. NAFO/COM Doc. 19-01, Serial No. N6901, 181 pp.

Olaya, V. 2009. Basic land-surface parameters. In: Hengl, T., Reuter, H.I., (Eds.). Geomorphometry. Concepts, Software, Applications. Elsevier, Amsterdam, pp. 141-169.

Pham, C.K., Murillo, F.J., Lirette, C., Maldonado, M., Colaço, A., Ottaviani, D., and Kenchington, E. 2019. Removal of deep-sea sponges by bottom trawling in the Flemish Cap area: conservation, ecology and economic assessment. Nature Sci. Rep. 9: 15843.

R Development Core Team. 2018. R: A language and environment for statistical computing. R Foundation for Statistical Computing. Vienna, Austria.

Ryan, W.B.F., Carbotte, S.M., Coplan, J.O., O'Hara, S., Melkonian, A., Arko, R., Weissel, R.A., Ferrini, V., Goodwillie, A., Nitsche, F., Bonczkowski, J., and Zemsky, R. 2009. Global Multi-Resolution Topography synthesis. Geochem. Geophys. Geosyst. 10: Q03014, doi: 10.1029/2008GC002332

Shank, T.M. 2010. New England and Corner Rise Seamounts. Mountains in the Sea. Oceanogr. 23: 104-105.

Shepard, A., Theroux, R.B., Cooper, R.A., and Uzmann, J.R. 1986. Ecology of Ceriantharia (Coelenterata, Anthozoa) of the northwest Atlantic from Cape Hatteras to Nova Scotia. Fish. Bull. 84: 625-646.

Tazioli, S., Bo, M., Boyer, M., Rotinsulu, H., and Bavestrello, G. 2007. Ecological observations of some common antipatharian corals in the marine park of Bunaken (North Sulawesi, Indonesia) Zool. Stud. 46: 227-241.

Wagner, D., Luck, D.G., and Toonen, R.J. 2012. Chapter Two – The Biology and Ecology of Black Corals (Cnidaria: Anthozoa: Hexacorallia: Antipatharia). Adv. Mar. Biol. 63: 67-132.

Waller, R., Watling, L., Auster, P., and Shank, T. 2007. Anthropogenic impacts on the Corner Rise Seamounts, north-west Atlantic Ocean. J. Mar. Biol. Ass. U.K. 87: 1075-1076.

Wang, L., and Liu, H. 2006. An efficient method for identifying and filling surface depressions in digital elevation models for hydrologic analysis and modelling. Int. J. Geogr. Inf. Sci. 20: 193-213.

Wang, Z., Lu, Y., Greenan, B., Brickman, D., and DeTracey, B. 2017. An eddy-resolving North Atlantic model (BNAM) to support ocean monitoring. Can. Tech. Rep. Hydrogr. Ocean Sci. 327: vii + 18 pp.

Wareham, V., Molodstova, T.N., Murillo, F.J., and Opresko, D.M. 2012. Recent progress in our understanding of the distribution of Black Corals (Anthipatharia: Anthozoa: Cnidaria) throughout the North Atlantic International Symposium on Deep-Sea Corals. Amsterdam (The Netherlands). 1 to 6 April 2012. Abstract: 164 p. Poster presentation.

Yokoyama, R., Shirasawa, M., and Pike, R.J. 2002. Visualizing topography by openness: A new application of image processing to digital elevation models. Photogramm. Eng. Rem. S. 68: 251-266.